HEPATITIS C PATIENTS TREATED WITH INTERFERON-ALPHA/RIBAVIRIN THERAPY DEVELOP AUTOANTIBODIES TO DISTINCT CYTOPLASMIC ROD/RING STRUCTURES COMPOSED OF CTP/GTP NUCLEOTIDE BIOSYNTHETIC ENZYMES

By

WENDY CARCAMO

A DISSERTATION PRESENTED TO THE GRADUATE SCHOOL
OF THE UNIVERSITY OF FLORIDA IN PARTIAL FULFILLMENT
OF THE REQUIREMENTS FOR THE DEGREE OF
DOCTOR OF PHILOSOPHY

UNIVERSITY OF FLORIDA

2012

To my parents for all their encouragement, love, and never-ending support; to my mentor for all his hard work and dedication to help me succeed

ACKNOWLEDGMENTS

It is with great appreciation and sincere thanks that I acknowledge the following individuals for their professional or personal role in my academic career. First and foremost, I would like to thank my family for always being there for me. I thank them for being extremely patience with all of my academic career choices.

I thank my mentor, Dr. Edward Chan, for supporting me in my PhD endeavor. He has guided me throughout my research and with my future career decisions. His support has allowed for our success.

I would also like to thank the members of my committee, Dr. Minoru Satoh, Dr. Naohiro Terada, Dr. Hideko Kasahara, and Dr. Robert Burne for their support and advice throughout my research.

I would like to thank our collaborators, Dr. Nicola Bizzaro, Dr. Chen Liu, Dr. David Ostrov, Dr. Giovanni Covini, Dr. Kevin Wang, Dr. Lung-Ji Chang, Dr. Luis Andrade, Dr. Maria Zajac-Kaye, Dr. Katherine Hankowski and Dr. David Purich who have helped with our study by providing reagents, samples and scientific discussions.

I thank all the current and past Chan lab members for their friendship, assistance, and collaboration. I especially would like to thank Dr. Shangli Lian and Dr. Kaleb Pauley for their support and guidance for perusing my PhD. I would like to thank Dr. Andrew Jakymiw, Dr. Songqing Li, and Dr. Keigo Ikedo for their help when I was just starting out in the lab. A special thanks to Bing Yao, Hyun-Min Jung, Dr. Angela Ceribelli, Lan La, Grant Abadal, Brad Pauley, John Calise, Paul Dominguez-Gutierrez, Stephanie Tamayo, Claire Krueger, and Dr. Abu Nahid for their help with my experiments.

TABLE OF CONTENTS

page

ACKNOWLEDGMENTS 4

LIST OF TABLES 8

LIST OF FIGURES 9

ABSTRACT 11

CHAPTER

1 INTRODUCTION 13

Autoantibodies in Rheumatic Diseases 13
Hepatitis C Virus and Disease 14
HCV and Its Life Cycle 15
HCV and Autoantibodies 16

2 INDUCTION OF CYTOPLASMIC RODS AND RINGS STRUCTURES BY INHIBITION OF THE CTP AND GTP SYNTHETIC PATHWAY IN MAMMALIAN CELLS 19

Background 19
Materials and Methods 20
Cell Culture 20
Embryonic Stem Cell Culture and Differentiation 21
Mouse Cardiomyocyte Collection and Preparation 21
Autoantibody Reagents 21
Immunoprecipitation 21
Indirect Immunofluorescence 22
Induction of RR Formation Using CTPS or IMPDH Inhibitors 22
siRNA Knockdown 23
Transfection of GFP Plasmid 23
Western Blotting 23
Statistical Analysis 24
Results 24
Rods and Rings in the Cytoplasm 24
Identification of CTPS1 and IMPDH2 as RR Components 26
Expression of Rods and Rings in Cultured Cells 27
Induction of Rods and Rings in Cultured HEp-2 Cells 28
Induction of RR in Other Cancer and Primary Cells 29
Induction of RR is Quantitatively Sensitive to the Level of Cellular IMPDH2 Protein 30
RR Expression in Embryonic Stem Cells (ESCs) 32
Discussion 33
RR-Like Structures are Evolutionarily Conserved 34

Embryonic Stem Cells Form RR in the Absence of Chemical Inducers 36

3 CYTOPLASMIC RODS AND RINGS AUTOANTIBODIES DEVELOPED DURING PEGYLATED INTERFERON AND RIBAVIRIN THERAPY IN PATIENTS WITH CHRONIC HEPATITIS C 49

Background 49
Methods 50
Patients 50
Cell Culture and Indirect Immunofluorescence Studies 51
Statistical Analysis 52
Results 53
Discussion 55

4 DIFFERENTIAL AUTOREACTIVITY TO IMPDH2 IN ANTI-RODS/RINGS ANTIBODIES: CLUES TO UNRESPONSIVENESS TO INTERFERON-ALPHA/RIBAVIRIN THERAPY IN US AND ITALIAN HCV PATIENTS 63

Background 63
Materials and Methods 65
Human Sera and Autoantibodies 65
Indirect Immunofluorescence (IIF) 65
Immunoprecipitation (IP) 66
Statistical Analysis 66
Results and Discussion 66
Autoantibodies to Cytoplasmic Rods and Rings in the US and Italian Cohorts 66
Prevalence of Anti-IMPDH2 Antibody by IP 67
Comparison of IIF Titer Versus Anti-IMPDH2 IP 68
Correlation of Anti-RR/IMPDH2 Prevalence and Titer with Therapeutic Outcome 68
Conclusions 70

5 GLUTAMINE DEPRIVATION INITIATES REVERSIBLE ASSEMBLY OF CYTOPLASMIC RODS AND RINGS 75

Background 75
Materials and Methods 77
Cell Culture 77
Indirect Immunofluorescence 77
Induction of RR Assembly by Glutamine Deprivation 77
Induction of RR Formation Using CTPS or IMPDH Inhibitors 78
Induction of RR Formation Using Glutamine Transport and Glutamine Synthetase Inhibitors 78
qRT-PCR 78
Western Blotting 79
Quantification and Statistical Analysis 79

Results 79
Glutamine Deprivation Induces Rod and Ring Formation 79
Glutamine Add-Back Disassembles RR Induced in Response to Glutamine Starvation 81
Supplement of Guanosine or Cytosine Induces the Disassembly of RR Formed in Response to Glutamine Starvation 82
MPA-Induced RR Disassemble After Replenishing with Guanosine 83
Inhibition of Glutamine Synthetase and Glutamine Transport Induce RR Formation 83
Discussion 84

6 COMPARISON OF RODS AND RINGS TO CYTOPLASMIC STRUCTURES COMPOSED OF CTPS OR IMPDH 93

Rods and Rings in the Cytoplasm 93
Nucleotide Biosynthesis Associated with RR 94
Assembly of Proteins for a Cellular Function 95
Rods/Rings Related Filament-Like Structures 95
Conservation of RR Across Species 99
Composition of RR 99
Formation of RR 100
Concluding Remarks 101

7 SUMMARY AND PERSPECTIVE 107

Biological Function of RR Structure 107
Rod Versus Ring Configurations 107
Induced Versus Native RR 107
Attempts to Identify Additional Components in RR 109
Cytoplasmic Versus Nuclear RR 111
Technical Difficulties in RR Detection 112
Clinical Implication of Anti-RR 112
Ribavirin as a Therapeutic Agent 112
MPA as a Therapeutic Agent 113
Development of RR Antibodies and Resistance to Treatment 113
Conclusions 116

LIST OF REFERENCES 126

BIOGRAPHICAL SKETCH 143

LIST OF TABLES

Table		page
2-1	Dose- and time-dependent induction of RR using different CTPS1 and IMPDH2 inhibitors.	48
3-1	Clinical, serological and immunological features of the patients at baseline, and response to treatment.	61
3-2	Clinical and laboratory characteristics of the 15 patients who seroconverted to RR antigen during pegylated IFN α2a/ribavirin therapy.	62
6-1	Comparison of various reported RR-like cytoplasmic filament structures.	106
7-1	Methods of RR induction and quantification of rods vs rings.	124
7-2	Antibodies tested for RR detection by direct immunofluorescence.	125

LIST OF FIGURES

Figure		page
1-1	HCV genome and polyprotein cleavage products.	18
2-1	The distribution of cytoplasmic rods and rings were independent of the Golgi complex and centrosomes, and these structures were not enriched in tubulin or vimentin.	38
2-2	Examples of various intermediate RR structures in HEp-2 cells stained with human serum 604 (green) and counterstained with DAPI (blue).	39
2-3	The expression of rods versus rings was not correlated with the cell cycle.	40
2-4	CTPS1 and IMPDH2 were highly enriched in RR and human anti-RR prototype serum It2006 recognized IMPDH2.	41
2-5	Inhibition of CTPS1- or IMPDH2-induced formation of rods and rings.	42
2-6	Inhibition of CTPS1-induced formation of RR in several human cancer cell lines	43
2-7	Inhibition of CTPS1-induced formation of RR in mouse primary cardiomyocytes, fibroblasts, and endothelial cells.	44
2-8	Overexpression of IMPDH2 prevented the induction of RR.	45
2-9	RR formation becomes increasingly sensitive to ribavirin when IMPDH protein level is reduced by specific siRNA knockdown.	46
2-10	Uninduced mouse embryonic stem cells (ESCs) expressed predominantly cytoplasmic rings that were disassembled during retinoic acid (RA)-induced differentiation and reassembled when treated with acivicin.	47
3-1	Cytoplasmic rods and rings structure stained by sera from HCV patients.	59
3-2	Rod and ring structure can be induced with ribavirin.	60
4-1	Antibody titer determined in two cohorts of HCV patients with autoantibodies to cytoplasmic structures called “rods and rings”.	71
4-2	Prevalence of anti-55kDa IMPDH2 in immunoprecipitation analysis of anti-RR positive sera.	72
4-3	Correlation of anti-RR IIF titer and anti-55kDa IMPDH2 IP intensity	73
4-4	Correlation of anti-RR antibodies and 55 kDa band IP intensity to IFN/R treatment outcome.	74

5-1 Glutamine deprivation induces rods and rings. 87

5-2 Longitudinal analysis of RR formation during glutamine starvation. 88

5-3 Glutamine add-back disassembles RR formed in response to glutamine starvation. 89

5-4 Supplement of guanosine or cytosine induces the disassembly of RR formed in response to glutamine starvation. 90

5-5 MPA-induced RR disassemble after replenishing with guanosine. 91

5-6 Inhibition of glutamine synthetase and glutamine transport induce RR formation 92

6-1 Rods and rings (RR) recognized by human autoantibodies. 103

6-2 A schematic of RR components CTPS1 and IMPDH2 along the purine and pyrimidine biosynthesis pathways. 104

6-3 Patient autoantibodies recognize multiple components of RR. 105

7-1 RR induction pathway showing hypothetical exchange between rods and rings. 117

7-2 Schematic of RR assembly. Rods and rings formed from monomers after induction with CTPS/IMPDH inhibitors (red inserts). 118

7-3 A schematic of putative RR components AICARFT and GARFT along the purine and pyrimidine biosynthesis pathways. 119

7-4 Rods and rings located within the nucleus. 120

7-5 Hypothetical role of ENT1 contributing to resistance to ribavirin therapy and HCV viral persistence *in vivo*. 121

7-6 Experimental schematic to test whether ENT1 resistance is linked to viral persistence. 122

7-7 Postulation of HCV antigens associated with RR. 123

Abstract of Dissertation Presented to the Graduate School
of the University of Florida in Partial Fulfillment of the
Requirements for the Degree of Doctor of Philosophy

HEPATITIS C PATIENTS TREATED WITH INTERFERON-ALPHA/RIBAVIRIN THERAPY DEVELOP AUTOANTIBODIES TO DISTINCT CYTOPLASMIC ROD/RING STRUCTURES COMPOSED OF CTP/GTP NUCLEOTIDE BIOSYNTHETIC ENZYMES

By

Wendy Carcamo

August 2012

Chair: Edward K. L. Chan
Major: Medical Sciences – Molecular Cell Biology

Hepatitis C (HCV) is a pandemic disease affecting an estimated 180 million individuals worldwide and infecting another 3-4 million people each year, making HCV a global public health issue. HCV is the main cause of chronic hepatitis, cirrhosis, and hepatocellular carcinoma. Despite significant improvements in antiviral intervention, only approximately 50% of treated patients with HCV clear the virus after treatment.

Human autoantibodies serve as useful disease-specific markers for systemic rheumatic and other autoimmune disorders. Cytoplasmic filamentous structures referred to as rods and rings (RR) were identified using human autoantibodies. Our data show that HCV patients who have been treated with pegylated-interferon-alpha and ribavirin (RBV) develop these antibodies. The distinct cytoplasmic rods (~3-10 µm in length) and rings (~2-5 µm in diameter) were visualized in HEp-2 cells by immunofluorescence using HCV patient sera. Co-localization studies revealed that although RR had filament-like features, they were not enriched in actin, tubulin, or vimentin, and were not associated with known cytoplasmic structures. Two proteins, cytidine triphosphate synthetase (CTPS) and inosine monophosphate dehydrogenase (IMPDH) were

identified as components of RR. CTPS and IMPDH are important enzymes in the cytidine triphosphate (CTP) and guanosine triphosphate (GTP) biosynthesis pathways, respectively. Two CTPS inhibitors, 6-diazo-5-oxo-L-norleucine (DON) and acivicin were used to test the effects of CTPS inhibition. RR were formed in the presence of these inhibitors in a concentration-dependent and time-dependent manner. Similar results were observed when cells were treated with RBV or mycophenolic acid (MPA), inhibitors of IMPDH. Additionally glutamine deprivation affects CTP/GTP levels which induced RR at a slower rate compared to CTP/GTP inhibitors. Thus, RR formation might be affected by reduction of intracellular CTP/GTP levels. Interestingly, RR were readily detected in the majority of untreated mouse embryonic stem cells (>95%). Upon retinoic acid-induced differentiation, RR disassembled in these cells, but reformed again when treated with acivicin. RR formation appears to represent a response to decrease in intracellular levels of CTP or GTP in cancer cell lines, mouse primary cells, and mouse embryonic stem cells. RR autoantibodies may develop in HCV patients from their immune system exposed to direct interaction of HCV and RR induced by pegylated-interferon-alpha and ribavirin therapy.

CHAPTER 1
INTRODUCTION

Autoantibodies in Rheumatic Diseases

Autoantibodies directed against intracellular antigens are characteristic features of human autoimmune diseases such as systemic lupus erythematosus (SLE), scleroderma, and Sjögren's syndrome (SjS), certain malignancies, and paraneoplastic syndromes (1-5). Studies in systemic rheumatic diseases have provided strong evidence that autoantibodies are produced and maintained by antigen-driven responses (3,6,7) and that autoantibodies can be reporters from the immune system revealing the identity of antigens involved in the autoimmune disease pathogenesis (1). Some of these autoantibodies serve as disease-specific markers and are directed against intracellular macromolecular complexes or particles such as nucleosomes, nucleoli, small nuclear ribonucleoproteins (snRNPs), centromere antigens, and Ro cytoplasmic RNPs (hY-RNP) (1,3,8). In the last two decades there has been significant progress in identifying many intracellular autoantigens.

The study of human autoantibodies and their use as probes of cell structure and function has had an important impact on the disciplines of molecular and cell biology (2). First, the majority of autoantibodies studied have been shown to bind to highly conserved determinants on ubiquitous cellular proteins (1,3). Second, many of the autoantibodies associated with systemic rheumatic diseases are often directed to functional macromolecules rather than to structural components (1,3). These include, histones, DNA and HMG of the nucleosome, the snRNP complex, various centromere and kinetochore components (CENPs), components of the nucleolus and other subcellular structures such as Cajal bodies (a.k.a. coiled bodies) (9) and GW bodies

(a.k.a. mammalian processing bodies or P bodies) (10). Third, in systems amenable to testing, autoantibodies have been shown capable of inhibiting the cellular functions served by the autoantigens (1,3). Examples include the inhibition of aminoacylation of transfer RNAs by anti-tRNA synthetase antibodies, the relaxation of supercoiled DNA by anti-topoisomerase I antibodies, inhibition of precursor mRNA splicing by anti-Sm/RNP antibodies, and the transcription of RNA by anti-RNA polymerases. Taken together, these observations suggest that the conserved epitopes recognized by human autoantibodies are often the functional or active sites of these intracellular proteins (1,3). For immunologists, one of the interesting objectives is the identification of macromolecules and organelles, such as the nucleolus (11,12), Golgi complex (13), and Cajal bodies (9) , as targets of autoimmune responses and how this may explain pathogenesis of autoimmune diseases. For cell biologists, attempts to unravel cellular events can be enhanced by the availability of specific autoantibody probes.

Hepatitis C Virus and Disease

Hepatitis C virus (HCV) is a small positive sense single-stranded RNA virus that causes acute and chronic hepatitis in humans (14,15). HCV is one of the major causative agents of liver disease worldwide, with more than 180 million people infected (15,16). It is estimated that 3-4 million people are newly infected each year (15). In the United States, HCV related chronic liver disease is a leading cause of liver transplantation and causes thousands of deaths annually (17). Although therapeutic options are improving, viral clearance fails in about 80% of infected patients, resulting in a chronic viral disease (18). In 4-20% of patients with chronic hepatitis, liver cirrhosis develops within 20 years, with 1-5% of these patients developing hepatocellular carcinoma (HCC). Persistent HCV infections are facilitated by the ability of virus to

incorporate adaptive mutations in the host and exist as genetically distinct quasispecies. Moreover, the persistent infection may also result from the ability of the virus to disrupt host defense by blocking phosphorylation and function of interferon regulatory factor-3 (IRF-3), an antiviral signaling molecule (19). Unlike hepatitis A and B viruses, there is no vaccine to prevent HCV infection; therefore, current treatment is a combination therapy of pegylated interferon-alpha (IFN-α) and ribavirin, which results in sustained clearance of serum HCV-RNA. However, this treatment is only efficacious in approximately 50% of patients (20-22). Several host factors such as age, stage of liver fibrosis, body mass index (BMI), liver steatosis, insulin resistance, ethnicity and IL28B single nucleotide polymorphisms, as well as viral genotype can potentially influence the treatment outcome (23,24). For instance, patients with HCV genotypes 2 and 3 respond more favorably to treatment than patients with genotype 1 and 4 (25). Therefore, new antiviral compounds that are more efficacious and better-tolerated need to be developed. One of the biggest challenges in developing and implementing therapy for HCV infection is finding the appropriate models to examine the translational capability.

HCV and Its Life Cycle

HCV was originally referred to as non-A non-B Hepatitis. In 1989, a major breakthrough in HCV research was discovered in which the complete sequence of the viral genome was identified and cloned by Choo and collaborators (26). HCV is the only member of the *Hepacivirus* genus that belongs to the *Flaviviridae* family (27,28). Structural analysis of the virus revealed that the genetic materials is surrounded by a protective nucleocapsid, composed mainly of the protein core (C), and further protected by a lipid envelope (29). The lipid envelope contains two major glycoproteins, envelope protein 1 (E1) and E2, that are embedded in the envelope (30). The genome consists of

a single open reading frame that is ~9,600 nucleotides long, which is made into a single polyprotein (3,010 or 3,033 amino acids) product (Figure 1-2) (31,32). The HCV genome is flanked by two non-translated regions, which are essential in the replication and synthesis of viral proteins. Viral and cellular proteases mediate the processing of the polyprotein into structural (core, E1, E2, and p7) and nonstructural proteins (NS2, NS3, NS4A, NS4B, NS5A and NS5B) as illustrated in Figure 1-2 (33-35). The HCV life cycle is entirely cytoplasmic and replication occurs mainly in hepatocytes, but the virus may also replicate in peripheral blood mononuclear cells (PBMCs). The virus enters the host cells through a complex interaction between virions and cell surface molecules CD81, LDL receptor, scavenger receptor class B type 1, Claudin-1 and Occludin (36-39). Additionally, Niemann-Pick C1-like 1 cholesterol absorption receptor was identified as a new HCV entry factor (40,41). Once inside the cell, the virus takes over the intracellular machinery to replicate (42). Due to its high mutation rate caused by the RNA-dependent RNA polymerase, which lacks 3'-5' exonuclease activity (43), HCV is considered a quasispecies composed of 6 genotypes with several subtypes (25). The 6 genotypes have differences in geographic distribution, disease progression, and response to therapy. Genotypes 1, 2 and 3 are distributed worldwide, with genotypes 1a and 1b accounting for 60% of global infections. In the United States, genotypes 1a and 2b are more commonly encountered.

HCV and Autoantibodies

HCV autoimmune manifestations range from non-organ-specific autoantibodies, seropositivity and cryoglobulins to immunological diseases such as glomerulonephritis, vasculitis, and mixed cryoglobulinemia (44-46). Commonly found autoantibodies in the sera of HCV-infected patients are organ- and non-organ-specific. In chronic HCV

infection, smooth muscles antibodies (SMA), which react with cytoskeleton antigens of smooth muscle cells, are found in 10-66% of cases. The prevalence of antinuclear antibodies (ANA) ranges between 6% and 22%, and they are usually presented at a low titer (1:40-1:80) (47-50). Anti-liver-kidney-microsomal antibodies (LKM1), antibodies against epitopes on cytochrome P450, are found in the cytoplasm of hepatocytes and proximal renal tubes. Anti-LKM 1 was detected in up to 10% of chronic HCV patients (51). Other antibodies such as anti-asialoglycoprotein receptor, anti-liver membrane antigen, anti-liver cytosol antigen, anti-hepatocyte plasma membrane, anti-thyroglobulin, anti-thyroid peroxidase, anti-thyroid microsome, anti-phospholipid, anti-neutrophil cytoplasmic, and many other autoantibodies have also been described in patients with HCV infection (52-54). Although the roles of these antibodies are unclear, each antibody is directed against a certain intracellular antigen released during cell death and presented to the immune system. Most studies have not observed significant difference in clinical and biochemical parameters between chronic HCV patients with or without positive serum autoantibodies (49,55).

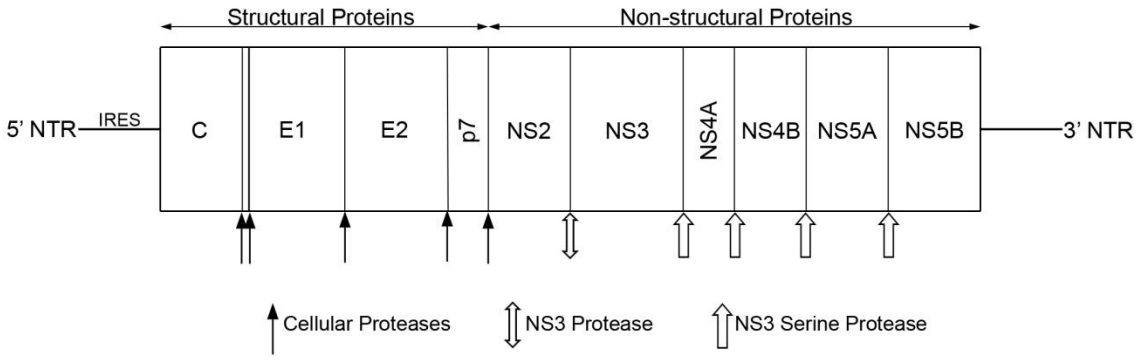

Figure 1-1. HCV genome and polyprotein cleavage products. A schematic representation of the HCV genome indicating the structural and non-structural regions, including the 5' and 3' NTRs. The polyprotein cleavage products are drawn within. The cleavage site and the corresponding protease are indicated (arrows). Schematic is modified from Bartenschlager and Lohmann (35).

CHAPTER 2
INDUCTION OF CYTOPLASMIC RODS AND RINGS STRUCTURES BY INHIBITION OF THE CTP AND GTP SYNTHETIC PATHWAY IN MAMMALIAN CELLS

Background

Over the past few decades many human autoantibodies have emerged as significant disease-specific markers for systemic rheumatic diseases (2). In these diseases, many autoantibodies are directed against intracellular macromolecular complexes or particles, such as nucleosomes and small nuclear/cytoplasmic ribonucleoproteins (2). Thus human autoantibodies have also served as useful probes for exploring subcellular structures and functions because of their unexpected specificity to novel self-antigens. Examples of significant uses of human autoantibodies in further characterization of novel subcellular structures included the identification of p80-coilin in Cajal bodies (formerly known as coiled bodies) (9) and GW182 in GW bodies (10). Within the past few years, our laboratories identified novel human autoantibodies that recognized unique cytoplasmic structures described provisionally as rods and rings (RR). The current study reports the identification of cytidine triphosphate synthase 1 (CTPS1) and inosine-1,2-monophosphate-dehydrogenase-2 (IMPDH2) as components associated with these mammalian RR.

CTPS1 and IMPDH2 are key enzymes in the biosynthetic pathway for CTP and GTP, respectively. CTPS1 catalyses the rate-limiting step in generating cytidine triphosphate (CTP) from uridine triphosphate (UTP). CTP is involved in nucleic acid and phospholipid biosynthesis and plays an important role in controlling cellular proliferation (56). Two isoforms, CTPS1 and CTPS2, have been identified with 74% amino acid similarity. The 67 kDa CTPS1 is a target for antiviral, antineoplastic, and antiparasitic

drug development. Currently available specific inhibitors of CTPS1 include acivicin and 6-diazo-5-oxo-L-norleucine (DON) (57).

The oxidation of inosine monophosphate (IMP) to xanthosine monophosphate (XMP) is the rate-limiting step in the *de novo* guanine synthetic pathway catalyzed by IMPDH2. IMPDH2 regulates cell proliferation. Due to its rate-limiting property, it has been a major target for immunosuppressive, antiviral, and cancer chemotherapy. Two isoforms of IMPDH have been identified sharing 84% amino acid similarity, and both are 56-58 kDa proteins that function as tetramers (58). A study on the regulation of IMPDH with mycophenolic acid (MPA) showed that MPA binds to IMPDH and causes a conformational change resulting in the formation of inactive angular aggregates (59). IMPDH2 inhibitors such as MPA, ribavirin, and tiazofurin are currently used for various medical conditions (60-63).

In the current report, inhibiting either CTPS1 or IMPDH2 using different compounds demonstrated induction of RR in a variety of cell types. More importantly, RR were observed in mouse embryonic stem cells (ESCs) and changes in its expression were correlated with differentiation.

Materials and Methods

Cell Culture

HeLa (human cervical cancer), HEp-2 (human epidermoid larynx carcinoma), and HCT116 (human colon cancer) were cultured in DMEM containing 10% Fetal Bovine Serum (FBS). Human oral cancer cells CAL 27 were cultured in DMEM containing 10% FBS and 1.5 g/L sodium bicarbonate. THP-1, human monocytes, and K562, human erythroleukemia cells, were cultured in RPMI 1640 with 25mM HEPES, and 10% FBS. All cells were cultured in a 37°C incubator with 5% CO2. Adherent cell lines were

maintained at 50% confluence. Suspension cells were maintained at optimum concentration of 10^6 cells/mL. All media contained 100 I.U./ml penicillin and 100 µg/ml streptomycin.

Embryonic Stem Cell Culture and Differentiation

The murine R1 ESCs were obtained from Dr. Andre Nagy (University of Toronto) and maintained according to Hamazaki *et al.* (64). ESCs were differentiated with 1 µM retinoic acid for 4 consecutive days as described (65).

Mouse Cardiomyocyte Collection and Preparation

The mouse cardiomyocytes were harvested and prepared according to Chan *et al*. (66).

Autoantibody Reagents

Autoantibodies with reactivity to RR were selected by authors GC and CAvM during routine screening anti-nuclear antibody assay typically used to help define whether selected patients have developed autoimmune response. All three human anti-RR sera used in this study had chronic hepatitis C virus (HCV) infection and were de-identified samples. These sera were selected largely related to their relative specificity in RR staining and in available quantity to allow further analyses. Serum It2006 was provided by GC, and serum 604 and 609 provided by CAvM, are considered prototype sera for anti-RR. The clinical characterization of these patients and others with anti-RR will be summarized in a subsequent report.

Immunoprecipitation

Immunoprecipitation of [^{35}S]-methionine-labeled K562 cells for the analysis of the proteins recognized by human autoimmune sera was performed as described (67).

Indirect Immunofluorescence

HEp-2 cell slides (INOVA Diagnostics, San Diego, CA) or various adherent cell types cultured in 8-well chamber slides (BD Falcon) were used for indirect immunofluorescence as described (68,69). The 8-well chamber slides were prepared using ~60,000 cells per well in 500µL of media. Non-adherent cells were prepared using the cytospin method to transfer cells onto glass slides as described (70). Fixation methods included acetone at -20°C for 5 min, acetone/methanol (3:1) at -20°C for 10 min, and 3% paraformaldehyde in PBS at room temperature for 10 min followed by 0.1% triton-X/PBS for another 10 min. For co-staining studies the following primary antibodies were used: rabbit anti-giantin (71), anti-pericentrin (a gift from Dr. Marvin Fritzler, University of Calgary), anti-CTPS1 (a gift from Dr. Jim Wilhelm, University of California, San Diego), anti-IMPDH2 (Abcam, Cambridge, MA: ab75790; Proteintech, Chicago, IL: 12948-1-AP), mouse anti-actin, anti-actinin (Sigma-Aldrich, St. Louis, MO: A7811), anti-tubulin, and anti-vimentin, and human anti-RR serum It2006, 604, and 609.

Induction of RR Formation Using CTPS or IMPDH Inhibitors

Acivicin (Enzo Life Sciences, Ann Arbor, MI; BML-El113-0010) and ribavirin (Sigma-Aldrich; R9644) were solubilized in water to 100 mM and 50 mM stock concentration, respectively. 6-diazo-5-oxo-L-norleucine (DON, Sigma-Aldrich; D2141) was solubilized in DMEM to a stock concentration of 100mM. Cells were seeded as monolayers and allowed to attach for 24 h. Subsequently, CTPS1 or IMPDH2 inhibitors were added to various final concentrations from 0.2 µM to 2 mM and were kept in cell incubator for times ranging from 15 min to 48 h.

siRNA Knockdown

All siRNAs used in this study were obtained from Dharmacon RNA Technologies (Lafayette, CO). The siRNAs were dissolved in molecular biology grade water and the resulting 20 µM stock was stored in aliquots at -80°C before use. The two predesigned siRNAs were: ON-TARGET plus SMART pool siRNA Human CTPS1 (target sequences: UAACAUUGAUGCAGGAACA, AGACUAAACCUACCCAGAA, GGUGUUAUAUCAGGAAUUG, and GUAUGCAGGUGCUCAAAUC), siGENOME SMARTpool siRNA IMPDH2 (target sequences: GGACAGACCUGAAGAAGAA, GCACGGCGCUUUGGUGUUC, GGAAAGUUGCCCAUUGUAA, and CUAAAGAAAUAUCGCGGUA). Transfection was performed using Lipofectamine 2000 (Invitrogen, Carlsbad, CA) as per the manufacturer's instruction. The siRNA was used at a final concentration of 100 nM. Knockdown efficiency was determined by real-time PCR analysis using CTPS primers (Applied Biosystems, Hs01041851_m1) or IMPDH2 primers (Applied Biosystems, Hs00168418_m1) plus Western blot for protein expression.

Transfection of GFP Plasmid

HeLa cells were seeded in 8 well chambers at 50-70% confluency. Cells were transfected with 0.35 µg GFP-IMPDH2 (RG202977, OriGene, Rockville, MD) or GFP vector alone using 0.53 µg of Lipofectamine 2000. The transfected cells examined after 24 h directly as live cells or were processed for indirect immunofluorescence.

Western Blotting

Protein levels were analyzed as described (72) using rabbit anti- CTPS (Abcam, 1:1000) or rabbit anti-IMPDH (Santa Cruz Biotechnology, Paso Robles, CA, 1:1000). For IP-Western, IgG was crosslinked to protein A Sepharose beads as described (73)

and human It2006 was used for immunoprecipitation and mouse monoclonal and rabbit anti-IMPDH from Santa Cruz Biotechnology were used for detection. Mouse anti-actin antibody 31G9 was used at 1:5,000 or ~1 µg/ml as a normalizer to control for loading.

Statistical Analysis

Cell counting was performed using Mayachitra Imago (Mayachitra, Santa Barbara, CA) to detect nuclei counterstained with DAPI. Unpaired, two-tailed Student's t-test and Fisher's exact test were used to compare independent groups. For all statistical analysis, Prism for Windows, version 5.0 (GraphPad Software, San Diego, CA) was used.

Results

Rods and Rings in the Cytoplasm

A distinct cytoplasmic pattern was first identified in routine antinuclear antibody (ANA) clinical test using HEp-2 cell slides purchased from INOVA Diagnostics Inc. The structures recognized by a prototype human serum 604 were distinct cytoplasmic rods (~3-10 µm in length) and rings (~2-5 µm in diameter, Figure 2-1). On average, there are one to two rods and/or rings per cell including some interesting apparent intermediate structures such as a figure "8", an elongated ring, twisted ring, rods with pin loops at one end, as well as some that appeared to be transitioning from rods to this peculiar form (Figure 2-2). Figure 2-1A shows RR structure and location with respect to the nucleus and the Golgi complex. Some rods often align adjacent to the nucleus (short arrows, ~40% frequency) or perpendicular to the nucleus (long arrows, ~40% frequency), and rings may be found in the cytoplasm (arrowheads, 5-10% frequency). RR are expressed in some mitotic cells; however, co-staining studies with anti-centromere protein F (CENP-F), showed that the expression of either rods or rings were

independent of the cell cycle, as they appear in all stages (Figure 2-3). CENP-F is a cell cycle marker that has little or no expression at the G1 phase and with increasing level during the S phase, reaching highest expression during late S and G2 phases.

To examine the relationship of RR and other known cytoplasmic organelles, co-localization studies were performed using known markers for cytoplasmic structures. Co-staining studies with antibodies to the Golgi complex showed that RR were independent of the Golgi complex (Figure 2-1A); although many rods appeared to be in the same vicinity as the Golgi complex, there are also many clear-cut examples of rods unassociated with this subcellular structure. Cytoplasmic structures, referred to as “actin rockets,” were previously described in bacteria-infected cells (74). To determine whether RR are related to actin rockets, co-staining with mouse anti-actin antibody was performed to show that RR are not enriched in actin (data not shown). Furthermore, upon careful examination at higher magnification, the HEp-2 cells in our laboratory were not contaminated with bacteria and cell viability was >99%. Since RR are filamentous, co-staining experiments were also performed to determine whether tubulin or vimentin, was enriched in RR. Figure 2-1D is a merged image of RR (Figure 2-1B) and tubulin (Figure 2-1C), showing that RR are not enriched in tubulin. Co-staining of human prototype serum 604 and anti-vimentin antibody ruled out enrichment of RR with enrichment of vimentin in RR. Figure 2-1G shows clear examples of RR with little or no vimentin staining.

Another initial consideration was that primary cilia, which function as nonmotile sensory organelles and have a rod-like appearance (75), could be a possible candidate. To rule out RR as primary cilia, a co-staining study with anti-pericentrin, which

recognizes centrosomes, was conducted. Centrosomes are the precursors of primary cilia and are often located at the ends of the primary cilia. Figure 2-1J revealed that centrosomes were not located at the ends of rods recognized by human prototype serum 604, and therefore are not primary cilia. In fact, there is no noticeable association of either rods or rings with centrosomes. Furthermore, upon closer examination, the fact that ring-type structures have never been observed for primary cilia is consistent with the conclusion.

These findings are highly reproducible using HEp-2 cell substrate from INOVA, as well as using home grown cells prepared with various commonly used fixatives in biological laboratories including acetone at -20°C for 5 minutes, acetone/methanol for 10 minutes, or 3% paraformaldehyde and 0.1% triton-X (after cells were treated with inhibitors – see below). Co-staining experiments with known subcellular markers showed no association with known cytoplasmic organelles such as GW bodies (data not shown).

Identification of CTPS1 and IMPDH2 as RR Components

During the initial stage of characterization, personal consultation with Dr. Joseph G. Gall, Carnegie Institution of Washington, Baltimore, MD, led to the consideration that CTPS1 may be a candidate RR protein because similar rod-like structures were observed in Drosophila embryos in their study of GFP insertional screening (76). This work has been recently published (77). Dr. Jim E. Wilhelm, University of California at San Diego, La Jolla, CA, kindly provided a rabbit anti-CTPS1 serum produced to a peptide of the *Drosophila* CTPS1. Co-staining studies with rabbit anti-CTPS1 antibody showed localization of CTPS1 to RR, identified with prototype human anti-RR serum It2006 (Figure 2-4A).

A second candidate RR protein was postulated in part because of an isolated ring-like structure in the cytoplasm presented in a poster at the 9th Dresden Symposium on Autoantibodies in Germany describing a single autoimmune serum recognizing the enzyme inosine monophosphate dehydrogenase 2 (IMPDH2) (78) and the consideration that CTPS1 and IMPDH2 are enzymes in closely linked pathways as discussed below. In the first experiment to demonstrate whether IMPDH2 was localized to RR, a commercially available rabbit anti-IMPDH2 antibody was used to co-stain HEp-2 cells. Figure 2-4B clearly shows anti-IMPDH2 staining of both rods and rings (arrows), as detected by It2006. Immunoprecipitation analysis using an extract of [^{35}S]-methionine-labeled K562 cells showed that rabbit anti-IMPDH2 and It2006 both pulled down a 55kDa protein (Figure 2-4C). Furthermore, IP-Western analysis confirmed that the 55kDa protein immunoprecipitated by It2006 was IMPDH2, since it was recognized by both mouse monoclonal anti-IMPDH2 and rabbit anti-IMPDH2 (Figure 2-4D).

Expression of Rods and Rings in Cultured Cells

HEp-2 cell slides from INOVA Diagnostics have been consistently positive for RR, tested from lot to lot, since this study was initiated over four years ago. The same was not true for HEp-2 cell ANA slides from other manufacturers examined to date, with staining varying from completely negative to cytoplasmic granular to diffuse. This could be the explanation for why the subcellular staining observed by Blüthner *et al.* (78) was largely different from ours, except for showing one or two isolated ring structures. These differences among products from several manufacturers remain a question not completely resolved, but may stem from differences in culture conditions or proprietary sample processing or both. Homegrown HEp-2 cells on coverslips or 8-chambered slides have not been generally positive for RR staining unless cells were kept in rapidly

dividing log phase and under subconfluent cell density. Confluent cultures were generally negative for RR. Variability from experiment to experiment was clearly observed, and on average only 5-30% of cells were positive for RR detectable by serum 604 or It2006. Cells were always co-stained with both human anti-RR and rabbit anti-giantin (Golgi marker) antibodies to ensure that variables were not introduced in the fixation and immunostaining steps in these experiments. Exactly how INOVA Diagnostics can produce highly consistent HEp-2 cell slides with >95% cells positive for RR staining remains unresolved, but clearly the difference must stem from their unique manufacturing methods. Thus, HEp-2 cells do not have RR under normal culture conditions and cells that do not ordinarily have RR have a diffuse cytoplasmic pattern when stained with prototype human serum (Figure 2-5A). However, it was noted that cells recently thawed from liquid nitrogen form RR in about 15% of the cells. Treating cultured cells with 0.015 - 0.5% of DMSO overnight to simulate freezing medium condition (often with 10% DMSO) did not induce formation of RR.

Induction of Rods and Rings in Cultured HEp-2 Cells

When CTPS1 and IMPDH2 were identified as RR components, the next series of experiments focused on the effects of inhibiting these enzymes. Effects of each drug treatment were analyzed by immunofluorescence (Figure 2-5). The first applied was the CTPS1 inhibitor DON on HEp-2 cells culture using a 2 mM concentration, as reported in literature (57,79). A surprising finding was that both rods and rings were readily detected in >95% of cells after overnight incubation (Figure 2-5B) compared to 0% in untreated control cells cultured in parallel (Figure 2-5A). The RR detected in DON-treated cells were identical in frequency as those observed in the INOVA HEp-2 slides. A second independent CTPS1 inhibitor acivicin (56,57), as well as the IMPDH2 inhibitor

ribavirin, also showed the ability to induce RR formation under similar conditions (Figure 2-5C and D). Inhibition of CTPS1 or IMPDH2 induced RR formation in a concentration and time-dependent manner. Table 2-1 shows the relative efficiencies of the three inhibitors in the induction of RR formation in HEp-2 cells, with ribavirin inducing RR formation in the shortest time and at lowest concentration analyzed. On average, cells treated with DON or acivicin had two RR per cell, while cells treated with ribavirin had more than two RR per cell. An unrelated compound, enoxacin, used as an oral broad-spectrum fluoroquinolone antibacterial agent observed to enhance miRNA activity (80) served as an additional negative control as it did not induce RR after 24 h treatment in various concentrations (10-100 nM). Thus, the inhibition of either CTPS1 or IMPDH2 appeared to be specific for the induction of RR in HEp-2 cells.

Induction of RR in Other Cancer and Primary Cells

To address whether the expression of RR is conserved, multiple cell lines were analyzed, including other adherent monolayer cell lines like HeLa (Figure 2-6A), CAL 27 (Figure 2-6B), and HCT116 (Figure 2-6D), as well as a suspension monocytic cell line THP-1 (Figure 2-6C). Cells were incubated with DON for 24 h and co-stained with serum It2006 and anti-giantin. All cell lines expressed RR in high frequency, comparable to those observed in HEp-2 cells. Untreated cells normally did not show expression of RR, but isolated HeLa cells showed some cytoplasmic granular staining and THP-1 some short “immature” rods. To determine whether the expression of RR could be observed in species other than human, mouse 3T3 fibroblasts and rat NRK cells were stained with It2006. Freshly defrosted 3T3 and NRK often showed expression of RR (~25% of cells) in the first one or two passages, but their expression disappeared completely in subsequent passages. Mouse primary cardiomyocytes, as

well as the often co-purified endothelial cells and fibroblasts during isolation from neonatal heart, did not form RR until induced with 2 mM DON in overnight culture (Figure 2-7). When counting all the cells, overall 88.4% had detectable RR, but cardiomyocytes detected by co-staining of actinin had up to 92.6% showing induced RR (Figure 2-7B). Thus, RR expression appeared to be conserved as they could be induced in multiple immortalized cells, as well as in primary cultured cells.

Induction of RR is Quantitatively Sensitive to the Level of Cellular IMPDH2 Protein

To monitor the formation of RR, the use of GFP fusion constructs was explored. HeLa cells were transfected with GFP-IMPDH2 (Figure 2-8A-C) or the GFP vector alone (Figure 2-8D-F). Following transfection, cells were treated with 2 mM of ribavirin for 24 h, after which cells were fixed and stained with rabbit anti-IMPDH2. GFP-IMPDH2 transfected cells had brighter fluorescence compared to untransfected cells confirming the expression of recombinant IMPDH2 (Figure 2-8A). Surprisingly, GFP-IMPDH2 transfected cells did not show RR after ribavirin induction whereas neighboring untransfected cells showed RR as expected (Figure 2-8C). To rule out transfection induced artifacts interfering with the induction of RR, the induction of RR in control GFP-vector transfected cells was not apparently affected by the transfection (Figure 2-8F). Therefore, the overexpression of IMPDH2 appeared to inhibit formation of RR even at high concentrations of ribavirin. Series of experiments were performed to explore whether the lowest expression of transfected GFP-IMPDH2 could produce cells with GFP-labeled RR by titrating the amount of transfected plasmid and by reducing the time of transfection. None of these experiment yielded live cells labeled with GFP-RR.

Since overexpression of IMPDH2 inhibited RR induction, the next series of experiments were to address whether knockdown of CTPS1 or IMPDH2 would affect

the induction of RR. The strategy adopted was to examine cells transfected with either CTPS1 siRNA (siCTPS1) or IMPDH2 siRNA (siIMPDH2). Thus HeLa cells were either untransfected, transfected with siCTPS1, or siIMPDH2 for 44 h, followed by an additional 4 h of incubation with three different concentrations of ribavirin at 2 mM, 0.2 µM, or 0.05 µM, respectively. Based on the data presented in Table 2-1A, the 2 mM ribavirin concentration was selected as the highest concentration tested, and 0.2 µM was selected as the lowest. Not shown in Table 2-1A for HEp-2 cells, 0.05 µM ribavirin was tested in HeLa cells and shown to be not effective in the induction of RR. The induction of RR was monitored by double immunofluorescence using rabbit anti-IMPDH2 antibody as well as It2006. Figure 2-9A shows the Western blot analysis after siIMPDH2 knockdown with reduction of IMPDH2 levels to 5-9% of untreated cells whereas siCTPS1 had little or no effect on the level of IMPDH2 as expected, although siCTPS1 was confirmed by real-time PCR to be functional with 62% CTPS1 mRNA knockdown. Number of cells with RR were counted and plotted as percentage (Figure 2-9B). While siCTPS1 transfection did not affect the percentage of cells positive for RR in all three concentrations of ribavirin examined, knockdown of IMPDH2 showed significant increase in the percentage of cells with detectable RR formation at both 0.2 µM and 0.05 µM of ribavirin ($p = 0.0001$ for 0.2 µM and 0.05 µM compared to untransfected and siCTPS1 transfected cells by Fisher's exact test). For the 2 mM ribavirin treatment, although RR were induced in 100% of cells transfected with siIMPDH or siCTPS1 RR, knockdown of IMPDH2 showed a decrease in the size of RR (with the average length of rod at 4.6 µm in siIMPDH2 transfected versus 6.9 µm in untransfected) along with the number of RR per cell (4.5 RR/cell in siIMPDH2

transfected versus 7.1 RR/cell in untransfected, p = 0.0024 by t-test) when compared to untransfected cells at 2 mM ribavirin. At 0.2 µM ribavirin, increased formation of RR was observed in cells with reduced levels of IMPDH2 (42.9% of cells in siIMPDH2 transfected vs 21.6% for siCTPS1, p = 0.0048). At 0.05 µM ribavirin, siIMPDH2 transfected cells had 22.4% cells with shorter rods (Figure 2-9D) compared to siCTPS1 transfected cells with 3.6% (Figure 2-9C, p = 0.0001). Thus the data show that the formation of RR by ribavirin was sensitive to the total IMPDH2 level and excess intracellular IMPDH2 makes cells resistant to the formation of RR.

RR Expression in Embryonic Stem Cells (ESCs)

From the data presented in the previous sections, except for unique case of the INOVA HEp-2 cells, various cultured cell types did not consistently form RR unless induced with one of the CTPS1/IMPDH2 inhibitors. The next question was whether certain cell types were uniquely capable of forming RR in the absence of inducers. ESCs are highly proliferative cells that can self-renew and are pluripotent. Undifferentiated, uninduced ESCs were found to form RR (Figure 2-10B) similar to those described in HEp-2 cells (Figure 2-1A) with 1 or 2 RR per cell. Interestingly, unlike HEp-2 cells or mouse 3T3 cells (Figure 2-10A), where only ~10% of cells had rings, >90% of ESC expressed rings, and <5% of cells had rods (Figure 2-10B). In contrast, ESCs that were differentiated with retinoic acid (RA) for 4 days no longer expressed RR (Figure 2-10C) but those differentiated ESCs remained capable of RR formation upon treatment of 2 mM acivicin for 24 h and the RR phenotype was similar to the original undifferentiated ESC (Figure 2-10D). RR expression could be induced in multiple cancerous and primary cells, but RR were found to be expressed in untreated stems cells.

Discussion

In this study, a novel cytoplasmic structure was identified by human autoantibodies produced by HCV patients through ANA testing. Most subcellular organelles disassemble prior to mitosis and reform after cell division. Although some mitotic cells were devoid of RR, either RR disassembly was incomplete or it did not occur at all in other cells, since up to 50% of mitotic cells clearly retained RR. At least one autoantigen, IMPDH2, recognized by the human anti-RR prototype serum It2006 was determined through IP-Western analysis. Co-localization studies determined CTPS1 to be a second component of RR. Inhibitors of the two enzymes induced formation of RR in cells that did not form RR during continuous culture. RR induction could be accomplished with low nanomolar inhibitor concentration. Overexpression of IMPDH2 prevented formation of RR while knockdown in IMPDH2 protein allowed for more sensitive induction of RR with ultralow concentrations of ribavirin that normally did not induce RR. Since CTPS1 and IMPDH2 are major enzymes controlling the biosynthetic pathway for CTP and GTP, respectively, the formation of RR using multiple independent inhibitors of these enzymes implies that this cytoplasmic structure was linked to these cellular metabolic pathways. The observations that the formation of RR is sensitive to the concentration of IMPDH2 (Figure 2-9) and that RR are present in some cases in untreated cells suggest that the formation of RR is linked to the functional level of these enzymes in cellular regulation related to ribonucleotide synthesis. Although both CTPS1 and IMPDH2 were identified as components of RR, due to the large size of these structures, one may speculate that there are many other components involved in RR formation. Since our initial observation of RR over four years ago, morphologically

similar structures were identified in two previous reports (59,81) as well as four recent reports (77,82-84).

RR-Like Structures are Evolutionarily Conserved

The first report of RR-like structures may be the 1987 study by Willingham *et al*. (81). They reported a cytoplasmic "fibrillar structure" identified by an IgG3 monoclonal antibody generated from a Balb/c mouse immunized with mouse tumor cells. These structures were identified using transmission electron microscopy and immuno-electron microscopy as "large single paracrystalline arrays of individual filaments," not enclosed by a lipid bilayer membrane. Their structures were similar in appearance and number per cell to the RR in this study. The unknown antigen recognized by the monoclonal antibody, an unknown 58 kDa protein in immunoprecipitation of lysate of [^{35}S]-methionine radiolabeled cells, was referred to as nematin (from nematodes). The identity of the antigen was not elucidated (81). Similar to our results, they reported that these structures were a) not related to tubulin or vimentin, and b) evolutionarily conserved in human, mouse, and rat. It was also reported that the nematin structure occurred following thawing of stored frozen cells (81) such as HEp-2, 3T3, and NRK cells as also observed in our laboratory.

The second study reporting RR-like structures was by Ji *et al*. identifying IMPDH2 protein aggregates formed from inhibition of enzymatic activity through MPA treatment (59). The structures were identified through immunofluorescence and electron microscopy analysis, with data comparable to the earlier study (81). Further analyses revealed that the aggregates were reversible with the addition of guanosine, guanine, guanosine monophosphate (GMP), guanosine diphosphate (GDP) and guanosine triphosphate (GTP). The structures in that study and in ours were induced with two

independent IMPDH2 inhibitors, MPA versus ribavirin. Both inducers inhibit IMPDH2 but MPA is a noncompetitive and reversible inhibitor (85), while ribavirin is a nonreversible inhibitor. However, our study has identified that the structures induced by IMPDH2 inhibition can be recognized by human autoantibodies. In addition, the RR structure was composed of CTPS1 and IMPDH2.

Ingerson-Mahar *et al.* demonstrated that CTPS formed filaments in *C. crescentus* (82). Identification of the structure was through electron cryotomography along the inner curvature of *C. crescentus*. The metabolic enzyme CTPS has a bifunctional role, as a filament that regulates curvature and performs its catalytic function. In addition, *Escherichia coli* CTPS homologue can also form filaments. A key difference was that treatment of DON in this study dissociated the CTPS filaments in bacteria, while DON induced the formation of RR in mammalian cells in our study.

The most recent report identified RR-like structure in both yeast and *Drosophila*. Noree *et al*. identified four novel filaments that were identified by screening yeast GFP strain collection (83). Through inhibition of CTPS, they determined that filaments were comprised of inhibited CTPS, similar to our results. In addition, they were able to visualize CTPS filaments in the *Drosophila* egg chamber, a subset of gut cells and neurons. Another report also identified an intracellular structure containing CTPS in *Drosophila* cells (77). The structures referred to as cytoophidia were identified in ovary and other tissues (86). The structure was recognized by an antibody against Cup protein, which was believed to have cross-reactivity to an antigen in the cytoophidia. GFP protein trap fly stocks from the Carnegie Protein Trap Library identified CTPS as

the component of cytoophidia. RR and cytoophidia may be similar conserved structures among different species.

Ramer *et al.* identified a large intracellular neuronal organelle that occurs in a subset of adult rat sympathetic ganglion neurons (84). The structure, identified by immunohistochemistry, plus confocal and electron microscopy, occurred mainly in a toroidal shape, but also twists or rods. The structures referred to as loukoumasomes, or donut-like structures were recognized by a monoclonal antibody that was raised against neuron-specific βIII-tubulin, but not recognized by other βIII-tubulin antibodies. One difference between this and our study was the increased toroidal (ring) structures in neurons, while we observed more rods than rings in all induced cancer cells, but more rings than rods in ESCs.

Embryonic Stem Cells Form RR in the Absence of Chemical Inducers

Although RR may appear to be highly conserved as discussed above, our preliminary screening in mouse tissues including liver, kidney, and spleen, using indirect immunofluorescence did not detect these structures. Undifferentiated ESCs form RR without the use of inhibitors while differentiated cells do not form RR and, interestingly, differentiated cells were still capable of RR formation upon induction with a CTPS1 inhibitor; however, this should not be interpreted as de-differentiation back to stem cells. A note of caution is needed as it is not clear whether ESCs RR are structurally and functionally the same as those of cancer cells treated with inhibitors. It is unclear whether the spontaneous formation of RR in ESCs is related to the functional activity of IMPDH2 or CTPS1. The ability to self-renew and pluripotency are two unique properties of stem cells, and these properties may have an effect on IMPDH2 and CTPS1 activity. It is possible that once stem cells differentiate, the cellular regulation of

CTPS1 or IMPDH2 may change and affect the formation of RR. One biological function of RR is related to CTP/GTP synthetic pathway as demonstrated here.

In summary, RR formation is regulated by CTPS1 and IMPDH2, important in purine and pyrimidine biosynthesis and critical for RNA and DNA synthesis. Studies have demonstrated that CTPS1 and IMPDH2 are aberrantly expressed in different cancers (56,87). CTPS1 and IMPDH2 are differentially expressed and, therefore, cells may regulate CTPS1 or IMPDH2 activity via the formation of RR. Further characterization and understanding of RR may lead to a new biomarker for diseases or novel markers for stem cells.

This work was published: Carcamo W.C., Satoh M., Kasahara H., Terada N., Hamazaki T., Chan J.Y.F., Yao B., Tamayo S., Reeves W.H., Liu C., Covini G., von Mühlen C.A., and Chan E.K.L. (2011) Induction of cytoplasmic rods and rings structures by inhibition of the CTP and GTP synthetic pathway in mammalian cells. PLoS One. E29690.

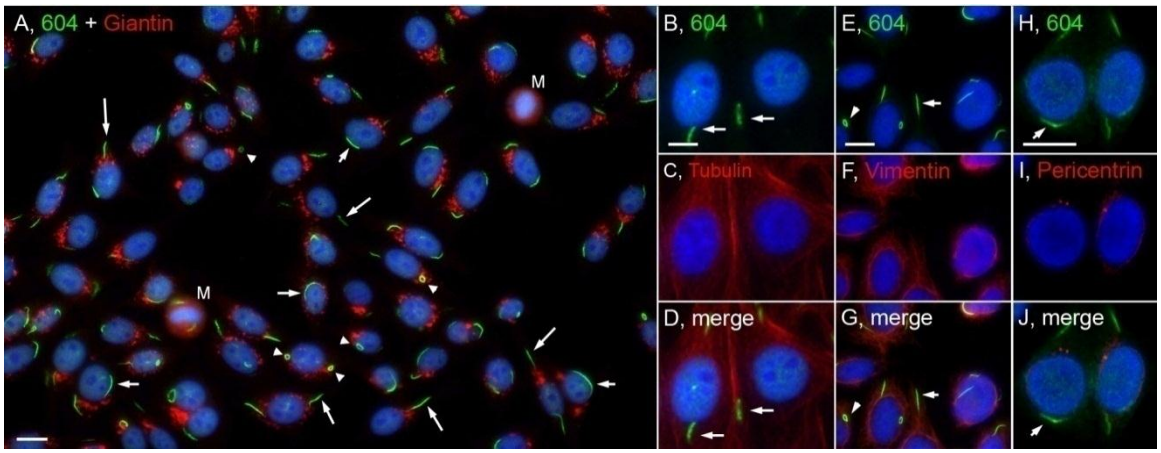

Figure 2-1. The distribution of cytoplasmic rods and rings were independent of the Golgi complex and centrosomes, and these structures were not enriched in tubulin or vimentin. A) Merged image of HEp-2 co-stained with human anti-RR prototype serum 604/Alexa 488 goat anti-human Ig (green) and rabbit anti-giantin (Golgi marker)/Alexa 568 goat anti-rabbit Ig (red). Rods are often presented adjacent (short arrows) or perpendicular (long arrows) to the nucleus while rings (arrowheads) are found either 1 or 2 to a cell. M, mitotic cell. HEp-2 cells were also co-stained with serum 604/Alexa 488 goat anti-human Ig (green, B,E,H) and different cytoplasmic markers using mouse anti-tubulin C), anti-vimentin F), anti-pericentrin I), followed by Alexa 568 goat anti-mouse Ig (red). Nuclei were counterstained with DAPI (blue). Bar, 10 µm.

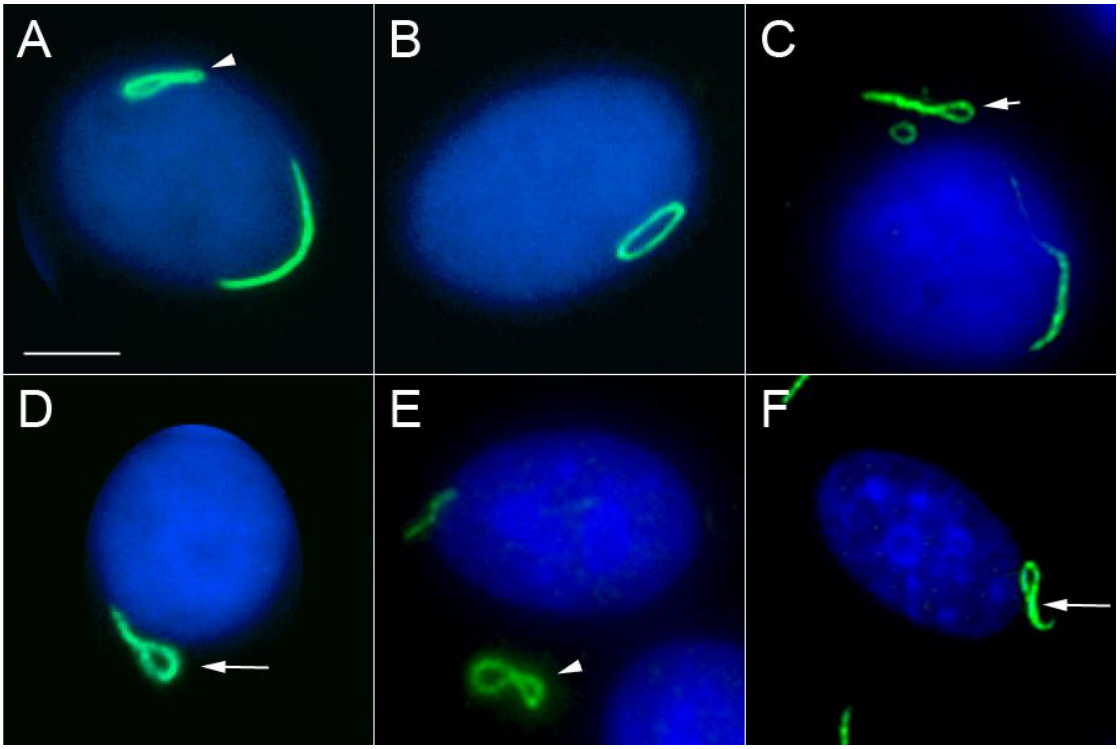

Figure 2-2. Examples of various intermediate RR structures in HEp-2 cells stained with human serum 604 (green) and counterstained with DAPI (blue). A) Figure “8” structure (arrowhead) with a curved rod adjacent to the nuclear envelope; B) elongated ring; C) elongated, twisted ring (short arrow); D) rod with a pin-loop (long arrow); E) Figure “8” structure (arrowhead); F) another rod with pin-loop (long arrow). Nuclei were counterstained with DAPI (blue). Bar, 5 µm.

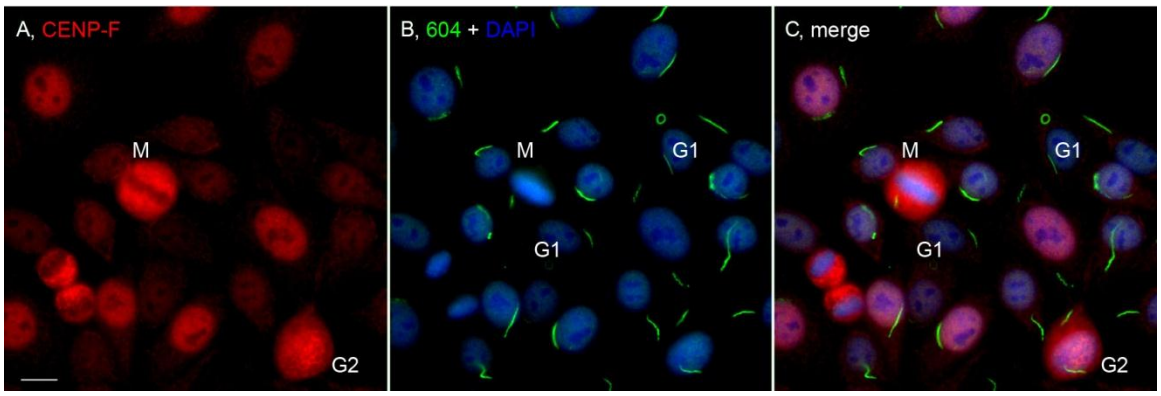

Figure 2-3. The expression of rods versus rings was not correlated with the cell cycle. HEp-2 cells were co-stained with rabbit anti-CENP-F/Alexa 568 goat anti-rabbit IgG A) and human anti-RR serum 604/Alexa 488 goat anti-human IgG B). G1 cells had little or no CENP-F staining, whereas late S/G2 and mitotic (M) cells showed strong staining for CENP-F. Nuclei counterstained with DAPI (blue). Bar, 10 μm.

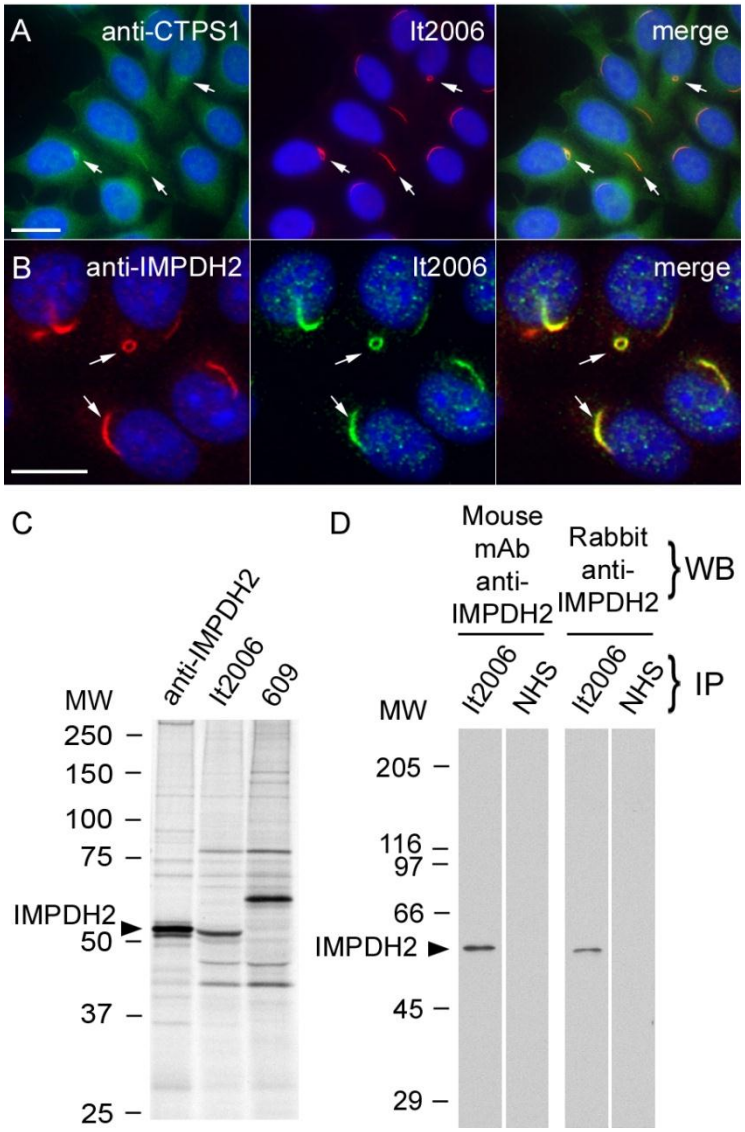

Figure 2-4. CTPS1 and IMPDH2 were highly enriched in RR and human anti-RR prototype serum It2006 recognized IMPDH2. A) Enrichment of CTPS1, detected by rabbit anti-CTPS1 (green), to RR (arrows) identified by It2006 (red). Nuclei were counterstained with DAPI (blue). B) IMPDH2 stained by rabbit anti-IMPDH2 (red) localized to RR (arrows) detected by It2006 (green). Bar, 10 µm. C) Immunoprecipitation (IP) analysis using an extract of [^{35}S]-methionine-labeled K562 cells and rabbit anti-IMPDH2, It2006, and a second human anti-RR serum 609. It2006 recognized a 55kDa protein band that co-migrated with IMPDH2 immunoprecipitated by rabbit anti-IMPDH2. Serum 609 did not immunoprecipitate the 55kDa protein. D) IP-Western blot demonstrated that serum It2006 immunoprecipitated IMPDH2, which was recognized by both mouse monoclonal and rabbit anti-IMPDH2 antibodies. NHS, control normal human serum.

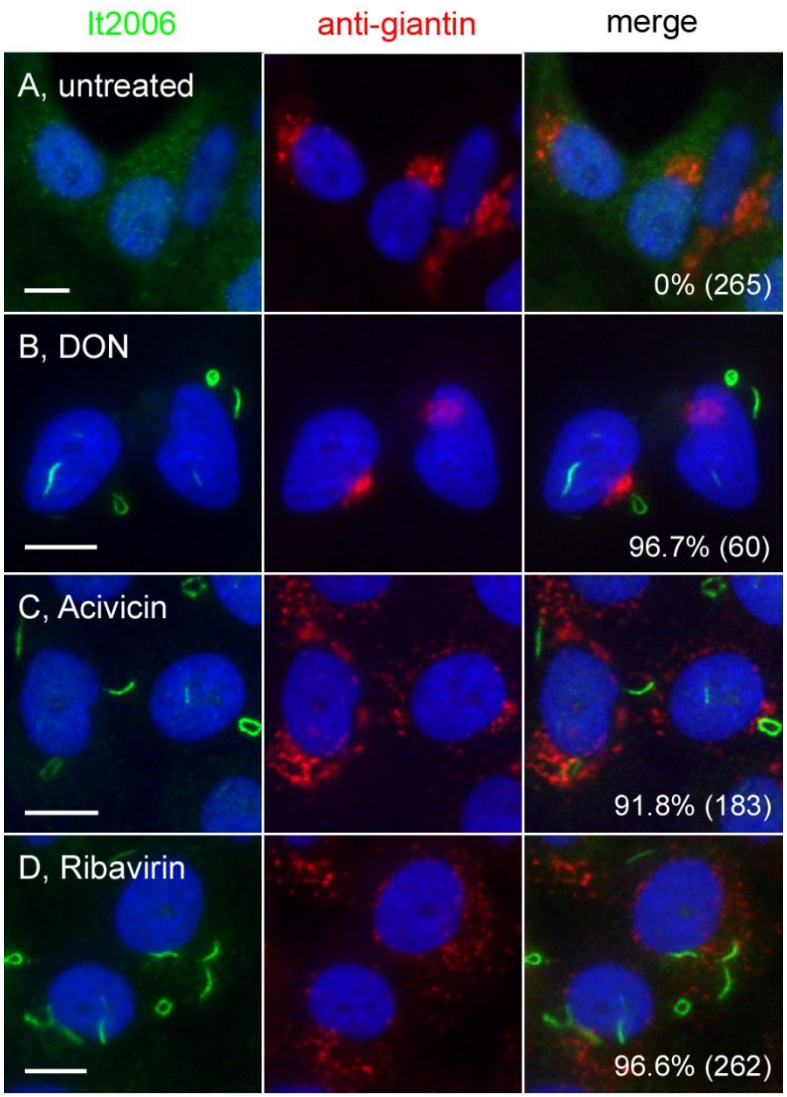

Figure 2-5. Inhibition of CTPS1- or IMPDH2-induced formation of rods and rings. Untreated HEp-2 cells A) and cells treated with inhibitors 2 mM DON (CTPS inhibitor, B), 2 mM acivicin (CTPS inhibitor, C), or 2 mM ribavirin (IMPDH2 inhibitor, D) for 24 h were co-stained with human anti-RR serum It2006 (green) and rabbit anti-giantin (red). Nuclei were counterstained with DAPI (blue). The percentage of cells with RR displayed for each experiment is shown in the lower right corner with the total number of cells counted indicated in parentheses. Bar, 10 μm.

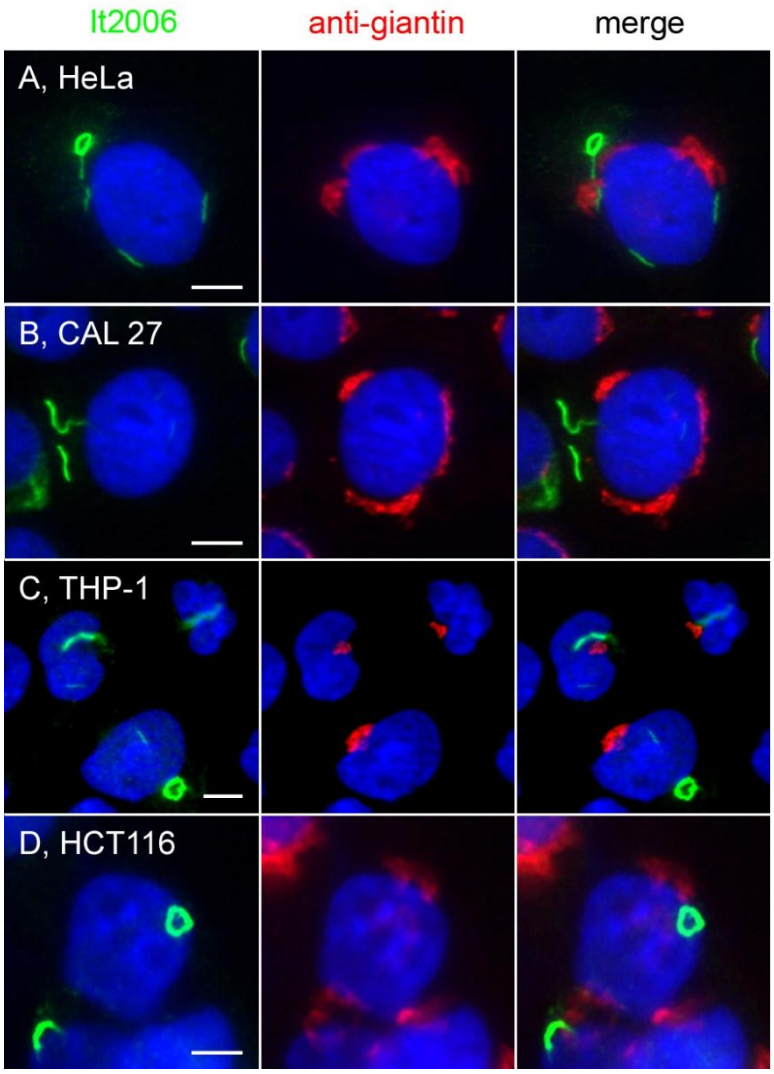

Figure 2-6. Inhibition of CTPS1-induced formation of RR in several human cancer cell lines. Induction of RR observed in human cancer cell lines HeLa A), CAL 27 B), THP-1 C), and HCT116 D) when treated with 2 mM DON in culture for 24 h, fixed, and co-stained with human anti-RR serum It2006 (green) and rabbit anti-giantin (red). Untreated controls showed few or no RR. Bar, 5 µm.

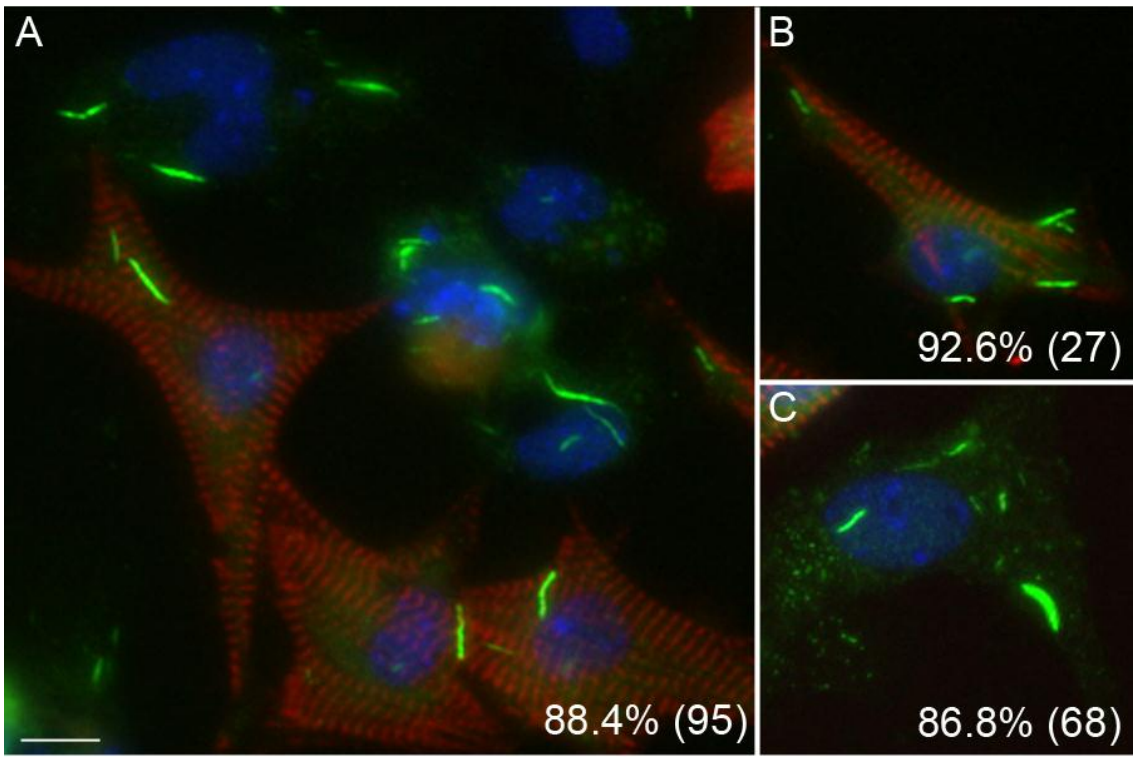

Figure 2-7. Inhibition of CTPS1-induced formation of RR in mouse primary cardiomyocytes, fibroblasts, and endothelial cells. Mouse primary cardiomyocytes preparation together with fibroblasts and endothelial cells, were treated with 2 mM DON and cultured for 24 h. Cells were co-stained with human anti-RR serum IT2006 (green) and mouse anti-actinin monoclonal antibody (red). Nuclei counterstained with DAPI (blue). Actinin-positive cardiomyocytes A, B, red) as well as actinin-negative fibroblast or endothelial cells A, C) all show distinct rods. The percentage of cells with RR displayed is shown in the lower right corner with the total number of cells counted indicated in parentheses A, all cells; B, actinin-positive cardiomyocytes only; C; actinin-negative fibroblast and endothelial cells). Bar, 10 µm.

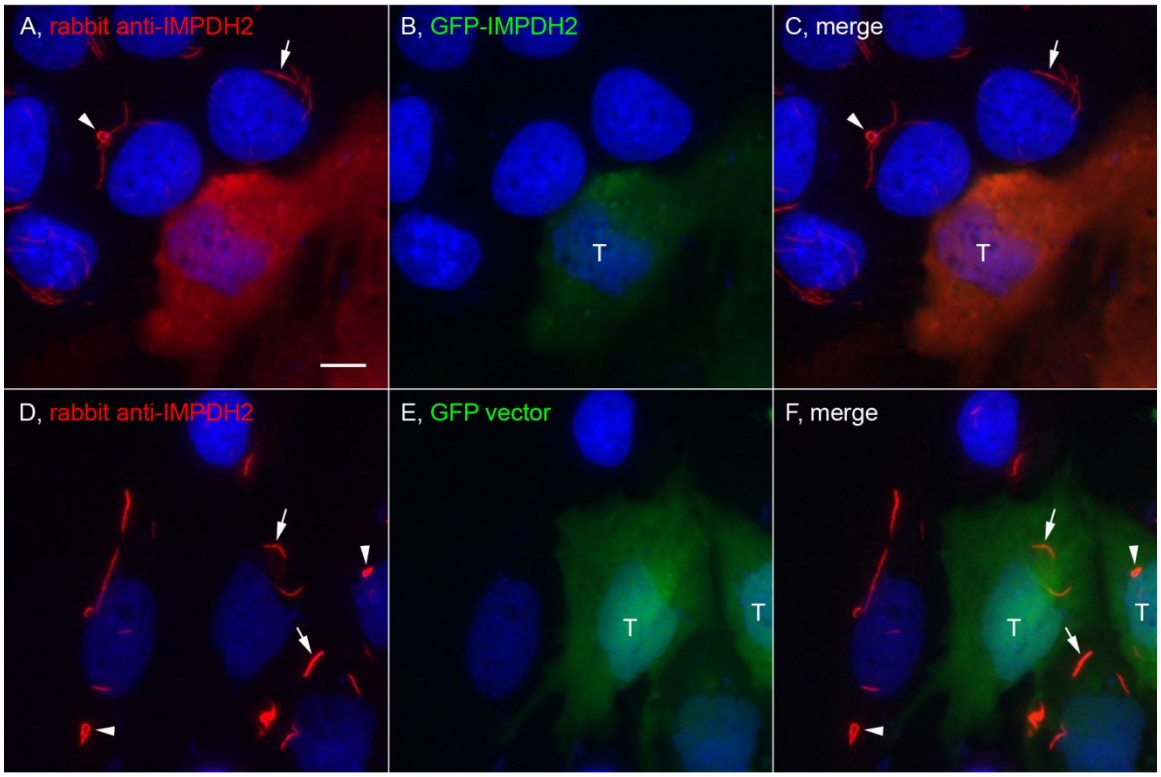

Figure 2-8. Overexpression of IMPDH2 prevented the induction of RR. HeLa cells were transfected with either GFP-IMPDH2 A-C) or GFP vector D-F) for 24 h and followed by 2 mM ribavirin incubation for 24 h. Cells were stained with rabbit anti-IMPDH2 (red) and counterstained with DAPI (Blue). GFP-IMPDH2 transfected cells (T) did not form RR while untransfected cells showed rods (arrows) and rings (arrowheads). RR were detected in both GFP vector transfected and untransfected cells. Nuclei Bar, 10 μm.

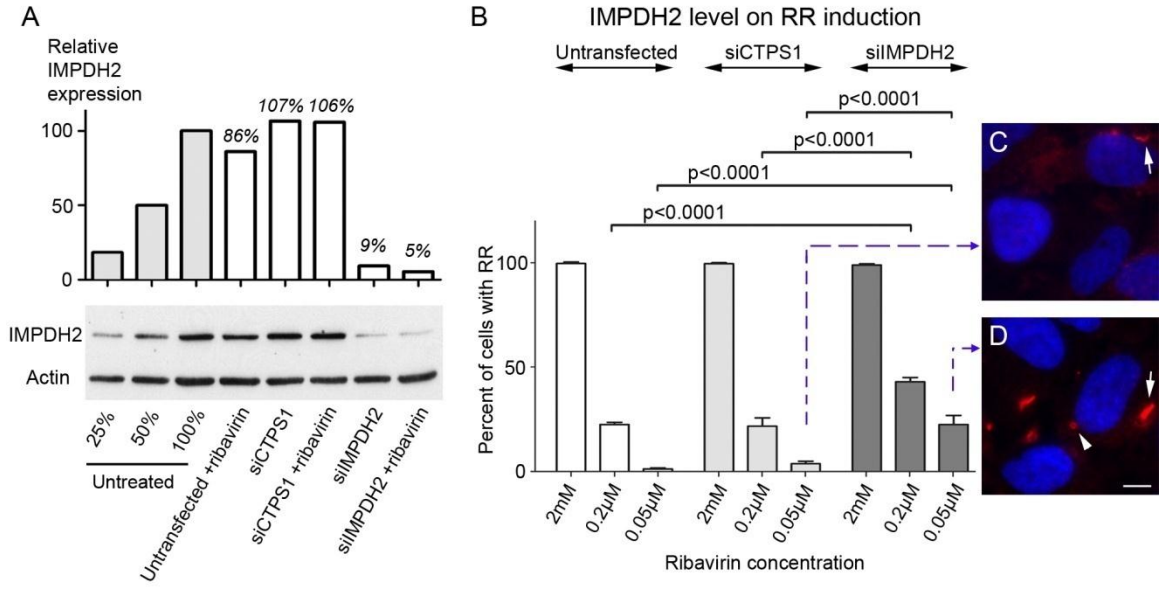

Figure 2-9. RR formation becomes increasingly sensitive to ribavirin when IMPDH protein level is reduced by specific siRNA knockdown. HeLa cells were either untransfected, transfected with siCTPS1, or siIMPDH2 for 44 h and followed by incubation of ribavirin at various concentrations for an additional 4 h. A) IMPDH2 expression was monitored by Western blot using rabbit anti-IMPDH2 antibody. Serial dilutions of untreated HeLa cell lysates (100%, 50%, and 25%) were used to help to comparatively quantitate the degree of protein knockdown. The level of actin was used as a loading control. Relative IMPDH2 protein levels were quantified using image J and normalized to the serial dilution standards. B) Percentage of cells with RR were quantified using Mayachitra Imago with a range of 131 to 298 cells counted per data point. Cells treated with siIMPDH2 had a significant increase in percentage of cells with RR at 0.2 μM and 0.05 μM of ribavirin analyzed by Fisher's exact test. C-D) Representative image of cells at the lowest concentration of ribavirin transfected with siCTPS1 or siIMPDH2. Arrows, rods; arrowhead, ring. Bar, 5 μm.

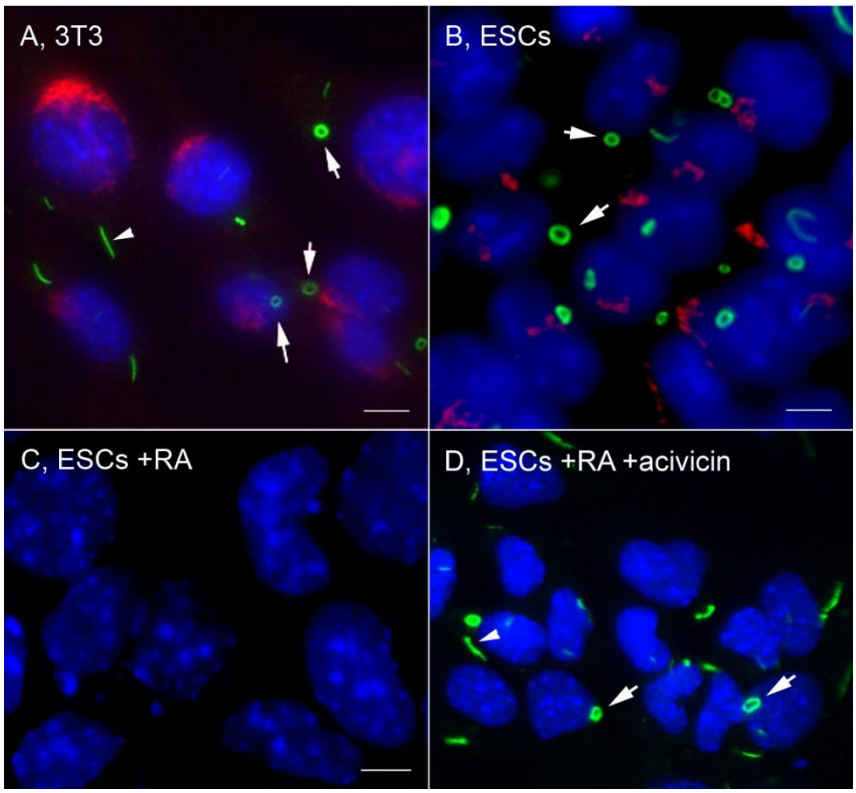

Figure 2-10. Uninduced mouse embryonic stem cells (ESCs) expressed predominantly cytoplasmic rings that were disassembled during retinoic acid (RA)-induced differentiation and reassembled when treated with acivicin. A) Mouse 3T3 cells for comparison shown with both rods (80-90%, arrowhead) and rings (10-20%, arrows). B) undifferentiated mouse ESCs shown with ~90% rings (arrows) and few rods. C) ESCs treated with RA for 4 days showed no RR. D) RR were induced in these RA-differentiated cells by treatment with 2 mM acivicin for 24 h. Cells were stained with human anti-RR serum It2006 (green, A-D) and co-stained with rabbit anti-giantin (red, A, B only). Nuclei counterstained with DAPI (blue). Bar, 5 μm.

Table 2-1. Dose- and time-dependent induction of RR using different CTPS1 and IMPDH2 inhibitors.

Concentration dependent induction of RR in HEp-2 cells after 24 h incubation by ribavirin, DON, and acivicin.

Drug concentration	Ribavirin	DON	Acivicin
2 mM	+++	+++	+++
1 mM	+++	+++	+++
0.5 mM	+++	+++	+++
0.25 mM	+++	++	+++
125 µM	+++	++	+++
62.5 µM	+++	++	+++
31.3 µM	+++	++	++
15.6 µM	+++	+	+
7.81 µM	+++	-	-
0.20 µM	+++	-	-

Differential time requirements for RR induction in HEp-2 cells treated with 2 mM of the respective compound.

Time after addition	Ribavirin	DON	Acivicin
30 min	+	-	-
1 h	+++	-	+
2 h	+++	+	++
3 h	+++	++	++
24 h	+++	+++	+++
48 h	+++	+++	+++

Legend indicates percent of cells with RR in (A) and (B): (-) = 0%, (+) = <25%, (++) = 50%, (+++) = >95%.

CHAPTER 3
CYTOPLASMIC RODS AND RINGS AUTOANTIBODIES DEVELOPED DURING PEGYLATED INTERFERON AND RIBAVIRIN THERAPY IN PATIENTS WITH CHRONIC HEPATITIS C

Background

Serum organ and non-organ specific autoantibodies are frequently detected in patients with chronic hepatitis C virus (HCV) infection, reflecting the wide spectrum of immune reactions associated with HCV (48,88-96). Experimental studies have in fact demonstrated the existence of an interaction between the HVR1-E2 region of the virus and CD81 receptors on the surface of B lymphocytes, which promotes B cell proliferation and activation, thereby stimulating antibody production (97,98). In addition, a significant homology motif between HCV polyproteins and tissue autoantigens has been postulated to suggest 'molecular mimicry' as a mechanism that may also play a role in priming specific autoantibodies in patients chronically infected by HCV (50,99-101). Finally, several clinical studies have reported deterioration of pre-existing autoimmune diseases in patients receiving interferon (IFN) therapy for hepatitis C, as well as *de novo* induction of autoimmune phenomena in HCV-infected patients on IFN-α monotherapy. In this setting, the most common phenomenon associated with IFN therapy is the *de novo* induction of serum tissue antibodies or boosting of the titer of pre-existing autoantibodies that in some patients, ends with the development of an autoimmune disease (102-111). The immune properties of IFN, at least in part, rely on its ability to enhance the expression of HLA class I and II antigens on cell membranes, promote T-cell activation and the subsequent release of cytokines, mechanisms that could account for the onset of autoimmune reactions during IFN therapy in patients with chronic hepatitis C (112).

To date, there is little data on autoimmunity in HCV patients being treated with the combination (PEG)-IFN plus ribavirin (RBV) (20,113,114). One main reason for this is that high titer of serum autoantibodies remains a widely accepted criteria against starting IFN therapy in patients with chronic hepatitis C, mainly as a consequence of the strict criteria of exclusion adopted in the design of registration trials rather than for the evidence of adverse reactions in practice. In other studies, the presence of tissue autoantibodies was associated with an increased risk of treatment failure (115-118).

We describe a novel autoantibody developed in patients with chronic hepatitis C during therapy with PEG-IFN and RBV that in immunofluorescence (IIF) studies appear like distinct rods and rings (RR) in the cytoplasm of HEp-2 cell slides, more commonly detected in patients who failed to respond to HCV therapy. In the present study, we determine the titer and prevalence of such anti-RR antibodies in HCV patients under treatment with PEG-IFN and RBV and its correlation with the outcome of treatment.

Methods

Patients

From 2004 to 2007, 156 previously untreated patients with chronic hepatitis C were consecutively treated with PEG-IFN/ RBV at the Liver Center, Istituto Clinico Humanitas, Rozzano, Italy. Seventy-five patients with sera available in our laboratory for autoantibody tests at baseline and during treatment were investigated. All subjects had histologically proven, compensated liver disease characterized by elevated serum alanine aminotransferase (ALT) activity, anti-HCV antibodies and serum HCV RNA for at least six months. Excluded were patients with autoimmune diseases, infection with the HBV or the HIV and with general contraindications to using either IFN or RBV (119). Patients were treated with subcutaneous injections of PEG-IFN-α2a (Pegasys;

Roche, Basel, Switzerland) 180 µg once weekly coupled with oral RBV (Copegus; Roche, Basel, Switzerland) at a dose of 1,000 mg per day for patients weighing 75 kg or less and 1,200 mg per day for those weighing more than 75 kg. All patients gave their written informed consent to receive therapy and permission for use of their medical records. HCV-1- and HCV-4- infected patients were treated for 48 weeks. HCV-2 and HCV-3 patients were treated for 24 weeks. Patients were classified as non-responders (NR) if HCV-RNA was still detectable at week 24 of therapy, as relapsers (REL) if HCV RNA was detected after the end of treatment in patients with a virological response, and as sustained virological responders (SVR) if HCV RNA was undetectable in the 24 weeks after the completion of therapy. As controls, sera were obtained from 105 primary biliary cirrhosis patients, 43 with primary sclerosing cholangitis, 56 with autoimmune hepatitis, 100 untreated HBV related chronic active hepatitis, 100 with hepatocellular carcinoma and 100 blood donors. This study meets and is in compliance with all ethical standards in medicine and information consent was obtained from all patients according to the Declaration of Helsinki.

Cell Culture and Indirect Immunofluorescence Studies

Different cell lines, such as normal human epidermoid larynx carcinoma HEp-2, human colon cancer cell line HCT116, human cervical cancer cell line HeLa, myelogenous leukaemia cell line K562, oral squamous cell carcinoma CAL 27 and rat kidney fibroblasts NRK, were cultured and prepared with multiple fixation methods that included acetone, -20°C, for 5 minutes, or 3% paraformaldehyde and 0.1% triton-X fixation as commonly used in many standard cell biology laboratories. For the induction of RR, RBV (Sigma-Aldrich, St Louis, MO, USA; R9644) was solubilized in water to a stock of 50 mM and was added to cultured cells seeded in monolayer at a final

concentration of 2 mM for 24 h. RR were detected using patient sera and anti-IMPDH2 antibodies (anti-inosine monophosphate dehydrogenase 2; Proteintech, Chicago, IL, USA; 12948-1-AP). Anti-nuclear (ANA), anti-smooth muscle (SMA), anti-mitochondrial (AMA) and anti-liver kidney microsomal (LKM) antibodies were detected by IIF at a serum dilution of 1:40 or higher in PBS and incubated for 45 min. using as substrates commercial HEp-2 (INOVA Diagnostics, San Diego, CA,USA) for ANA, whereas cryostat sections of rat kidney were used to detect SMA, AMA and LKM antibodies. Slides were then rinsed in PBS two times for 10 min. Goat anti-human-immunoglobulin G conjugated to fluorescein isothiocyanate (Cappel, ICN Biomedicals Inc., Aurora, Ohio) or Alexa 488 goat anti-human Ig (Invitrogen, Carlsbad, CA, USA) was used as secondary antibody diluted 1:100 in PBS and incubated on slides for 30 min. Slides were then rinsed again in PBS 2x for 10 min, mounted with cover slip and observed with a fluorescence microscope. IIF slides were read by a single investigator (GC) under standardized experimental conditions.

Statistical Analysis

The following 18 biological and clinical variables were analyzed for statistical significance: sex, age, ALT, aspartate transaminase, gamma-glutamyl transpeptidase, bilirubin level, prothrombin time, HCV genotype, HCV viremia level, presence of autoantibody at baseline (ANA, SMA, LKM and AMA), treatment outcome (long-term response and relapse/non response), steatosis, cirrhosis, diabetes mellitus and HCC development during post-treatment follow-up. Data are expressed as number and percentage or mean and range, unless otherwise stated. The differences between different groups were compared using Student’s t-test and Mann Whitney U test for continuous data; χ^2, and Fisher's exact test for categorical data as appropriate. A P-

value of <0.05 was considered to be statistically significant. All analysis where made with Stata10 (StataCorp. College Station, TX, USA).

Results

A total of 75 HCV infected patients were treated with standard of care PEG-IFN-α2a plus RBV regimens. Forty four patients (59%) were male, with a mean age of 49±11 years. Histological evidence of cirrhosis was present in 8 subjects (11%). The overall prevalence of serum autoantibodies at baseline was detected in 26 subjects (35%); the prevalence of ANA, SMA and anti-LKM-1 was 24, 8, and 3% respectively. None of the patients were AMA-positive. No patient met the criteria of probable or definite autoimmune hepatitis on the basis of the International Autoimmune Hepatitis Group score (120). Demographic, clinical and laboratory features of the patients are shown in Table 3-1.

The IIF study on HEp-2 cells substrate revealed the presence of antibodies reacting with a cytoplasmic structure in 15 patients (20%) with HCV who received PEG-IFN/RBV (Table 3-2). Human prototype serum It2006 recognized rods ranging approximately 3-10 μm in length and rings ranging approximately 2-5 μm diameter (Figure 3-1A). These cytoplasmic structures, here referred to as ‘rods and rings’ or RR, were found in more than 95% of HEp-2 cells. Usually there were only one to two RR per HEp-2 cell. Rods may align either close to the nuclear envelope (Figure 3-1C) or extend perpendicularly from the nucleus (Figure 3-1B), while rings are found in low frequency (approximately 10% of all cells) only in the cytoplasm (Figure 3-1D).

Colocalization experiments with known markers showed no association with any known cytoplasmic organelles, including Golgi complex, mitochondria, centrosomes, and GW bodies which are cytoplasmic foci known to mediate gene expression via the

small RNA-guided translation silencing process (121,122). Table 3-2 summarizes the relevant clinical features of the 15 patients who tested positive for anti-RR. Interestingly, anti-RR autoantibodies were found in the sera collected in HCV patients during PEG-IFN-α2a plus RBV treatment only (15/75, 20%) whereas it was never detected before antiviral therapy (0/75) or in any of the control groups listed in Methods.

Although the INOVA HEp-2 cell substrate was consistently positive (>95% of cells) for RR structures, home grown HEp-2 cells using standard conditions were mainly negative. In fact, among the few commercial ANA slides tested, none other than the INOVA slides showed >1% cells with RR, making these other products extremely difficult for the accurate detection of anti-RR. Preliminary experiments were performed to determine whether IFN or RBV treatment would induce the formation of RR in *in vitro* culture. Several attempts of IFN treatment in HEp-2 or HeLa cells did not yield expression of RR when treated cells were stained by prototype anti-RR serum It2006. In contrast, RBV treatment readily induced RR formation. Figure 3-2A shows HEp-2 cells that were untreated gave primarily diffuse cytoplasmic staining and no detection of RR; however after treating cells with 2 mM of RBV for 24 h, RBV appeared to induce the aggregation of the protein into RR (Figure 3-2B). Furthermore, different cell lines such as normal rat kidney fibroblasts NRK or immortalized human cancer cell line such as HCT116, HeLa, K562, CAL 27 have been examined after RBV treatment and RR were induced in all cells stained with anti-RR positive sera (122). Thus, current data suggest that the RR staining pattern is not unique to HEp-2 cells but also detected in various immortalized human cell lines and also in cells derived from rodents.

The prevalence of anti-RR antibody is significantly higher in non-responders/relapsers (10/30, 33%) than in responder patients (5/45, 11%; Fisher p-value= 0.037; Table 1). In other words, the prevalence of REL/NR in anti-RR-positive group (10/15=67%) is higher than that of anti-RR-negative group (20/60=33%; Fisher P=0.037). Interestingly, seven anti-RR positive patients had HCV genotype 2a/2c or 3 (five genotype 2 and two genotype 3); of those seven easy to cure patients, three were non-responders or relapsers. None of the anti-RR positive patients had cirrhosis.

Discussion

This study describes a novel serum antibody (anti-RR) reacting against a cytoplasmic structure that can be detected by IIF using HEp-2 cells as substrate in HCV patients treated with PEG-IFN-α2a plus RBV. The overall prevalence of anti-RR antibodies was 20% of HCV treated patients. RRs are the first autoantigen described in literature arising during this treatment. In fact, only few drugs are reported in hepatology to induce autoantibodies to cytoplasmic antigens but all of them are organ-specific like anti-LKM-2 (123), anti-gastric parietal cells (106), anti-thyroid (91,124), anti-pancreatic islet cells (107), anti-glutamic acid decarboxylase (111) and anti-adrenal cortex (107). Interestingly, anti-RR antibodies were detected in PEG-IFN/RBV-treated patients only. In fact, baseline sera of HCV patients and of controls did not show any reactivity for anti-RR antibodies, thus suggesting an important role of PEG-IFN/RBV in triggering RR seroconversion.

Although INOVA HEp-2 cells express RR and are suitable for the detection of anti-RR antibodies, a few other pre-made HEp-2 slides marketed for ANA testing are negative for RR staining using the same prototype serum and other anti-RR positive sera (data not shown). Our novel data show that many cell lines treated with RBV *in*

vitro induced the formation of RR (Figure 3-2B); the induction led to greater than 95% of the cells to expressing RR compared to untreated cells not expressing RR. Induction of RR could happen also *in vivo* in human hepatocytes during antiviral therapy and these changes may induce the immune system resulting in the production of anti-RR.

In general, the most common autoantibody encountered in HCV- treated patients is ANA. Even if all published studies describe only fluorescence ANA patterns without focusing on their identity, it is reasonable to think that their specificities are heterogeneous like in HCC (96) being directed against different nuclear antigens, suggesting a nonspecific reaction of the immune system to nuclear antigens (114,125). By contrast, the production of anti-RR antibodies in HCV sera is quite different than ANA. In fact, the most important difference is that ANA appears independently from HCV therapy although anti-RR develop only during treatment and are apparently directed exclusively against a single antigenic structure; thus, anti-RR appears to mimic reactivity of serum autoantibodies which develop in the course of systemic autoimmune disease where each disease is associated with a specific profile of autoantibody specificities (1,2). For example, systemic lupus erythematosus is characterized by a high prevalence of ANA directed to the same structures such as DNA and spliceosomal proteins. In this context, the high prevalence of anti-RR antibodies that react to the same cytoplasm structure suggests their direct biological role in HCV treated patients. This hypothesis is supported by our data in which anti-RR positivity seems to alter antiviral response with significantly higher prevalence of anti-RR in non-responders/relapsers than sustained responders (33% versus 11%; P-value = 0.037). This evidence is further enhanced in HCV genotype 2 and 3 patients where

approximately half of anti-RR positive patients failed to respond to therapy, further suggesting a correlation between anti-RR antibodies and response to antiviral therapy.

In our recent study (122), at least one autoantigen recognized by the prototype anti-RR is the enzyme inosine monophosphate dehydrogenase 2 (IMPDH2), which catalyses the oxidation of inosine monophosphate to xanthosine monophosphate in the rate-limiting step in the *de novo* guanine synthetic pathway responsible for the GTP production. It is intriguing that IMPDH2 is the enzyme known to be inhibited by RBV *in vitro* and at the same time RBV induced the formation of RR in all cell lines examined to date, including primary mouse cells such as fibroblasts and endothelial cells. We speculate that RR can also form *in vivo* in the hepatocytes during RBV treatment; in some predisposed patients, IMPDH2 condensation into RR may induce the immune system to develop antibodies. This observation is extremely important also for immunologists to understand the development of drug-induced autoantibodies; in fact, this is the first study that elucidates a mechanistic action of a drug to induce autoantibodies through a topographic rearrangement of cytoplasmic proteins. As this is a retrospective study, our sera were collected at different times after starting treatment. For this reason we are not able to determinate the kinetics of rising anti-RR and we do not know whether these autoantibodies disappear after the end of therapy. With all the caveats of the limited sample size of the present study, one could speculate that anti-RR reflect an immune reactivity to cytoplasmic structure of the liver cells that interact with IFN/RBV therapy. Our current observations in HCV patients undergoing antiviral therapy need to be expanded to clarify the association between anti-RR and response to treatment.

This work was published: Covini G., Carcamo W.C., Bredi E., von Mühlen C.A., Colombo M., and Chan E.K. (2011) Cytoplasmic rods and rings autoantibodies developed during pegylated interferon and ribavirin therapy in patients with chronic hepatitis C. Antivir Ther. In Press.

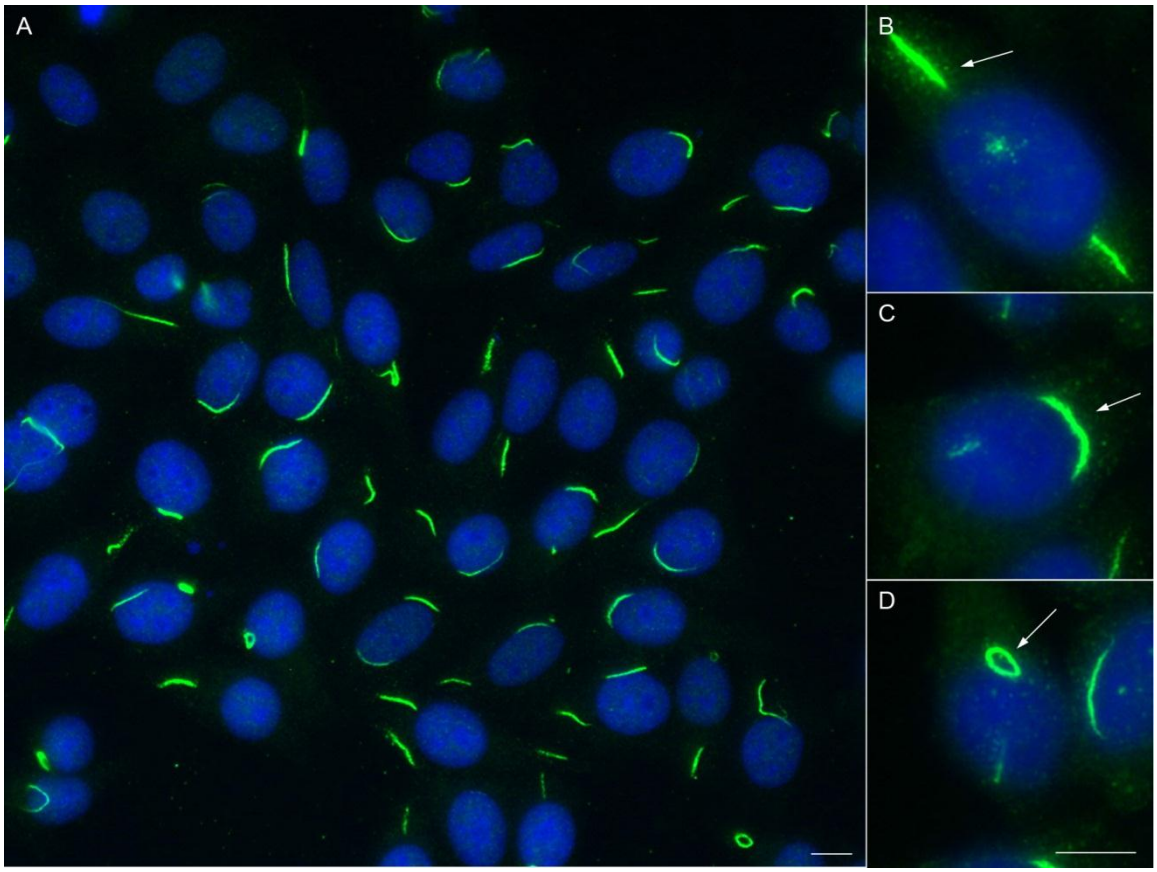

Figure 3-1. Cytoplasmic rods and rings structure stained by sera from HCV patients. INOVA HEp-2 cells stained with human anti-rods and rings (RR) serum It2006/Alexa 488 goat anti-human-immunoglobulin G (green). Nuclei were counterstained with DAPI (blue). Arrows indicate rods or rings. A) 20x magnification of HEp-2 cells; B) HEp-2 cell with rod perpendicular to the nucleus; C) HEp-2 cell with rod adjacent to the nucleus; D) HEp-2 cell with ring in cytoplasm. Scale bar 10 µM.

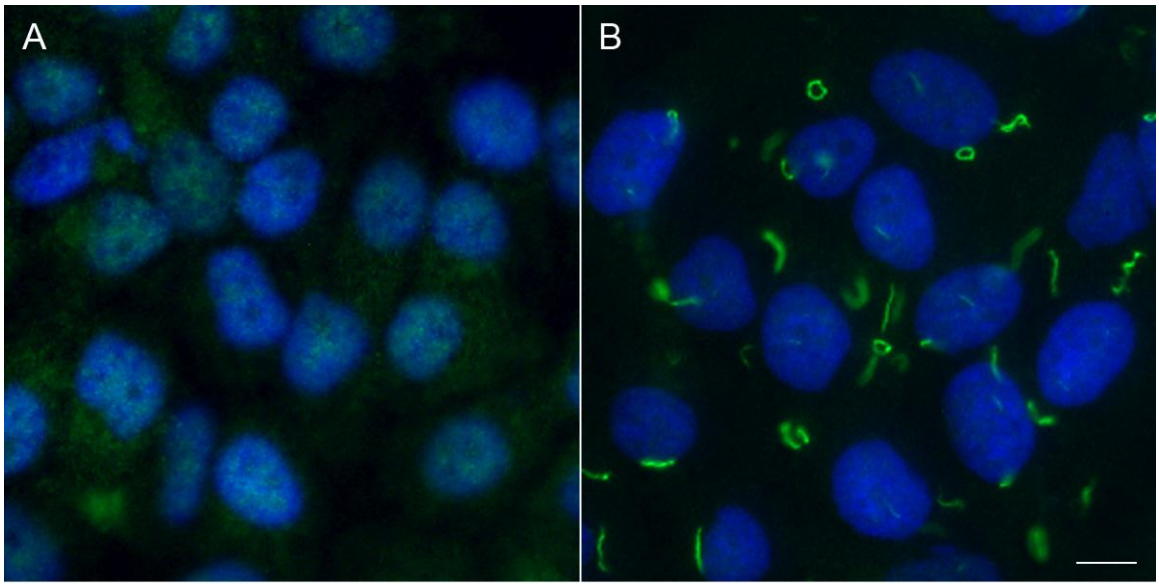

Figure 3-2. Rod and ring structure can be induced with ribavirin. HEp-2 cells were stained with human anti-rods and rings (RR) serum It2006/Alexa 488 goat anti-human -immunoglobulin G (green). HEp-2 cells are shown A) untreated or B) treated with 2 mM of ribavirin for 24 h. Nuclei were counterstained with DAPI (blue). Scale bar 10 µM. A) shows HEP-2 cells that were untreated gave primarily diffuse cytoplasmic staining and no detection of RR, however B) after treating cells with 2 mM of ribavirin for 24 h, ribavirin appeared to induce the aggregation of the protein into RR.

Table 3-1. Clinical, serological and immunological features of the patients at baseline, and response to treatment.

Parameters	Total Patients (n = 75)	Patients with RR Ab (n = 15)	Patients without RR Ab (n = 60)	*P* value
Patients, no.				
Male	44 (59)	9 (60)	35 (58)	NS
Female	31 (41)	6 (40)	25 (42)	
Age, years	49 ± 11	48 ± 11	49 ± 12	NS
ALT, UI/L	112 (23-408)	123 (32-408)	110 (23-389)	NS
Genotype *				NS
HCV-RNA **				NS
ANA, no.	18 (24)	4 (27)	14 (23)	NS
ASMA, no.	6 (8)	3 (20)	3 (5)	NS
LKM, no.	2 (3)	1 (7)	1 (2)	NS
AMA, no.	0 (0)	0 (0)	0 (0)	NS
Steatosis,	16 (21)	2 (13)	14 (23)	NS
Cirrhosis, no.	8 (11)	0 (0)	8 (13)	NS
Diabetes, no.	5 (7)	0 (0)	5 (8)	NS
Treatment out come				
SVR	45 (60)	5 (33)	40 (67)	0.037
REL / NR	30 (40)	10 (67)	20 (33)	

Values presented as n (%) unless otherwise indicated.

* Patients were classified according to their genotype, but no statistical correlation was found among the two groups.

** Patients' viremia at the baseline were stratified as <400.000 UI/L, 400000-800000 UI/L, >800000 UI/L. These findings were not statistically relevant. Ab, antibody; ALT, alanine aminotransferase; AMA, anti-mitochondrial antibody; ANA, anti-nuclear antibody; ASMA, anti-smooth muscle antibody; LKM, anti-liver kidney microsomal; NS, Not statistically significant (P > 0.05); REL / NR, Relapsers / Non Responders; RR, rods and rings; SVR, Sustained Virological Response.

Table 3-2. Clinical and laboratory characteristics of the 15 patients who seroconverted to RR antigen during pegylated IFN α2a/ribavirin therapy.

Patients	Sex	Age	Genotype	HCV-RNA IU/L x 105	SVR	ANA	ASMA	AMA	LKM	anti-RR titer
1	M	59	1a	0,3	Yes	Neg	Neg	Neg	Neg	1:320
2	M	46	1b	4,0	No	Neg	Neg	Neg	Neg	> 1:320
3	F	55	2a/2c	3,0	No	1:160*	Neg	Neg	Neg	1:160
4	F	44	3a	7,0	No	Neg	Neg	Neg	Neg	1:320
5	F	45	3a	6,0	Yes	Neg	1:160**	Neg	Neg	1:320
6	M	41	2a/2c	7,0	Yes	Neg	Neg	Neg	Neg	1:160
7	F	58	1b	5,7	No	1:160*	Neg	Neg	Neg	1:320
8	M	36	1b	7,0	No	Neg	Neg	Neg	Neg	> 1:320
9	M	41	1b	3,0	No	Neg	1:160**	Neg	Neg	1:160
10	M	56	1b	7,0	No	1:80*	Neg	Neg	Neg	> 1:320
11	M	42	1b	6,0	No	Neg	Neg	Neg	Neg	1:160
12	F	55	2a/2c	7,0	Yes	Neg	1:160**	Neg	Neg	1:320
13	F	60	1b	7,0	No	Neg	Neg	Neg	Neg	> 1:320
14	M	47	2a/2c	6,0	No	Neg	Neg	Neg	Neg	> 1:320
15	M	17	2a/2c	3,5	Yes	1:160*	Neg	Neg	1:160	> 1:320

*Speckled.

**Vessel smooth muscle antibody. AMA, anti-mitochondrial antibody; ANA, anti-nuclear antibody; ASMA, anti-smooth muscle antibody; F, female; LKM, antiliver kidney microsomal; M, male; Neg, negative; RR, rods and rings; SVR, sustained virological responder.

CHAPTER 4
DIFFERENTIAL AUTOREACTIVITY TO IMPDH2 IN ANTI-RODS/RINGS ANTIBODIES: CLUES TO UNRESPONSIVENESS TO INTERFERON-ALPHA/RIBAVIRIN THERAPY IN US AND ITALIAN HCV PATIENTS

Background

Hepatitis C virus (HCV) is an enveloped positive single-stranded RNA virus classified in the genus *Hepacivirus* of the family *Flaviviridae* (126). It was identified in 1989 and is a major cause of chronic liver disease, frequently leading to liver cirrhosis and eventually to hepatocellular carcinoma (14,26,127). An estimated 170 million people are infected worldwide and there is no vaccine available for this viral infection (128). The virus genome encodes a polyprotein of approximately 3000 amino acids that is flanked by 5′ and 3′ non-coding regions (129,130). Translation of the polyprotein is mediated by an internal ribosome entry site embedded within the 5′ non-coding regions, and the individual viral proteins are produced upon cleavage of the polyprotein by host and viral proteases. These include three structural proteins (core, E1, and E2), the p7 protein and six non-structural proteins (NS2, NS3, NS4A, NS4B, NS5A, and NS5B), which are involved in virion assembly and viral RNA replication (129,130). The virus is classified into eleven different genotypes and more than a hundred subtypes, and it also manifests itself in sera or tissues of patients with the appearance of quasi species (25,131). The current treatment of HCV is a combination of pegylated-interferon alpha (IFN-α) and ribavirin (RBV, IFN/R). Although the addition of RBV to the IFN treatment has significantly improved the outcomes, only half of patients infected with HCV respond to therapy (132). For the ultimate goal in treatment is to achieve a sustained virological response (SVR; defined as undetectable HCV RNA for at least 24 weeks post-therapy), new drugs have been approved for the treatment of HCV (133).

Patients with HCV may also develop aberrant immunological alterations, such as autoantibody production, autoimmune thyroid disorders, B cell lymphomas, and mixed cryoglobulinemia (134-136). HCV patients can produce non-organ specific autoantibodies such as anti-nuclear antibodies (ANA), anti-smooth muscle antibodies and anti-LKM1 antibodies, with much higher prevalence than healthy people (48,89). Since HCV enters hepatocytes through binding of its envelope protein E2 with CD81, also expressed in B-lymphocytes, Pileri *et al.* proposed that HCV binding to B-lymphocytes lowers the B cell activation threshold and therefore facilitates the production of autoantibodies (97). Autoantibodies are commonly used for diagnosis of certain autoimmune conditions such as systemic lupus erythematosus, scleroderma, and polymyositis (2,137), but data on the association of autoantibodies to the clinical and biochemical profile of chronic HCV hepatitis or response to treatment are still controversial (88,116,138).

A novel autoantibody that recognizes distinct cytoplasmic rods and rings (RR) structures was first identified in sera of HCV patients that were screened using commercial ANA slides (122). Localization of two specific enzymes, inosine monophosphate dehydrogenase 2 (IMPDH2) and cytidine triphosphate synthetase (CTPS1), to these structures was identified in our previous study (122). RR were induced in cultured cancer cells when exposed to IMPDH2 inhibitors RBV or acivicin, or CTPS1 inhibitor 6-diazo-5-oxo-L-norleucine (DON) (122). Anti-RR antibodies were specific to HCV patients treated with IFN-α and RBV but not prior to treatment (139). The aim of the present study is to identify the clinical significance of anti-RR autoantibodies developed during IFN/R therapy in HCV infected patients.

Materials and Methods

Human Sera and Autoantibodies

One patient cohort consists of patients from the University of Florida (US), where samples (n=2000) were obtained from the Department of Pathology and tested for anti-RR antibodies via indirect immunofluorescence (IIF) using HEp-2 slides (INOVA Diagnostics, San Diego, CA). US patients were classified as non-responders (NR) or sustained virological response (SVR) according to the following criteria: NR show no decrease in viral load after completion of 24 months of treatment, while SVR have no viral RNA detection 6 months after completion of treatment. The second cohort consists of 48 sera prescreened positive for anti-RR from an Italian cohort, obtained from three hospital clinics in north-eastern Italy. Serum samples were selected among patients with HCV infection and those that displayed a positive anti-RR pattern on HEp-2 cells. These samples were screened by IIF again for the presence of anti-RR antibodies using HEp-2 slides as described in the next paragraph, and 46 were confirmed as positive. Italian patients were classified as NR or SVR and an additional category of relapsers was included, to indicate previously SVR patients who tested positive for HCV RNA after 6 months of IFN/R treatment.

Indirect Immunofluorescence (IIF)

IIF analysis of autoantibodies in human sera was performed as described, using commercial HEp-2 ANA slides (INOVA Diagnostics, San Diego, CA) (122). To determine anti-RR titer, samples were 2 fold serially diluted in PBS containing 0.1% bovine serum albumin, with a starting dilution of 1:50 and ending dilution of 1:819,200. Titer analysis for anti-RR was determined by two readers (WCC and SJC) and endpoint titer was defined by more than 50% of cells with detectable RR staining. Fluorescent

images were captured with a Zeiss Axiovert 200M microscope fitted with a Zeiss AxioCam MRm camera using a 40x (0.75 NA) objective. The majority of anti-RR positive samples had titer below 1:100,000. Titers over 1:100,000 were determined with the aid of a Zeiss AxioCam MRm camera.

Immunoprecipitation (IP)

IP of lysate from [^{35}S]-methionine-labeled K562 cells for the analysis of the proteins recognized by human autoimmune sera was performed as previously described (67,122).

Statistical Analysis

The statistical analysis was performed using the GraphPad Prism 5 software for Windows (La Jolla, CA). The one-way analysis of variance (ANOVA), student's *T*-test, Mann-Whitney Test, Fisher's exact test or regression analysis were performed. A p value of < 0.05 was considered statistically significant.

Results and Discussion

Autoantibodies to Cytoplasmic Rods and Rings in the US and Italian Cohorts

HCV patients from both US and Italian cohorts were confirmed to have antibodies to rods and rings using INOVA HEp-2 slides at 1:50 dilution of sera. IIF staining of HEp-2 cells typically showed 1 to 2 distinct cytoplasmic rods (~3-10 μm in length) and/or rings (2-5 μm diameter, Figure 1A). Both US and Italian patients recognize the same RR as determined by costaining using a rabbit anti-IMPDH2 antibody (data not shown). It was previously demonstrated that IMPDH2 is a component of RR and rabbit anti-IMPDH2 antibodies costain RR detected by sera of HCV patients (122). This confirms that the structures recognized by Italian and US patients are the same. Determination of the ultrahigh anti-RR titers was accomplished with the aid of the Zeiss AxioCam

camera, otherwise RR were visualized by eye at titers as high as 1:102,400. Figure 1 A-C shows representative anti-RR staining from HCV patient with titer at 1:400, 1:102,400, and 1:819,200, respectively. The highest dilution used was 1:819,200, and three patients in each cohort had titers higher than this upper limit. The US cohort had titers that ranged from 1:50 to >1:819,200 with a median titer of 1:1,200, while the Italian cohort had titers that ranged from 1:200 to >1:819,200 with a median titer of 1:25,600 (Figure 1D). In the Italian cohort, a total of 18 females and 28 males had anti-RR. Although the anti-RR titer was slightly higher in females it was not significantly different when compared to anti-RR titer in males. However, IMPDH2 IP intensity was significantly higher in females versus males ($p=0.049$). In the Italian cohort, the age range was 36-75 years with a median of 59.5. It is unclear why there is a big difference in the median titers between the two cohorts.

Prevalence of Anti-IMPDH2 Antibody by IP

It was previously shown that IMPDH2 is a component of RR and some anti-RR recognize IMPDH2 as autoantigen (122) although the prevalence of anti-IMPDH2 has not been determined. Therefore, sera from the two cohorts were tested by IP for the prevalence of anti-55kDa IMPDH2. Figure 2 shows representative IP of ^{35}S-methionine labeled K562 cell lysate using selected patients from both US and Italian cohorts. Not all patients immunoprecipitated IMPDH2 (arrow in Figure 2A,B). In the Italian cohort, 44 anti-RR positive patients (96%) immunoprecipitated IMPDH2 and only 2 patients with anti-RR antibodies did not have the 55kDa band, previously shown to be IMPDH2 (122). In addition, none of the patients without anti-RR antibodies immunoprecipitated the IMPDH2 band (data not shown). However, in the US cohort, only 25 anti-RR positive patients (53%) had the IMPDH2 band, while the other 22 anti-RR-positive patients did

not immunoprecipitate the IMPDH2 band. Other antigens recognized by sera that are anti-IMPDH2 negative but anti-RR positive remain yet to be identified. Figure 2C shows the number of patients who were classified by IMPDH2 band intensity from 0 to 4 (weakest to strongest). Patients in the Italian cohort immunoprecipitate IMPDH2 with stronger intensity compared to patients in the US cohort. This difference may be due to the heterogeneity of the patients in the US cohort versus the Italian cohort; IMPDH2 is the predominant RR autoantigen in the Italian cohort while the US cohort develops anti-RR antibodies that may recognize additional components apart from IMPDH2, such as CTPS1, a previously identified component of RR, or other unknown components.

Comparison of IIF Titer Versus Anti-IMPDH2 IP

Anti-RR titer evaluated by IIF was correlated to the intensity of the IMPDH2 band in IP for both cohorts (Figure 3). Patients in the US and Italian cohort with higher anti-RR titers immunoprecipitated the IMPDH2 bands with higher intensity ($p < 0.0001$ and 0.0034, respectively). This strong correlation validates the finding that anti-55kDa IMPDH2 is the predominant autoantibody in the anti-RR response in these patients. This is clearly true in the Italian cohort with 96% anti-RR positive for the 55kDa IMPDH2 band. It is interesting that a significantly lower percent is seen in the US cohort. It remains to be determined what is the autoantigenic component(s) undetected in IP with those 47% who are negative for anti-IMPDH2.

Correlation of Anti-RR/IMPDH2 Prevalence and Titer with Therapeutic Outcome

The aim of our study was to determine whether the production and titer of anti-RR antibodies are different between US versus Italian patients and whether they are associated with the response to IFN/R therapy. A correlation was observed between anti-RR titers and response to treatment in the US cohort, and in fact patients classified

as NR had significantly higher anti-RR titers compared to SVR (mean=1:3,000 vs 1:100; p=0.0016, Fig. 4A). Patients in the Italian cohort were classified into three categories (Fig. 4B) and NR patients had lower titers than SVR, while relapsers had significantly higher titer when compared to NR and SVR (p=0.0040 and p=0.015, respectively, Fig. 4B). When the intensity of the IMPDH2 band was compared between NR versus SVR in the US cohort, 8 out of 9 patients with strong (3+4+) IP band intensity were non-responders (Fig. 4C). For patients in the Italian cohort, relapsers had a significantly stronger 55 kDa band IP intensity compared to SVR (p = 0.031) or NR (p = 0.016) patients (Fig. 4D).

The differences between the two cohorts could be due to the heterogeneity of the patients and to the different classification of patients for the US cohort (divided into two main groups, NR and SVR) and for the Italian cohort (divided instead in 3 groups: NR, SVR and relapsers). Covini *et al.* demonstrated that anti-RR antibodies were specific to HCV patients that had received the IFN/R therapy, and anti-RR antibodies were more often detected in non-responders/relapsers than in responder patients (33% vs 11%, p=0.037) (139). Although they observed the difference in prevalence of anti-RR antibodies, they did not examine anti-RR titers. An additional recent study by Seelig *et al*. on anti-RR antibodies did not examine correlations of antibodies with clinical and therapeutical response (140). The mechanism for the production of anti-RR antibodies remains unknown but we speculate that a subset of patients develop anti-RR antibodies due to exposure of turnover of RR structures induced by RBV during IFN/R therapy. Pileri *et al*. proposed that HCV binds to CD81 on B-lymphocytes through its envelope protein E2, thus lowering the activation threshold on the B cells and facilitating the

production of autoantibodies (97). B cell activation in addition to RR formation by ribavirin may play a role in the development of anti-RR antibodies.

Conclusions

Our results show for the first time that anti-RR antibody titer has a strong correlation to treatment response from two independent HCV patient cohorts in the US and Italy. Interestingly, in the Italian cohort 96% of anti-RR sera identified by IIF immunoprecipitate the IMPDH2 band, whereas in the US cohort, only 53% anti-RR positive by IIF showed the IMPDH2 IP band. Patients with high titer anti-RR antibodies tend to be non-responders or relapsers. Future studies are needed to examine the environmental or genetic element(s) that might contribute to the formation of anti-RR against IMPDH2, and their potential application in HCV follow-up.

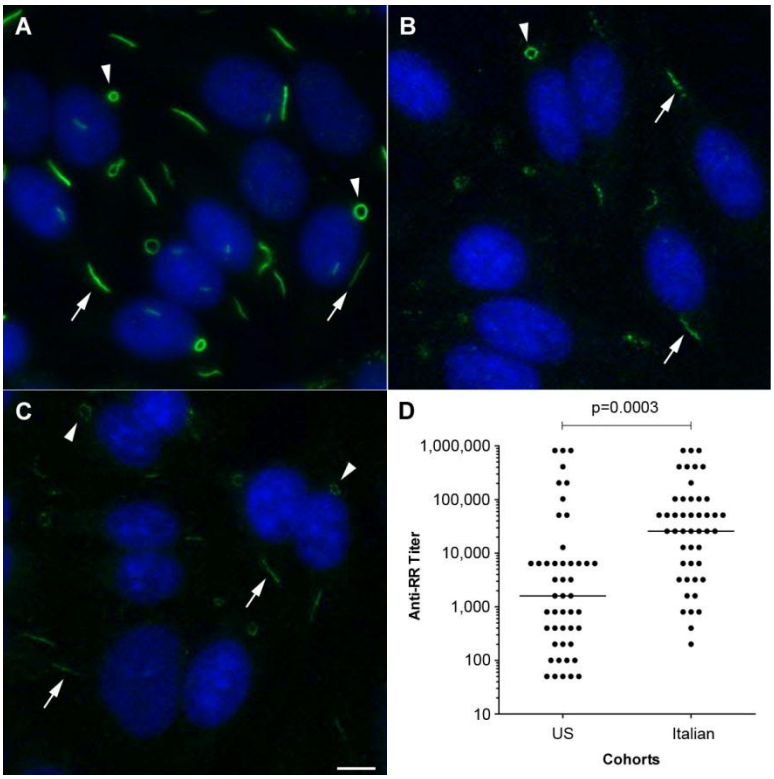

Figure 4-1. Antibody titer determined in two cohorts of HCV patients with autoantibodies to cytoplasmic structures called “rods and rings”. HEp-2 ANA slide stained with HCV patient sera at various dilutions. Representative images of rods and rings (RR, green) from sera diluted at 1:400 A), 1:102,400 B), and 1:819,200 C) dilution. Nuclei were counterstained with DAPI (blue). Scale bar, 10 µm. D) Anti-RR titers of US and Italian cohorts determined using 2 fold dilution of sera on HEp-2 ANA slides. Each dot represents a single positive anti-RR patient; patients that were negative for anti-RR antibodies are not represented.

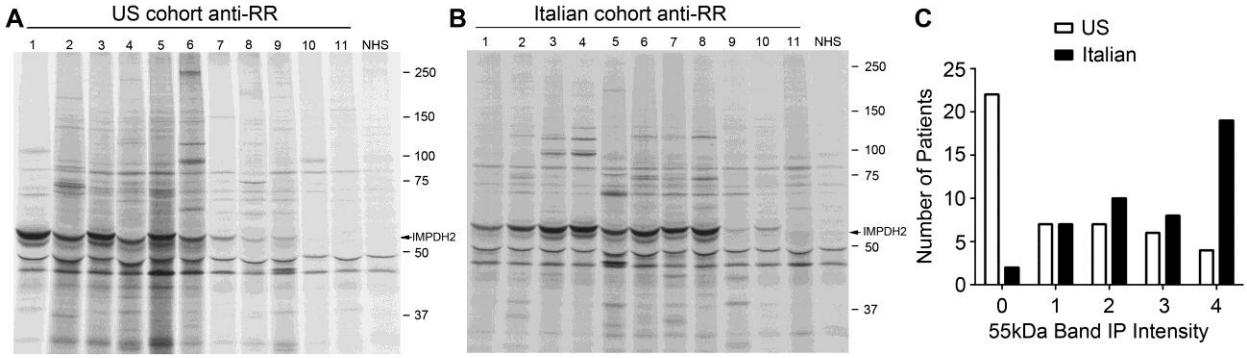

Figure 4-2. Prevalence of anti-55kDa IMPDH2 in immunoprecipitation analysis of anti-RR positive sera. Immunoprecipitation of ^{35}S-methionine labeled K562 cell extract was performed with all anti-RR positive patient sera from A) US and B) Italian cohorts. Numbers correspond to individual samples. The 55kDa band corresponding to IMPDH2 is indicated by arrows. C) Semi-quantitative analysis of all patients from both cohorts, measuring the intensity of the 55kDa band detected in IP using a scale from 0 (negative) to 4 (strongest). NHS, normal human serum.

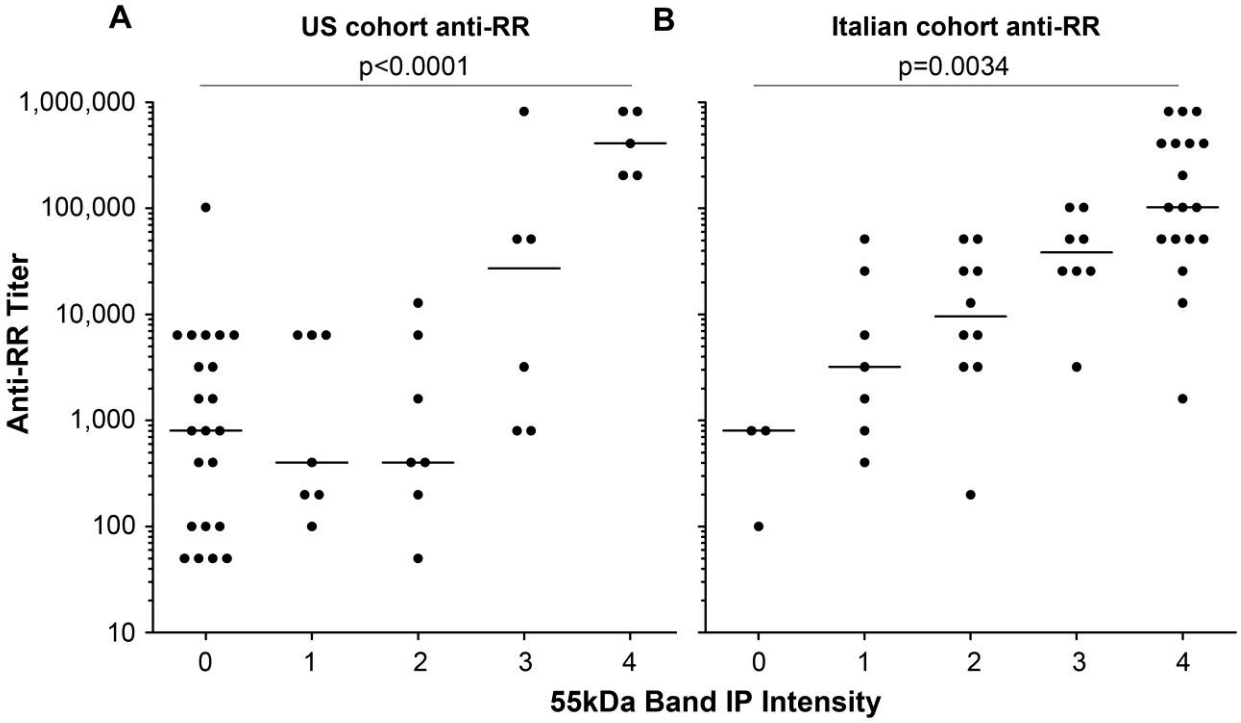

Figure 4-3. Correlation of anti-RR IIF titer and anti-55kDa IMPDH2 IP intensity. The intensity of the 55kDa IP band was correlated to anti-RR titer for each patient, as shown in A) for the US cohort and B) for the Italian cohort. Each dot represents one individual. Lines in each graph correspond to the median.

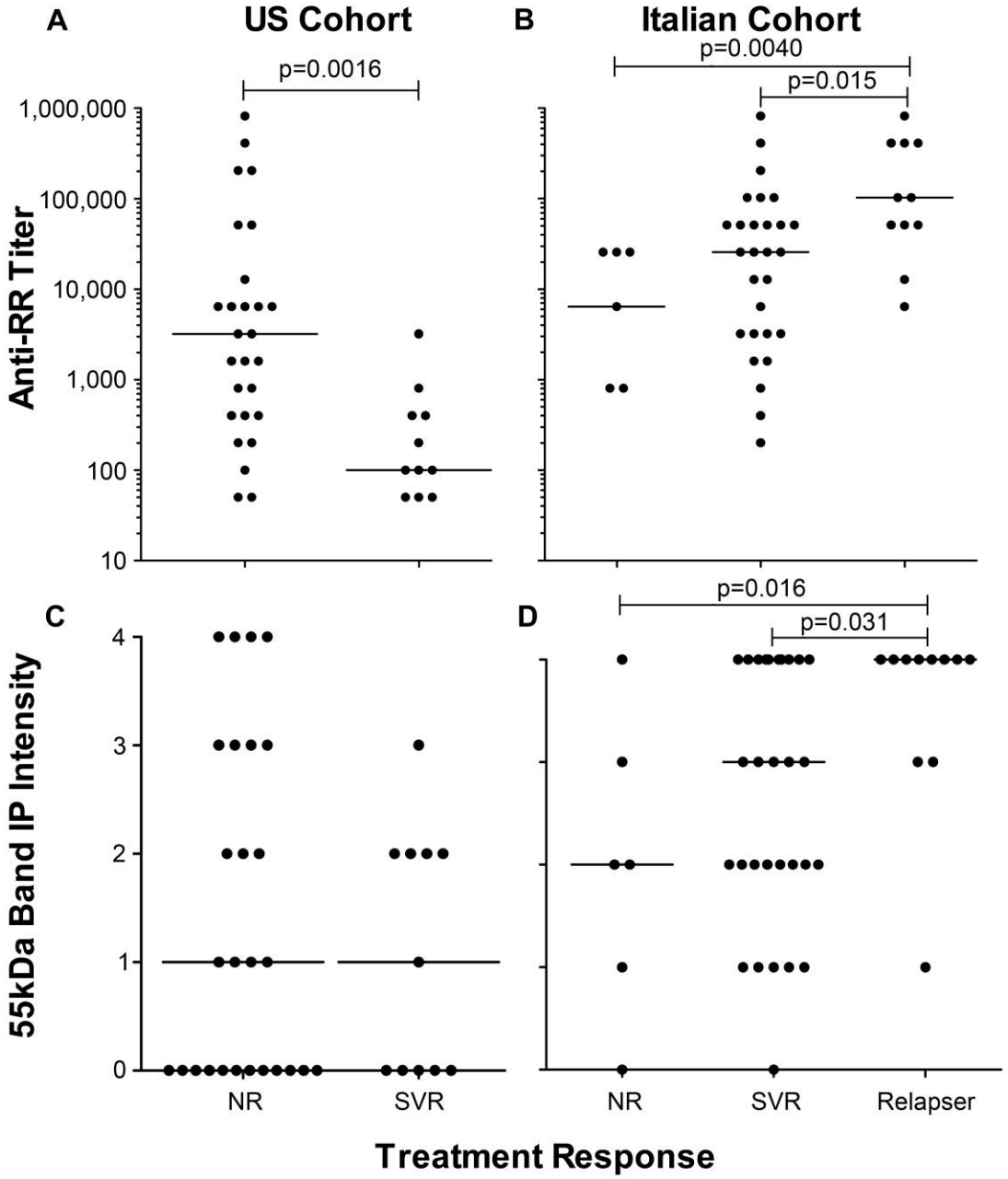

Figure 4-4. Correlation of anti-RR antibodies and 55 kDa band IP intensity to IFN/R treatment outcome. Patients were divided according to their response to treatment. The US cohort A, C) was divided into two groups, NR and SVR, while the Italian cohort B,D) was divided into NR, SVR and relapsers. The intensity of the 55kDa IP band was visually graded from 0 (negative) to 4 (strongest). Lines in each graph represent the median. NR, non-responders; SVR sustained virological responders; relapsers, responsive to therapy but after 6 months HCV RNA was detectable.

CHAPTER 5
GLUTAMINE DEPRIVATION INITIATES REVERSIBLE ASSEMBLY OF CYTOPLASMIC RODS AND RINGS

Background

Cytoplasmic structures referred to as rods and rings (RR) were identified by indirect immunofluorescence with human autoantibodies in cancer cell lines and mouse embryonic stem cells (122). Co-staining experiments demonstrated that rods and rings are not part of nor do they colocalize with the Golgi complex or other known organelles. Although RR are filament-like structures, there are not enriched in actin, tubulin, or vimentin. Two proteins, cytidine triphosphate synthetase (CTPS) and inosine monophosphate dehydrogenase (IMPDH), have been identified as components of RR. Two CTPS1 inhibitors, 6-diazo-5-oxo-L-norleucine (DON) and acivicin, and two IMPDH2 inhibitors, ribavirin and mycophenolic acid, induce RR formation, which is dependent on concentration and treatment time of the respective inhibitors (122). To date, the four chemical inhibitors that can induce RR assembly share a common metabolic repression mechanism involving the inhibition of enzymes associated with the nucleotide biosynthesis pathway.

CTPS1 and IMPDH2 are enzymes involved in the pyrimidine and purine biosynthesis pathways, respectively. CTPS1 is the rate-limiting enzyme and catalyzes the conversion of uridine triphosphate into cytidine triphosphate (CTP), a key precursor of DNA, RNA, and phospholipids, with the use of glutamine as a nitrogen provider. CTPS exists as two isoforms, CTPS1 and CTPS2, with 74% identity in humans. CTPS1 is a 591 amino acid protein with a molecular weight of 67 kDa; it is composed of an N-terminal synthetase domain and a C-terminal glutaminase domain. Ammonium is cleaved off of glutamine by the glutaminase domain to form glutamate. The synthetase

domain uses the ammonium ion to generate CTP from ATP-phosphorylated UTP. CTP synthetase activity is affected by all four ribonucleoside triphosphates *in vitro* (141). CTP acts as a feedback inhibitor by binding to the synthetase domain (142,143), while GTP is an allosteric activator (144). IMPDH2 is the committing enzyme involved in the purine biosynthesis pathway and catalyzes the conversion of inosine monophosphate into xanthine monophosphate, which is subsequently converted to guanine monophosphate (GMP) (145). IMPDH is a key enzyme in the regulation of cell proliferation and differentiation (146,147). Human IMPDH also has two isoforms, IMPDH1 and IMPDH2, with 84% sequence identity and a molecular weight of 55 kDa. IMPDH activity can be affected by way of IMP site inhibitors, NAD site inhibitors, or allosteric site inhibitors (148).

Glutamine is the most abundant free amino acid in the body and plays a role in many cell-specific processes, such as metabolism, protein synthesis, and cell proliferation. Glutamine is also involved in changes in protein activity, gene and protein expression, and intracellular metabolite concentrations (149). Extracellular administration of glutamine can stimulate purine and pyrimidine synthesis. The first step in the *de novo* synthesis of purines is the conversion of ribose-5-phosphate to glutamine phosphorybosylpyrophosphate by amidophosphorybosyltransferase. Glutamine, carbon dioxide, and ATP are required for the production of carbamyl phosphate in the *de novo* synthesis of pyrimidines (150). Extracellular glutamine level of 0.7 mM is a requirement that is met by a large majority of standard cell culture media, as most common formulations contain between 1.0 and 4.5 mM (151).

Previous reports identified CTPS1 and IMPDH2 as components of RR and that four inhibitors could induce the formation of RR in various cell lines (122). The current report investigates the effects of glutamine deprivation on RR assembly in human cancer cells.

Materials and Methods

Cell Culture

HeLa cells (human cervical cancer, ATCC, Manassas, VA) were cultured in DMEM containing 10% Fetal Bovine Serum (FBS) in a 37°C incubator with 5% CO_2. Adherent cell lines were maintained at 50% confluence. All medium contained 100 I.U./ml penicillin and 100 µg/ml streptomycin.

Indirect Immunofluorescence

HeLa cells were cultured in 8-well chamber slides (BD Falcon) and were used for indirect immunofluorescence as described (68,69). The 8-well chamber slides were prepared using ~50,000 cells per well in 500 µL of medium. Fixation method was 3% paraformaldehyde in PBS at room temperature for 10 min followed by 0.5% triton-X/PBS for another 5 min. For co-staining studies, rabbit anti-IMPDH2 (Proteintech, Chicago, IL: 12948-1-AP) and human anti-RR prototype serum It2006 were used and followed by secondary antibodies Alexa 488 goat anti-human Ig and Alexa 568 goat anti-rabbit Ig.

Induction of RR Assembly by Glutamine Deprivation

HeLa cells were cultured in 8-well chamber slides exactly as described above except in medium without glutamine (DMEM, Cellgro; 15-013-Cl). Glutamine-minus medium was replaced each day for 2 days. On the third day, cells were either harvested or supplemented with L-glutamine (Cellgro: 25-005-Cl), cytosine (Sigma-Aldrich;

C3506), guanosine (Sigma-Aldrich; G6264) or thymidine (Sigma-Aldrich; T1895) at designated concentrations ranging from 0.1 to 125 mM for another 24 h.

Induction of RR Formation Using CTPS or IMPDH Inhibitors

Mycophenolic acid (MPA; Sigma-Aldrich; M5255) was solubilized in ethanol to a 31 mM stock concentration. 6-diazo-5-oxo-L-norleucine (DON, Sigma-Aldrich; D2141) was solubilized in DMEM to a stock concentration of 100 mM. Cells were seeded as monolayers and allowed to attach for 24 h. CTPS1 or IMPDH2 inhibitors were then added in various final concentrations ranging from 0.2 µM to 2 mM and cells were kept for an additional 24 h.

Induction of RR Formation Using Glutamine Transport and Glutamine Synthetase Inhibitors

Cells were maintained in glutamine free medium and treated with methionine sulfoximide (Sigma; M5379) or γ-L-glutamyl-p-nitroanilide (Fisher Scientific; BP2656). Methionine sulfoximide was solubilized in warm water to a 100mM stock concentration. γ-L-glutamyl-p-nitroanilide was solubilized in water to a 10mM stock concentration. Cells were treated for 24 h with either inhibitor.

qRT-PCR

Total RNA samples were harvested using the mirVana Total RNA Isolation Kit (Applied Biosystems) after 48 h in culture or at specific time point indicated. Reverse transcription was performed using the High Capacity cDNA Reverse Transcription Kit (Applied Biosystems). The relative mRNA levels of target genes were measured in duplicates using TaqMan Fast Universal Master Mix (Applied Biosystems) with the corresponding TaqMan Gene Expression Assay (Applied Biosystems). GAPDH was used as an internal control and was run in duplex with the targets.

Western Blotting

The expression levels of CTPS and IMPDH were analyzed using rabbit anti-CTPS (Abcam, 1:1000) and rabbit anti-IMPDH (Santa Cruz Biotechnology, Paso Robles, CA, 1:1000) as described (72). The level of GAPDH was determined by rabbit anti-GAPDH antibody (Sigma, 1:2,000) as a normalizer to control for loading. Protein was quantitated using ImageJ and normalized to GAPDH.

Quantification and Statistical Analysis

Cell counting was performed using Mayachitra Imago (Mayachitra, Santa Barbara, CA) to detect nuclei counterstained with DAPI. Quantification of the size of RR was accomplished using the threshold feature in Mayachitra Imago software. The intensity threshold was set to 50 (detects RR with total intensity pixels higher than 50) for the analysis of images. The size of the structures was defined by their area in pixels. Unpaired, two-tailed Student's t-test and Fisher's exact test were used to compare independent groups. Prism for Windows version 5.0 (GraphPad Software, San Diego, CA) was used for all statistical analysis.

Results

Glutamine Deprivation Induces Rod and Ring Formation

RR were previously identified as cytoplasmic structures composed of CTPS1 and IMPDH2 after using CTPS1 or IMPDH2 inhibitors (122). CTPS1 and IMPDH2 are involved in the purine and pyrimidine biosynthesis pathways, which both utilize glutamine extensively (57). In the pyrimidine biosynthesis pathway, CTPS1 utilizes glutamine to convert UTP into CTP. Due to the importance of glutamine in these pathways, our notion was to examine whether cells deprived of glutamine or serum can also lead to the formation of RR. Cells were cultured with or without glutamine at

various concentrations of FBS: 10%, 5%, 1%, 0.1% and 0%. Cells maintained in medium containing 10% FBS but deprived of glutamine for 2 days formed RR in an average of 48.7% of cells after 2 days of starvation (Figure 5-1A). RR detection was confirmed by costaining using a rabbit anti-IMPDH2 antibody and the prototype human anti-RR serum It2006 as previously described (122). In contrast, cells cultured in normal medium with glutamine showed diffused cytoplasmic staining and RR were not detected (Figure 5-1C). Cells cultured in 1% FBS without glutamine had RR in 10.7% of cells (Figure 5-1B) and significant cell death was noted. In culture medium containing glutamine, a decrease in FBS from 10% (Figure 5-1C) to 1% induced only few RR (Figure 5-1D). When FBS concentration was lowered than 1%, there were too much cell death and no RR was detected. Changing glutamine levels from 0.5 to 15 mM was previously reported to have an effect on protein and gene expression (152). Messenger RNA (mRNA) levels of CTPS1 and IMPDH2 were elevated after cells were deprived of glutamine in the presence of 10% FBS when compared to cells maintained in medium with 10% FBS and glutamine (Figure 5-1E). In contrast to the ~2 fold increase in mRNA, only a small increase was observed in CTPS1 and 56% increase in IMPDH2 protein levels in cells deprived of glutamine compared to cells in normal medium (Figure 5-1F). This data suggest that the formation of RR enriched in IMPDH2 is primarily resulted from the assembly of soluble cytoplasmic enzyme pool and at the same time, there is increase synthesis of intracellular IMPDH2.

The assembly of cytoplasmic RR in response to glutamine deprivation was further examined in cells treated for 1, 2, and 3 days (Figure 5-2). RR were not detected in cells maintained in medium containing glutamine. A diffused cytoplasmic staining was

observed when co-stained with human serum It2006 and rabbit anti-IMPDH2 antibodies (Figure 5-2A-C). However, when the medium was replaced with medium deprived in glutamine, RR formation was observed clearly at day 2 (Figure 5-2G-I). At day 1, short structures that resemble rods were detectable in the cytoplasm (Figure 5-2D-F); these short rods were still detected among the long rods and rings at day 2 (Figure 5-2G-I). At day 3, the majority of short rods disappeared and predominantly mature long RR remained (Figure 5-2J-L). Counting of short and long RR showed the reduction of the short structures from 68.5% in day 1 to 10.1% at day 3 (Figure 5-2M). This is consistent with the hypothesis that mature RR in later time points are assembled from shorter structures from earlier time points. Since RR formation was almost complete after 2 days of glutamine deprivation, all subsequent experiments were conducted with 2 days of glutamine deprivation.

Glutamine Add-Back Disassembles RR Induced in Response to Glutamine Starvation

RR formed in response to glutamine deprivation for 48 hours disassembled within 24 h after the addition of 2.5 mM glutamine (Figure 5-3). Cells with glutamine add-back had diffused cytoplasmic staining (Figure 5-3G-I), as observed in cells in normal medium with glutamine (Figure 5-3A-C). Normal culture medium containing 4 mM glutamine; therefore, the addition of 2.5 mM glutamine was below the normal concentration. Addition of glutamine at concentrations as high as 125 mM all led to the disassembly of RR (data not shown). Addition of similar amount glutamine to cells maintained in normal culture medium did not lead to RR formation (data not shown). It is interesting that the increase in CTPS1 and IMPDH2 mRNA levels in cells depleted of glutamine was reduced back to normal in cells that were given the glutamine add-back

(Figure 5-3J). Since the RR induced in response to glutamine deprivation was co-stained human prototype anti-RR serum, these RR are likely identical to previously reported RR induced by IMPDH2/CTPS inhibitors (122).

Supplement of Guanosine or Cytosine Induces the Disassembly of RR Formed in Response to Glutamine Starvation

Glutamine is involved in several pathways, and its requirement in the purine and pyrimidine biosynthesis pathways is notable for this discussion. The steps in these pathways that utilize glutamine are shown in Figure 5-4A. Glutamine is required in the first and fourth step of the *de novo* pathway of purine biosynthesis. In addition, glutamine is also required in the second step of the synthesis of GMP from IMP. In the pyrimidine biosynthesis pathway, glutamine is utilized by CTPS1 in the conversion of UTP to CTP. Thus, depletion of glutamine prevents the formation of CTP and GTP.

Intracellular levels of CTP and GTP can be increased by adding cytosine and guanosine, respectively, to culture medium (153,154). RR induced in response to glutamine deprivation disassembled in a concentration-dependent manner with the addition of cytosine and guanosine. HeLa cells that were deprived of glutamine for 48 h showed abundant RR (Figure 5-4B). Addition of 1 mM guanosine completely disassembled RR induced by glutamine deprivation (Figure 5-4C), while 1 mM of cytosine partially disassembly of RR into short cytoplasmic punctuates (Figure 5-4D). Addition of guanosine and cytosine at 0.1 mM showed no apparent change in RR (data not shown). Thymidine, which is converted into thymidine triphosphate, did not affect the RR induced by glutamine deprivation (Figure 5-4E).

MPA-Induced RR Disassemble After Replenishing with Guanosine

Mycophenolic acid (MPA) is a reversible inhibitor of IMPDH2 that can induce RR formation in a concentration-dependent manner (Figure 5-5A). MPA can induce RR in as little as 30 minutes and 2 µM concentrations. Addition of guanosine to cells treated with MPA for 24 h led to a decrease the size of RR induced by MPA (Figure 5-5B). However, MPA-induced RR in cells treated with glutamine or cytosine were not affected (Figure 5-5C-D). RR induced by MPA had longer RR and cells contained 1 or more long RR compared to RR disassembled after addition of guanosine (Figure 5-5E-G; p-value=0.0001). Longer rods were considered to have more than 70 px. Guanosine treated cells had on average 2 or more short rods per cell and only 1 out of 10 cells contained a long RR. In this analysis, rings were quantitated identical to linearized rods.

Inhibition of Glutamine Synthetase and Glutamine Transport Induce RR Formation

Intracellular level of glutamine is a summation from extracellular supplement glutamine, endogenous de novo synthesis, and the efficiency of transport from extracellular source. The next experiment was to determine whether inhibitors for de novo glutamine synthesis and glutamine transport would affect the formation of RR. DON functions as an inhibitor of CTPS1 and glutamine synthetase. It was previously shown that DON can induce RR formation in a concentration-dependent manner (122). As expected, treatment with 1 mM of DON for 24 h induced RR formation (Figure 5-6B). Methionine sulfoximine, a glutamine synthetase specific inhibitor, was used to determine if inhibition of glutamine synthetase could induce RR assembly. RR were induced with 1 mM methionine sulfoximine (Figure 5-6C). Affecting intracellular

glutamine levels by inhibiting glutamine transporter solute carrier family 1 member 5 in HeLa cells using 1 mM γ-L-glutamyl-p-nitroanilide induced RR assembly (Figure 5-6D).

Discussion

Previous studies on the formation of cytoplasmic structures composed of CTPS in yeast determined that nutrient deprivation could induce the formation of CTPS filaments. It was determined that glucose depletion is a potent inducer of CTPS filaments in yeast (83). Another study observed the formation of cytoophidia, also RR-like filaments composed of CTPS, induced in human and *Drosophila* cells with glutamine analogs; such as DON or azaserine (155). Both DON and azaserine inhibit enzymes that require glutamine. The study in yeast supports that RR in our study and filament formation in yeast is in response to decrease in necessary factors for cellular division or proliferation. Additionally glucose deprivation in hamster fibroblast affected the levels (pool sizes) of intracellular of UTP, GTP and CTP (156). Therefore, glucose deprivation and glutamine deprivation may both decrease in CTP and GTP causing formation of filaments in yeast and RR in HeLa cells. The use of glutamine analogs to induce cytoophidia in *Drosophila* may suggest the importance of glutamine in preventing formation of cytoophidia or RR in HeLa cells.

Glutamine serves many roles in different cellular processes and is essential for cell viability and growth (157). In this study, RR are formed in response to glutamine starvation. Glutamine starvation requires a minimum of 24 h to visualize the formation of short rods. Although visibly shorter (or immature) rods were observed at 24 h, these structures continue to aggregate and reach full size by 72 h after starvation is initiated. It is easy to visualize this progression of the structure: at 24 hours, a diffused cytoplasmic staining in conjunction with short, immature rods shows the beginning stages of

aggregation. At 48 hours, there is notably less diffused staining, as more protein has been assimilated into the maturing RR. At 72 hours, when fully mature RR are formed, there is almost no diffused cytoplasmic staining visible, suggesting that all remaining IMPDH2 is incorporated into RR.

Glutamine deprivation prevents the formation of CTP and GTP by affecting enzymes in the purine and pyrimidine biosynthesis pathways (149,158). RR formation is therefore in response to decreased intracellular levels of CTP and GTP. This notion is supported by the addition of extracellular guanosine and cytosine, converted into CTP and GTP after transport and entry into cells (153,154), in the present study could reverse the process as demonstrated by RR disassembly when cells are replenished with guanosine and cytosine. Thus, the assembly for RR from the polymerizing of IMPDH2 (and probably CTPS1) appears to be in response to decreased production of CTP and GTP after glutamine deprivation or by inhibition of enzymatic activity of CTPS1 or IMPDH2. Additionally, the requirement of glutamine in the induction of RR was supported by data from the glutamine synthetase inhibitors. The observed induction of RR by DON and methionine sulfoximide is therefore consistent with notion that decrease intracellular levels of glutamine cause RR assembly.

A previous study also showed that MPA-induced RR-like filaments were disassembled by incubating cells with guanosine (59). Our data confirmed this finding with MPA-induced RR disassembled when supplemented with guanosine, but not with glutamine or cytosine. MPA inhibits IMPDH2 enzymatic activity, which prevents the formation of GTP. Replenishing GTP by the addition of guanosine after IMPDH2 inhibition can disassemble RR, while replenishing CTP levels after inhibiting IMPDH2

did not. Additional data confirms that RR also form in response to changes in CTP levels caused by glutamine deprivation and that these structures can be disassembled with guanosine, cytosine or glutamine. Therefore, changes GTP and CTP levels can induce RR formation.

Genes that mediate the synthesis of necessary metabolites are tightly regulated by various cellular mechanisms. These cellular mechanisms must respond to internal and external factors in order to respond to cellular needs. RR may be a structural mechanism that forms in response to decreased glutamine, CTP, or GTP levels. This study demonstrates that restoring glutamine levels after glutamine deprivation can disassemble cytoplasmic RR. RR may also serve to regulate IMPDH and CTPS mRNA and protein levels in response to nutrient stresses.

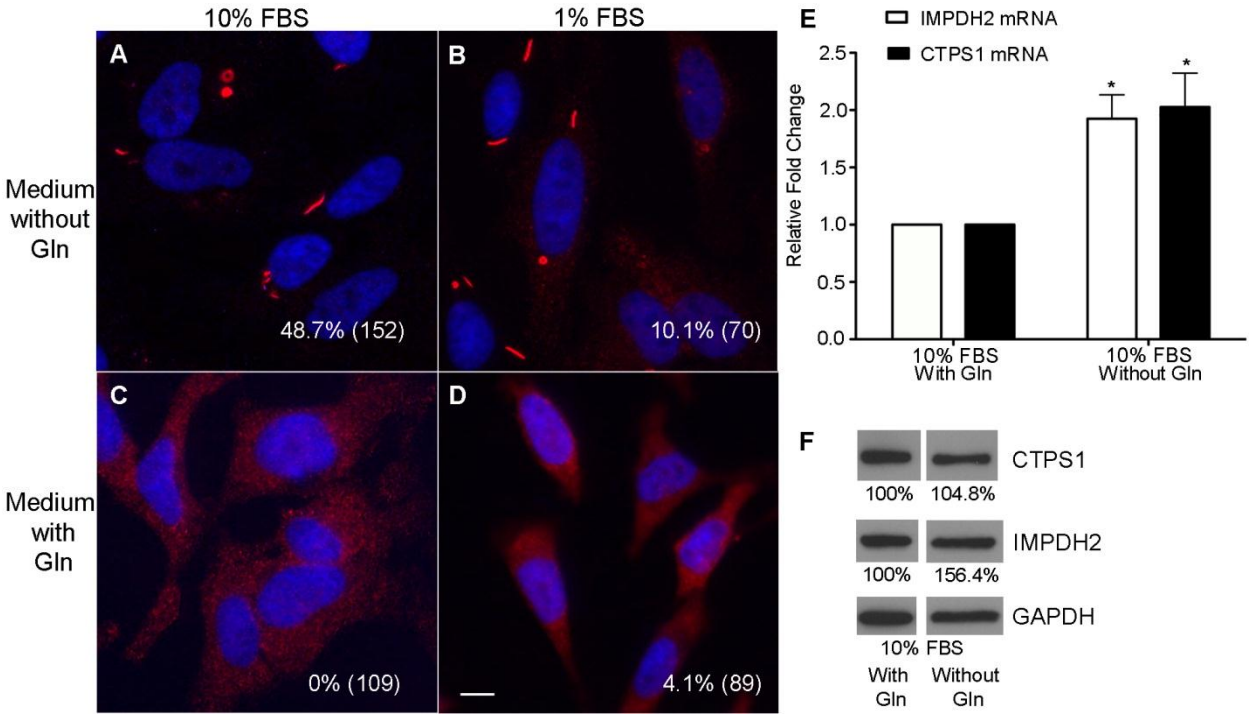

Figure 5-1. Glutamine deprivation induces rods and rings. HeLa cells maintained in DMEM medium with 10% FBS without glutamine A), DMEM medium with 1% FBS without glutamine B) DMEM medium with 10% FBS C), and DMEM medium with 1% FBS D) for 48 h were stained with rabbit anti-IMPDH2 (red). Nuclei were counterstained with DAPI (blue). The average percentage of cells with RR are displayed in the lower right corner, with total number of cells counted in parenthesis. E) mRNA levels of CTPS1 and IMPDH2 are significantly elevated in cells depleted of glutamine. mRNA levels were normalized to GAPDH. F) Western blot of CTPS1 and IMPDH2 protein levels using GAPDH as a loading control in HeLa cells maintained in 10% FBS medium with glutamine or without glutamine. There was an increase (156.4%) in IMPDH2 protein levels after glutamine deprivation in 10% FBS. Data are from three independent experiments (A-D, mean; E, mean ± s.d.). *$P < 0.05$; (two-tailed unpaired t-test) compared with cells maintained in DMEM medium with 10% FBS. Scale bar, 5 μm.

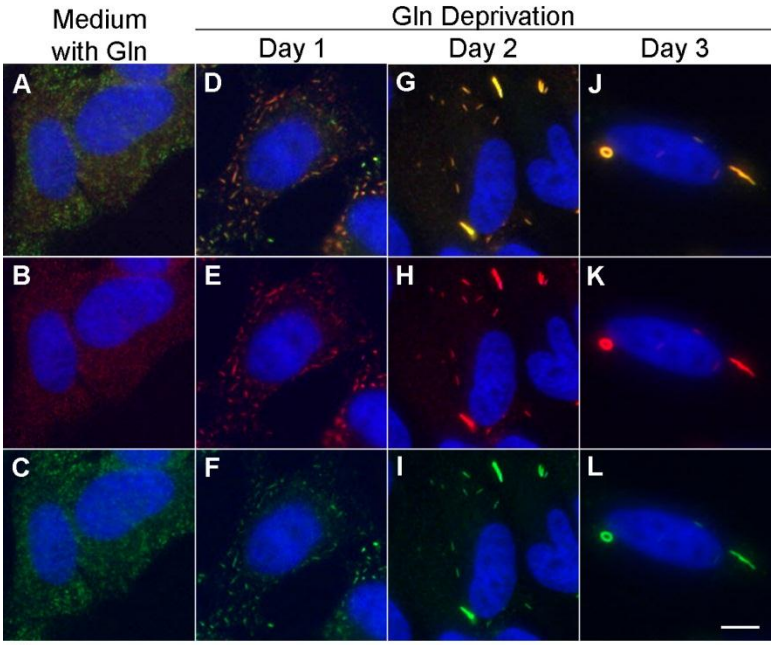

M

	Controls *(106)*	Day 1 *(64)*	Day 2 *(118)*	Day 3 *(44)*
Cells with short RR alone	0%	68.8%	14.8%	10.1%
Cells with short and long RR	0%	0%	45.2%	32.1%
Cells with long RR alone	0%	0%	4.8%	40.6%

Figure 5-2. Longitudinal analysis of RR formation during glutamine starvation. HeLa cells were maintained in normal DMEM medium with 10% FBS A-C), or in glutamine-depleted medium with 10% FBS for 1 day D-F), 2 days G-I), and 3 days J-L). Cells were co-stained with human anti-RR serum It2006 (green; C, F, I, L) and rabbit anti-IMPDH2 (red; B, E, H, K). Merged images are shown in A, D, G, and J. Nuclei were counterstained with DAPI (blue). (M) Summary of the percentage of cells with short RR alone, short and long RR, and long RR alone for each day of glutamine starvation and control. Total number of cells counted are shown in parentheses.

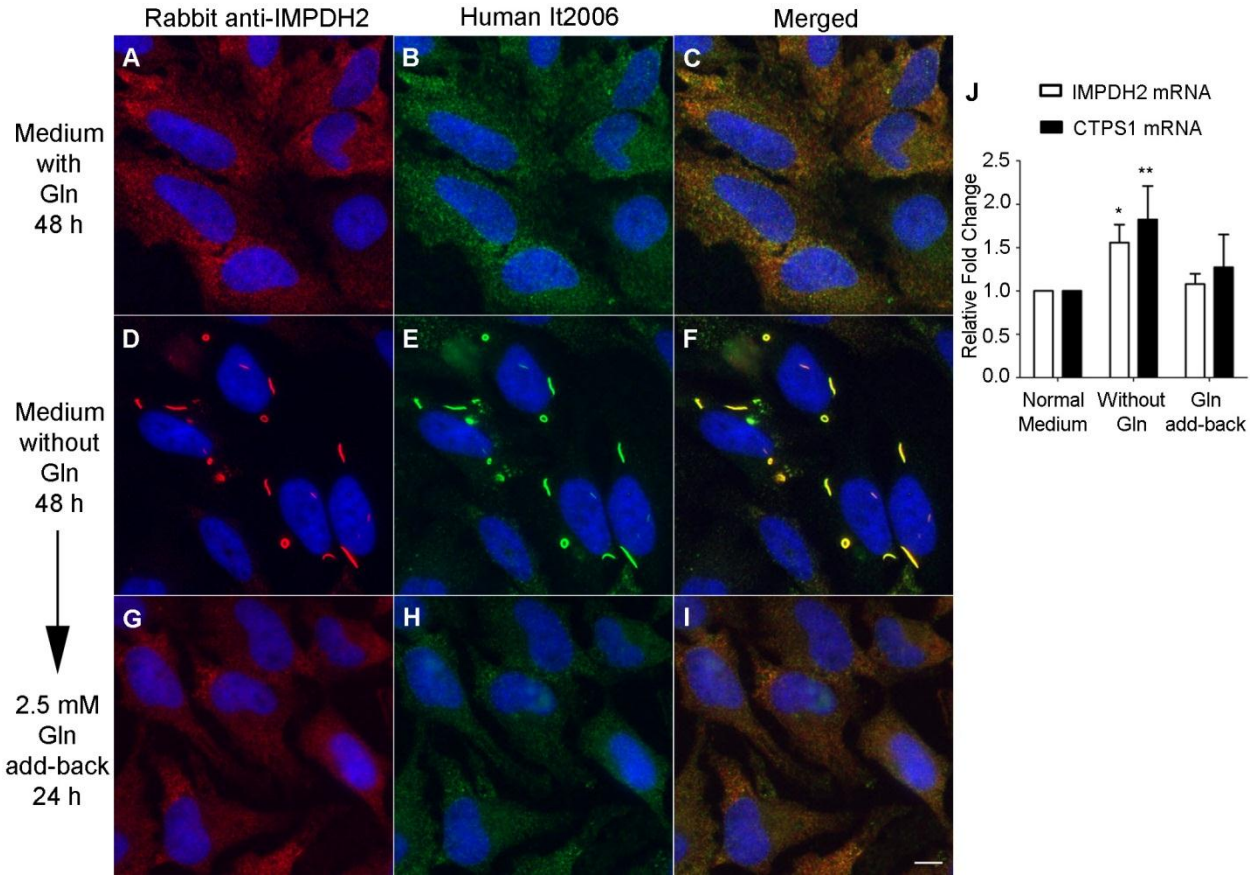

Figure 5-3. Glutamine add-back disassembles RR formed in response to glutamine starvation. A-C) RR were not detected in HeLa cells maintained in normal DMEM medium with 10% FBS. D-F) RR formed in cells maintained in glutamine deprived medium for 48 h. G-I) Glutamine deprivation-induced RR disassembled when cells were supplemented with 2.5 mM glutamine for 24 h. Scale bar, 5 μm. J) mRNA levels of CTPS1 and IMPDH2 were elevated in glutamine deprived cells and returned to normal in cells supplemented with 2.5 mM glutamine. mRNA levels were normalized to GAPDH.

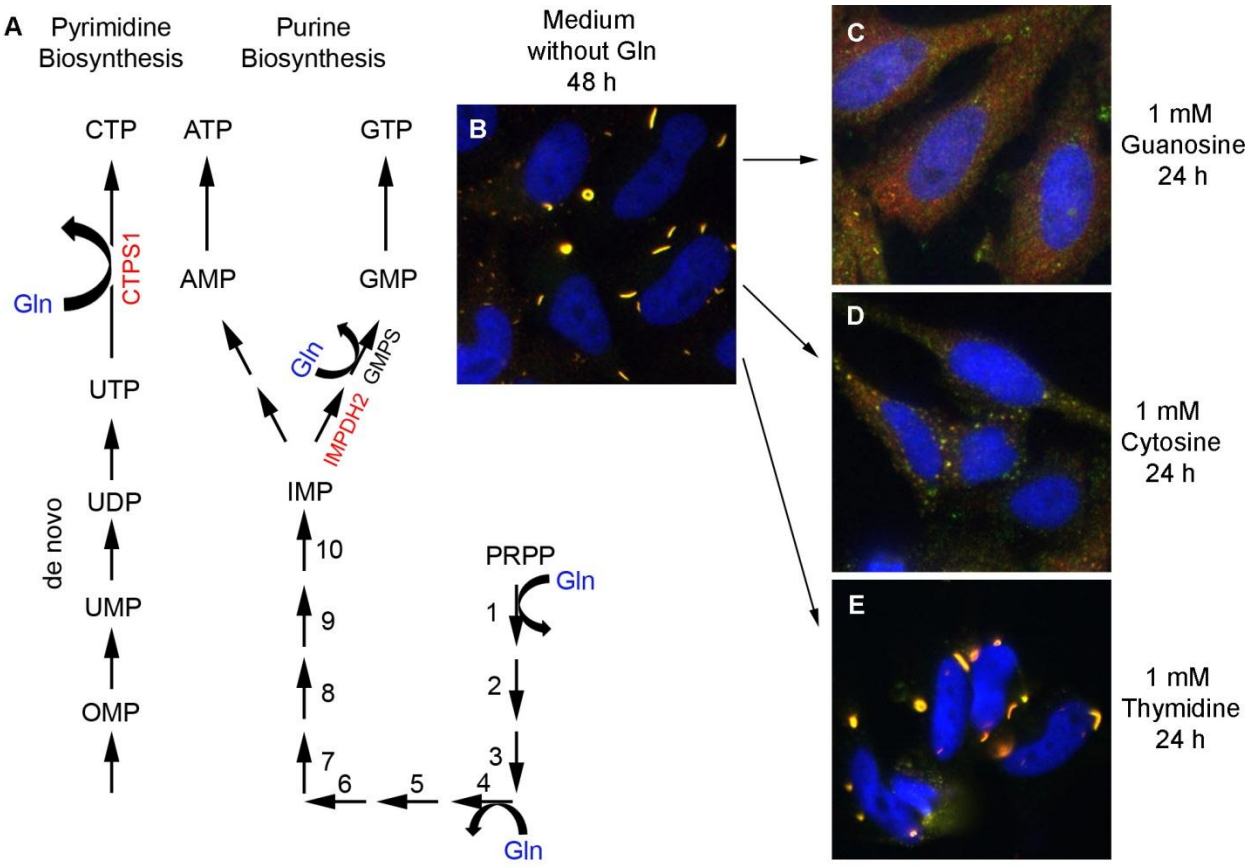

Figure 5-4. Supplement of guanosine or cytosine induces the disassembly of RR formed in response to glutamine starvation. A) Purine and pyrimidine biosynthesis pathways with RR components shown in red and steps requiring glutamine in blue. IMPDH2 is an enzyme involved in the GTP biosynthesis pathway catalyzing the conversion of IMP to GMP, which is a precursor to the production of GTP. CTPS1 is an enzyme involved in the CTP biosynthesis pathway and catalyzes the conversion of UTP to CTP. Arrows and numbers signify steps in the pathway. RR are detected in HeLa cells maintained in medium with 10% FBS minus glutamine for 48 h B). Glutamine-deprived cells are treated with 1 mM guanosine C), 1 mM cytosine D), or 1 mM thymidine for 24 h E). The pathway schematic is adapted from Hofer *et al.*(57).

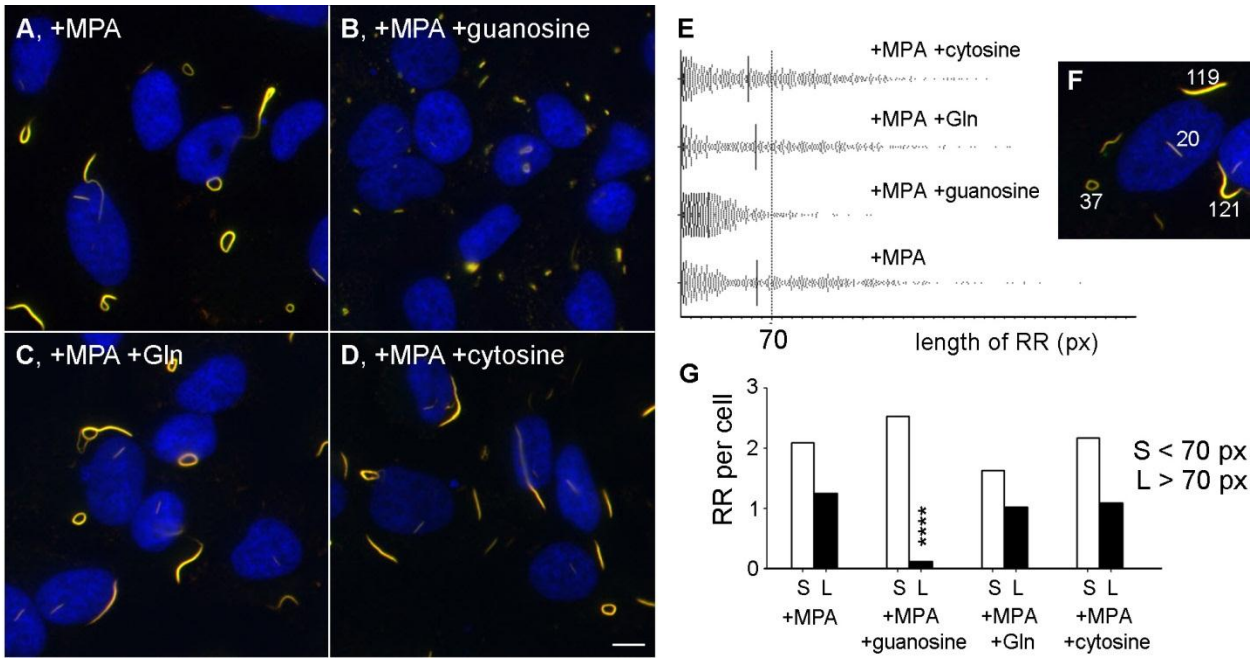

Figure 5-5. MPA-induced RR disassemble after replenishing with guanosine. HeLa cells were treated with 1 mM MPA for 24 h to induce RR formation A). Replicate wells were treated with 1 mM guanosine B), 2.5 mM glutamine C), or 1 mM cytosine D). Scale bar, 10 μm. Length of rods defined in pixel density (px) were quantitated by Mayachitra Imago and plotted for each condition (E, >300 cells analyzed for each). Px values for typical RR structures are shown F). By defining short rods (S) as <70 px and long rods L) as >70 px, the number of short and long RR structures are plotted for each conditions G).

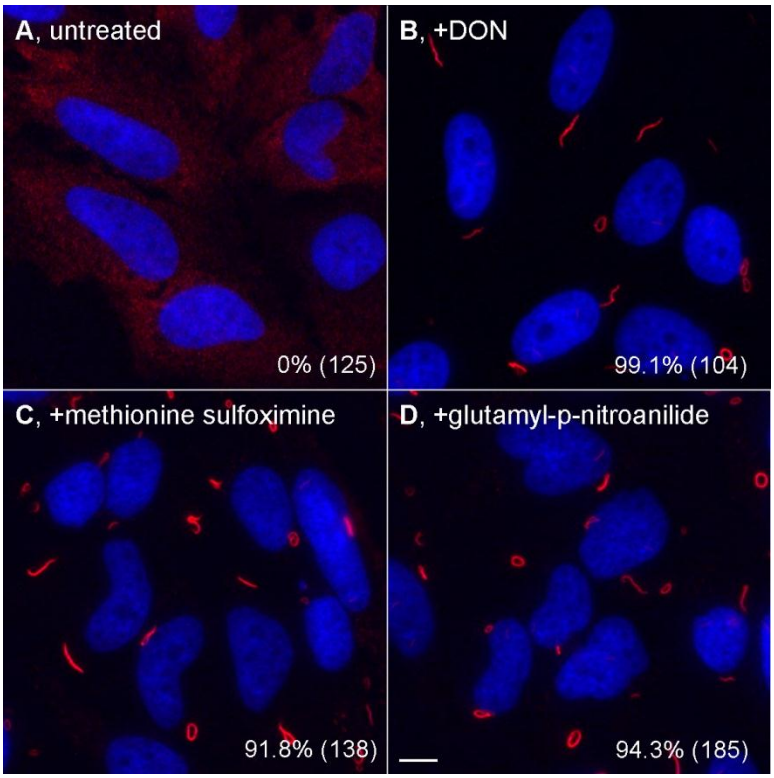

Figure 5-6. Inhibition of glutamine synthetase and glutamine transport induce RR formation. RR were not detected in HeLa cells maintained in DMEM medium with 10% FBS A). HeLa cells were treated with 1 mM DON B), 1 mM methionine sulfoximine C), or 1 mM γ-L-glutamyl-p-nitroanilide D) for 24 hours induced RR formation. Scale bar, 5 μm.

CHAPTER 6
COMPARISON OF RODS AND RINGS TO CYTOPLASMIC STRUCTURES COMPOSED OF CTPS OR IMPDH

Rods and Rings in the Cytoplasm

We have recently reported interesting cytoplasmic structures, referred to as rods and rings (RR, Figure 6-1), detected by using autoantibodies in specific patient sera (122). Many of the patients have hepatitis C (HCV) infection, and are producing anti-RR autoantibodies after treatment with a standard combination therapy of pegylated interferon and ribavirin (139). These structures contain cytidine triphosphate synthetase 1 (CTPS1) and inosine monophosphate dehydrogenase 2 (IMPDH2), proteins of 67kDa and 55kDa respectively (122). Staining by sera from HCV patients and rabbit anti-IMPDH antibodies shows perfect colocalization to RR structures. CTPS inhibitors, 6-diazo-5-oxo-L-norleucine (DON) and acivicin, as well as the IMPDH2 inhibitor ribavirin induce formation of RR in a dose-dependent manner. The induction of RR is confirmed in all cancer cell lines and primary cells examined. Interestingly, RR are visualized in undifferentiated mouse embryonic stem cells (ESCs) without the need of adding inhibitors, and were disassembled after differentiation with retinoic acid (122). Since RR are found in ESCs without the use of inhibitors, RR expression may be a very interesting biomarker for ESCs. Various other publications have described novel cytoplasmic filament-like structures that are composed of enzymes involved in either cytidine triphosphate (CTP) or guanosine triphosphate (GTP) nucleotide biosynthesis. Here, we review all the relevant findings which allow us to speculate the main function of RR in enhancing production of CTP/GTP when their cellular levels are lowered and the formation of RR is thus sensitive to lowered levels of GTP/CTP.

Nucleotide Biosynthesis Associated with RR

The observation that two known components in RR are CTPS1 and IMPDH2 implicates these structures in CTP and GTP biosynthesis. CTP and GTP are essential building blocks of DNA and RNA and are involved in a multitude of pathways in both prokaryotes and eukaryotes. They serve as energy carriers, participate in cellular signaling, and act as important cofactors in enzymatic reactions. Nucleotide biosynthesis can occur via *de novo* pathways or the salvage pathway and is tightly regulated by the cell. CTPS is a glutamine amido transferase enzyme that catalyzes the conversion of uridine triphosphate (UTP) to CTP and is a key enzyme in nucleic acid and phospholipid biosynthesis (Figure 6-2). Two human isoforms, CTPS1 and CTPS2, exist and are 74% identical at the amino acid level (56). There are two CTPS isozymes in *Saccharomyces cerevisiae*, URA7 and URA8, which correspond to the mammalian CTPS1 and CTPS2, respectively. The enzyme consists of the N-terminal synthetase domain and the C-terminal glutaminase domain. The latter catalyzes the deamination of glutamine. CTPS is an established target for antiviral, antineoplastic, and antiparasitic therapy (57,159,160).

IMPDH is also tightly regulated and catalyzes the conversion of IMP into xanthosine 5'–monophosphate, which is the rate-limiting step in the *de novo* synthesis of guanine nucleotides (146,161). IMPDH exists as two 55kDa isoforms, IMPDHI and IMPDH2, with 84% amino acid sequence identity, and forms independent tetramers when active (162). IMPDH is an important regulator of cell proliferation and is a known target in the treatment of neoplastic and viral diseases. Mycophenolic acid (MPA), an IMPDH inhibitor, has been used as an immunosuppressive agent for organ transplants

and autoimmune diseases (163-165). Another IMPDH inhibitor, ribavirin, is currently being used in the treatment of HCV (63,166).

Assembly of Proteins for a Cellular Function

Assembly of intercellular protein complexes can serve important functional purposes. GW Bodies is a cytoplasmic structure, assembled from miRNA/mRNA-protein complexes, that plays a role in RNA interference and mRNA degradation (121,167). Previous studies have also identified purinosomes and U bodies as functional cytoplasmic structures (168,169). Various studies show that inhibition of certain enzyme activity by chemical inhibitors, or by altering nutrient levels, can induce formation of other filaments. Acetyl-CoA involved in fatty acid synthesis has been shown to assemble into filaments in mammalian cells and yeast in response to citrate (170,171). Acetyl-CoA filaments as well as glutamine synthetase filaments in yeast show enzyme activity and nutrient starvation play a role in filament polymerization (172-174). Nutrient deprivation plays a similar role in reducing nucleotide levels compared to using the nucleotide biosynthetic enzyme inhibitors as described above and, therefore, depleting nucleotide levels may be a direct cause for the formation of RR. Since CTPS1 and IMPDH2 are key RR components, it is speculated that formation of RR helps increase cellular production of GTP and CTP.

Rods/Rings Related Filament-Like Structures

Upon scanning the literature, it appears that several reports have come across similar RR-like structures. The earliest report is the work by Willingham *et al.* in 1987, who described a novel cytoplasmic filament named as nematin, practically identical to rods shown in Figure 6-1 (81). The structures were observed by immunofluorescence staining using a monoclonal antibody, referred to as anti-nematin. The monoclonal

antibody was derived from a BALB/c mouse that was immunized with SR-BALB 3T3 cells and thus can be classified as an autoantibody as it was later shown positive for staining of mouse 3T3 cells. Most cells exhibited only one of these structures, but occasionally more than one were present. Some structures took on a distinct donut-shaped structure, which appears indistinguishable from the ring shown in Figure 6-1. Through colocalization studies, the filaments were identified to be independent of tubulin or vimentin. The presence of these filaments was examined in nine different mammalian cell lines and they determined that rat and mouse cells expressed the nematin structure at a higher frequency, while chick embryo cells contained virtually no such structures. Fixation methods affected the stability of the structures, with formaldehyde acting as the best fixative. Through the use of light and electron microscopy and microinjection, they identified this filament as a novel cytoplasmic structure without a lipid bilayer membrane. They concluded that the antigen recognized by the monoclonal antibody was a protein and that it may be a differentiation marker. Although the antigen was not identified, immunoprecipitation analysis revealed that the antigen was a 58kDa protein, very close in size to IMPDH. One additional common finding is that cells were found to have a higher frequency of RR right after thawing and that DMSO treatment does not induce RR formation. This study was not continued to determine the identity of the antigen, but these similarities suggest that this may be the first publication to identify the novel cytoplasmic structure that we have described as RR.

The second report of a filament composed of a nucleotide biosynthetic enzyme was from Ji *et al.*, who discovered that IMPDH inhibitors induced rods composed of

IMPDH and that the structure was reversible with the addition of GTP (59). Cells treated with MPA induced the clustering of IMPDH in as little as 30 minutes, with full linear/rod and annular/ring observed after 24 hours. MPA treatment also caused a mobility shift of IMPDH band in SDS-PAGE detectable in Western blotting. The band shift was preventable with the use of guanosine, which also caused the disassembly of the IMPDH aggregates. The aggregation of IMPDH was associated with the loss of enzymatic activity, as expected from the putative inhibitory action of MPA. They determined that GTP levels are important for the prevention and reversal of IMPDH aggregates. The structures identified by Ji *et al.* are the same as RR, although only IMPDH2 was identified. RR formation was also detected in HeLa cells treated with MPA using a rabbit anti-IMPDH antibody as well as our patient autoantibody (unpublished).

There are several recent studies reporting RR-like structures in different systems. Ji-Long Liu identified a RR-like intracellular structure containing CTPS in *Drosophila* cells (77). The structures, referred to as cytoophidia ("cell serpents"), were identified in all major *Drosophila* cell types within the ovary and other tissues, such as brain, gut, trachea, testis, accessory gland, salivary gland, and lymph gland. The structure was recognized by an antibody against Cup protein that was believed to have cross-reactivity. Using two GFP protein trap fly stocks from the Carnegie Protein Trap Library, CTPS was identified as a component of cytoophidia (77). Cytoophidia were also determined to be associated with the microtubular network but not associated with centrioles. Two types of structures were identified as macro- and micro-cytoophidium based on their length. In a follow-up study, the same laboratory reported similar structures in human HeLa P4 cells using an anti-CTPS antibody (155). Cytoophidia

formation was increased by treatment with DON. Knocking down CTPS caused the cytoophidia to disappear, however it is unknown if the disappearance is due to the requirement of CTPS or the decrease in protein. Azaserine, another CTPS inhibitor, showed effects similar to those of DON. Identification of cytoophidia in HeLa and clustering of CTPS suggests that this structure is identical to rods and rings. Cytoophidia and RR have clear similarities, as both structures have been determined to be unassociated with centrioles. Although the expression frequency of cytoophidia varies, both structures can be induced with DON and both structures were detected with antibodies to CTPS.

Another recent study from Noree *et al.* identified nine proteins that formed rod-like filaments in *S. cerevisiae* (83). The filaments were identified using GFP-tagged proteins; they also verified that the tag did not play a role in the formation of the filaments by changing the GFP tag to an HA epitope tag and observed the same filaments. Additionally, the tagged version of each protein did not affect growth or viability of cells. The nine proteins are Glt1p (glutamate synthase), Psa1p (GDP-mannose pyrophosphorylase), Ura7p/Ura8p (CTP synthase), Gcd2p (eIF2B-δ), Gcd6p (eIF2B-ε), GCD7p (eIF2B-β), Gcn3p (eIF2B-α) and Sui2p (eIF2B-α). Some of the nine proteins colocalized to form four distinct filaments. They observed that the Ura7p filaments were increased when cells were grown to saturation and concluded that this was due to a decrease in available carbon sources. In addition, treating cells with sodium azide to alter energy status caused an increase in Ura7p and Psa1p filaments. CTPS filaments were identified in all three cell types in the *Drosophila* egg chamber. They concluded that the different complexes form in response to environmental conditions either to

promote or inhibit particular enzymatic processes, and not as a stress response. Additionally, CTPS filament assembly is caused by the regulation of enzyme activity by the binding of specific ligands such as CTP.

The third recent report is from Ingerson-Mahar *et al.* identifying a possible function of CTPS filaments in the fresh water bacterium *Caulobacter crescentus* (82). They demonstrated that CTPS formed filaments along the inner curve of the bacterium using electron cryotomography. This bacterial CTPS enzyme has a bifunctional role; as a filament, it regulates the curvature of *C. crescentus* and performs its catalytic function. They treated cells with the irreversible CTPS inhibitor DON and showed the disruption of the CTPS filament. They determined via electron cryotomography that CTPS colocalizes with the filament and is required for its formation. In addition, *Escherichia coli* CTPS homologue was able to form filaments both *in vivo* and *in vitro*. They concluded that CTPS is a negative regulator of cell curvature by mediating CreS. However, the mechanism of how CTPS controls cellular curvature remains unclear.

Conservation of RR Across Species

RR-like filaments have been identified in a wide range of species as described above (86). RR-like filaments have been identified in human, bovine, mouse, rat, *Drosophila,* yeast, and bacteria. Filament sizes range from <1 µm to 50 µm, with bacteria expressing the smallest structures and *Drosophila* expressing the largest ones (summarized in Table 6-1). The structures have also been identified in some cancer cell lines, primary cells, and stem cells as discussed above.

Composition of RR

Although CTPS1 and IMPDH2 are known RR components, immunoprecipitation of K562 cell extract using anti-RR positive HCV patient sera shows some anti-RR

antibody-positive sera, 604, 605, and 611, pull down a common 55kDa doublet (Figure 6-3A, red dots), which corresponds to IMPDH1/2. Yet other sera with anti-RR antibodies by immunofluorescence do not immunoprecipitate IMPDH protein (Figure 6-3A, 603, 606, 608, 609, 610, and 612). Immunofluorescence analysis show serum 609 (anti-RR-positive, 55kDa doublet-negative) and serum 611 (anti-RR-positive, 55kDa doublet-positive) both recognize the same structure costained with rabbit anti-IMPDH2 (Figure 6-3B-J). Amongst the studies reported to date, two identified IMPDH and five identified CTPS as component of the RR-like filaments as summarized in Table 6-1. Liu speculates that these structures may be composed of additional components as seen in the yeast Ura7p and Ura8p filaments (86). Willingham *et al.* identified that nematin filaments were not enriched in vimentin or tubulin (81). Our study also concluded that RR are neither enriched in vimentin, tubulin, or actin, nor associated with any known cytoplasmic structures (122). In addition, we investigated the colocalization of RR with centrioles and determined that RR are not primary cilia, because the structures are not attached to the centrioles.

Formation of RR

RR are not found in most mammalian culture cells in more than a few percent of cells. Inhibitors of CTPS and IMPDH are known to induce RR formation in 90-100% of cells detectable by both patient autoantibodies and rabbit anti-IMPDH2 antibodies (122). Comparing IMPDH inhibitors ribavirin/MPA to CTPS inhibitors DON/acivicin at relatively high concentration (2 mM), IMPDH inhibitors are consistently faster in inducing RR in only 15-30 minutes versus CTPS inhibitors which require 2-3 hours to induce comparable levels of RR (122). Most studies report that inhibition of these enzymes causes RR-like filament formation, with the only exception in *C. crescentus* when CTPS

inhibitor DON disassembles CTPS filament as described earlier (82). Noree *et al.* specifically identified Ura7p (CTPS) filaments as being affected by levels of nutrients (83). Some key differences between reports are summarized in Table 6-1.

Concluding Remarks

Recent studies show that cells can regulate nucleotide biosynthesis by clustering critical enzymes into RR although their mechanism of formation and functions are not completely understood. RR contain two nucleotide biosynthetic enzymes CTPS and IMPDH but we speculate that these structures may be composed of other enzymes of the same pathways, based in part on its relatively large physical dimension and on the fact that there are many other anti-RR autoantibodies that do not appear to recognize CTPS/IMPDH. Assembly of both CTPS and IMPDH may be due to the close interaction between both enzymes during nucleotide biosynthesis. Many studies suggest the possibility of a conserved RR structure composed of nucleotide biosynthetic enzymes and is a sensor to lowered levels of GTP/CTP.

Our identification of abundant RR in mouse undifferentiated embryonic stem cells is intriguing, as it is the only native condition, to date; these structures are found without extrinsic manipulation. Chen *et al.* has described effects of DON on the filaments and *Drosophila* oogenesis suggesting their biological function in development (155). We have also identified the fact that HCV patients treated with interferon-alpha and ribavirin produce autoantibodies against RR. Covini *et al*. examined the prevalence of anti-RR antibodies in other diseases and concluded that anti-RR antibodies are highly specific to HCV patients after treatment, but not before treatment (139). Anti-RR antibodies were determined to be more prevalent in patients that do not respond to therapy. Additional studies have also shown correlation of anti-RR antibody production with HCV and that

the antigen of anti-RR antibodies is IMPDH2 (139,140). Since HCV patients are treated with ribavirin and we have shown that ribavirin can induce RR formation *in vitro* (122), ribavirin treatment in HCV patients may cause RR formation, which leads to the induction of autoantibodies against these structures when they are released to the host immune system during turnover. Studies thus far implicate novel clinical and biological significance of RR structures.

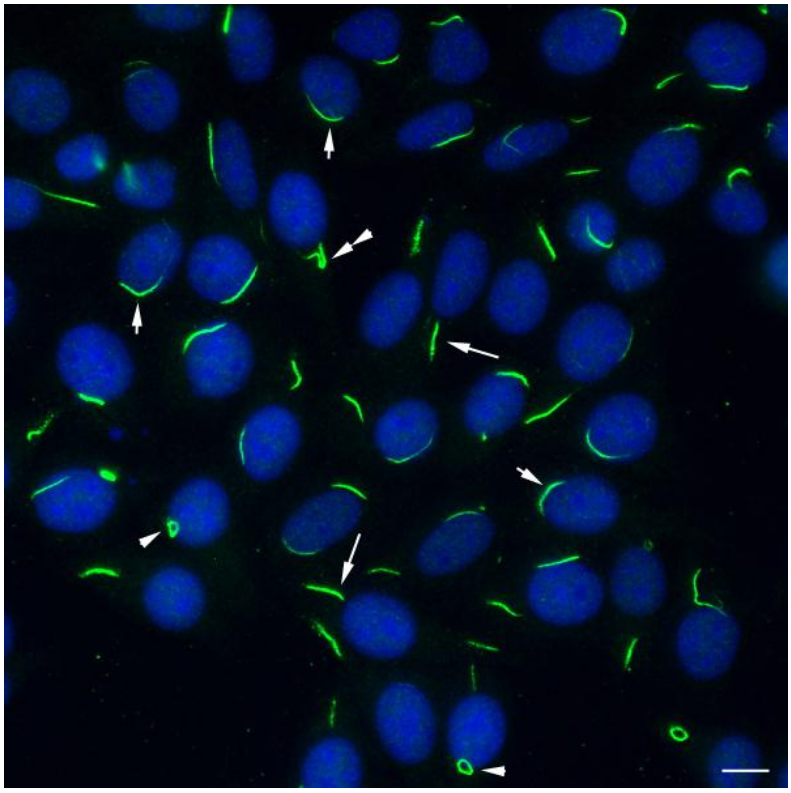

Figure 6-1. Rods and rings (RR) recognized by human autoantibodies. HEp-2 cells are stained with human prototype anti-RR serum It2006 followed by Alexa 488 goat anti-human IgG (green) and nuclei counterstained with DAPI (Blue). Rods are sometimes presented perpendicular to the nucleus (long arrows) or adjacent to the nuclear envelope (short arrows). Rings (arrowheads) and other transition structures (double arrowhead) are found either 1 or 2 to a cell. Scale bar, 10 µm.

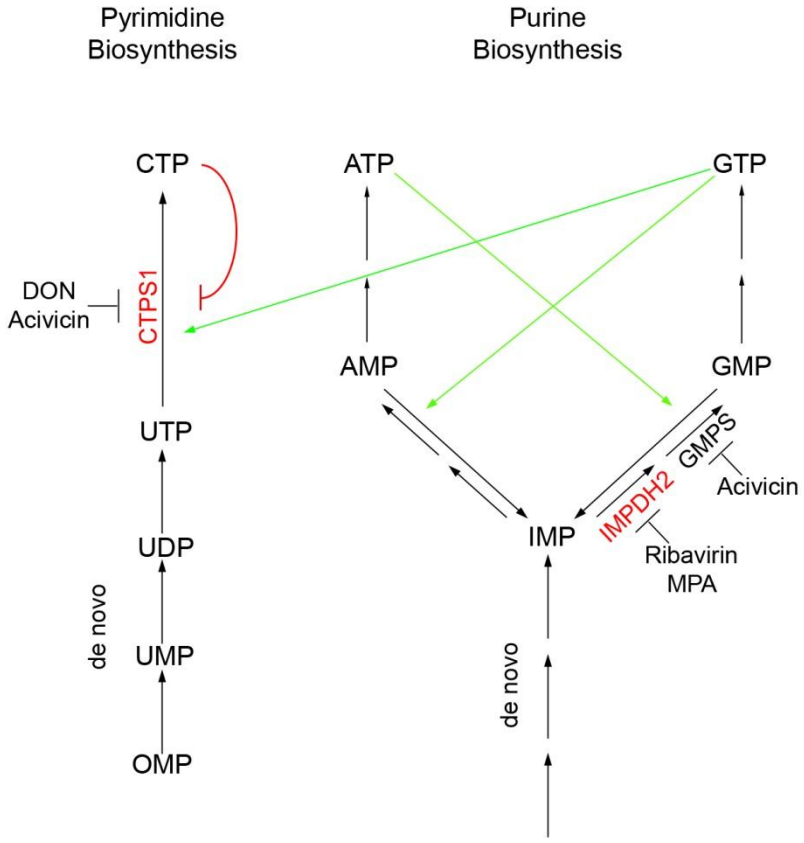

Figure 6-2. A schematic of RR components CTPS1 and IMPDH2 along the purine and pyrimidine biosynthesis pathways. RR components are shown in red. IMPDH2 is an enzyme involved in the GTP biosynthesis pathway catalyzing the conversion of IMP to GMP that is a precursor to the production of GTP. CTPS1 is an enzyme involved in the CTP biosynthesis pathway and catalyzes the conversion of UTP to CTP. The site of inhibition is indicated for DON, acivicin, ribavirin and MPA. Arrows signify a step in the pathway. Green arrows signify activation of pyrimidine and purine biosynthesis pathways by ATP and GTP. Red arrow signifies inhibition of pyrimidine biosynthesis pathway by end product CTP. The pathway schematic is adapted from Hofer *et al. (57).*

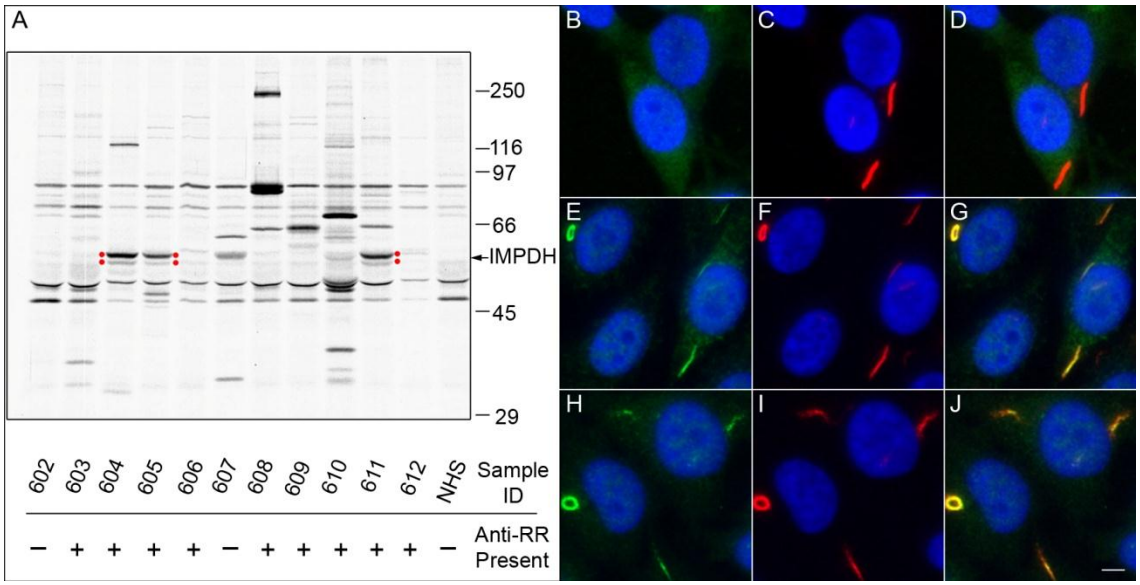

Figure 6-3. Patient autoantibodies recognize multiple components of RR. A) Immunoprecipitation of K562 cell lysates using hepatitis C patient sera 602-612 and correlation with the presence of anti-RR antibodies by immunofluorescence. Sera 604, 605, and 611 show common 55kDa doublet (red dots) corresponding to IMPDH and they are also positive for anti-RR antibodies. In contrast, sera 603, 606, 608, 609, 610, and 612 have anti-RR antibodies but do not immunoprecipitate the 55kDa band. To confirm RR detected from patients was all the same structure, double staining of HEp-2 cells was performed with rabbit anti-IMPDH2 C, F, I) and serum 607(anti-RR negative, B), serum 609 (anti-RR positive but did not immunoprecipitate the 55kDa doublet, E), or serum 611 (anti-RR positive and immunoprecipitated the 55kDa doublet, H). Since RR is recognized by both serum 611 and 609, serum 609 most likely recognizes other unidentified RR component(s). Nuclei are counterstained with DAPI. D, G, J, merged images. Scale bar, 10 µm.

Table 6-1. Comparison of various reported RR-like cytoplasmic filament structures.

Investigator	Rods/rings; Components	Sizes	Induction method	Detection	Species/cell types			
Carcamo *et al.* (122)	both detected; CTPS1, IMPDH2	3-10 µm rod length; 2-5 µm ring diameter	CTPS1 and IMPDH2 inhibitors: DON, acivicin, ribavirin	IMDPH2 and CTPS1 antibodies and human autoantibodies	Human: HeLa, HEp-2, K562, HCT116; mouse 3T3, primary cardiomyocytes, fibroblasts, ESCs	Similarities vs. Carcamo *et al.* (122)	Differences vs. Carcamo *et al.* (122)	Other comments
Willingham *et al.* (81)	both detected; nematin, 58kDa	0.5-3 µm rod length	not induced	mouse IgG3 mAb	human KB; bovine MDBK; rat NRK; mouse 3T3	Not enriched in vimentin or tubulin Prevalent in newly thawed cells Fixation methods affect structure	mAb stains mouse skin and CNS Not abundant in human cell lines	
Ji *et al.* (59)	both detected; IMPDH	0.1->1 µm in diameter	IMPDH2 inhibitor MPA	IMPDH antibody	Human: MCF7, CEM, K66/B5	Untreated cells show IMPDH disperse in cytoplasm Aggregates appear 30 min after MPA treatment; mature rods by 24 h No association with other organelles	Mobility shift of IMPDH after MPA treatment by Western	Rods disassemble in cells added guanosine, guanine, GMP,GDP,GTP MPA causes aggregation of IMPDH on polylysine-coated glass slides
Liu (77)	both detected as cytoophidia; CTPS	<1-50 µm rod length, depends on stages	not induced	three CTPS antibodies, GFP-CTPS	Drosophila follicle cells, nurse cells, oocytes	Cytoophidia are not associated with centrioles	CTPS functional in cytoophidium Associated with the microtubular network but do not overlap	
Chen *et al.* (155)	both detected; CTPS	2-10 µm rod length	CTPS inhibitor DON	CTPS antibody	Human HeLa P4	DON increases the formation of cytoophidia	Only 40% RR can be induced at 4µg/mL of DON	DON induced apoptosis and induced filament formation in Drosophila ovaries
Noree *et al.* (83)	only rods; CTPS Ura7p	0.5-3 µm length	nutrient deprivation or inhibition of CTPS	GFP-protein in yeast	S. cerevisiae, D. melanogaster	Filament formation is due to regulation of enzymatic activity	The tag on the protein does not affect the formation of the filament	Kinase inhibitor staurosporine increased filament formation
Ingerson-Mahar *et al.* (82)	only rods; CTPS	390-790 nm length	not induced or CTPS over-expression	mcherry-CTPS	C. crescentus, E. coli		DON disrupts rods Overexpression increase length of rods	CTPS interacts with CreS

CHAPTER 7
SUMMARY AND PERSPECTIVE

Biological Function of RR Structure

Rod Versus Ring Configurations

As described in Chapter 2, the cytoplasmic structure provisionally named rods and rings was identified using HCV patient sera. The rods and rings are distinct structures visualized via indirect immunofluorescences. It is unknown whether rods and rings have different function; however, it is reasonable to consider that there is interconversion between rods and rings. This speculation is derived in part from the intermediate structures (Figure 2-2) that are observed via immunofluorescences. Although, rods and rings were induced in various cells lines, there are differences in size and the fractions of cells forming rods versus rings. HeLa cells were determined to have rods measuring 5-10 µm while THP-1 cells formed shorter rods, measuring 2-3 µm. Additional data suggests that the structures start off short and increase in size until reaching full/mature size of 5-10 µm; this was described in Chapter 5 using glutamine deprivation to induce RR (Figure 5-2).

Induced Versus Native RR

As described in Chapter 2, RR can be induced in cancer cells and primary cells using IMPDH2/CTPS1 inhibitors in as short as 15 minutes with IMPDH inhibitors and 3 hours with CTPS inhibitors. Figure 7-1 summarizes the putative formation of RR using IMPDH2/CTPS1 inhibitors and the induction time required for the formation of mature RR. Additionally, RR can be induced in cancer cells via glutamine deprivation after 48 hours as illustrated in Chapter 5. However, RR are observed in almost 100% of cultured undifferentiated mouse embryonic stem cells without the addition of inhibitors or

treatment to induce glutamine deprivation. Since mouse ESCs are highly active in cell division, this suggests different functional role for RR in these cells. RR structures induced with CTPS1/IMPDH2 inhibitors or by glutamine deprivation as well as RR in mESCs can be detected with patient anti-RR sera, anti-IMPDH2, and anti-CTPS1 antibodies, suggesting that induced RR versus native RR are similar structures. However, it is unclear whether they have the same molecular composition, due to observed differences in the ratio of rods to rings in cells that are induced versus native RR. Rods and rings, as independent structures, may hold different functions as 91% of ESCs form rings while cells that are treated with CTPS/IMPDH inhibitors or deprived of glutamine have 90% rods (Table 7-1). After induction of RR with CTPS1/IMPDH2 inhibitors proliferation is decreased, this is observed clearly with a decrease in number of mitotic cells after treatment with inhibitors compared to controls. While ESCs that form RR have a higher percentage of rings (~91%) and have a high proliferation rate, IMPDH2 and CTPS1 associated with RR may be active as these enzymes are required for cell proliferation (56,163). A hypothetical schematic for RR formation is shown in Figure 7-2. RR that are formed after inhibition with CTPS1/IMPDH2 inhibitors are aggregated proteins that have the active sites blocked by the inhibitor shown in red (Figure 7-2). However, RR in ESCs may be composed of active enzymes because although the same structures are observed, inhibitors are not present to block the active sites (Figure 7-2). Additionally, ESCs express more rings than rods suggesting that rings may be aggregates of active enzymes. RR induced via glutamine deprivation may also be composed of active enzymes (Figure 7-2). However, RR formed during glutamine deprivation could be in response to blocking of enzymatic activity of certain

enzymes such as CTPS1, which requires glutamine to produce CTP. Since production of CTP and GTP is still required for cells to survive, some structures may be composed of active enzymes. Therefore, rods and rings induced by CTPS1 and IMPDH2 inhibitors may be composed of the inactive enzymes while rods and rings observed in untreated rapidly proliferating cells or induced in response to glutamine deprivation may be composed of active enzymes.

Attempts to Identify Additional Components in RR

As stated above, rods and rings are composed of IMPDH2 and CTPS1, and likely to include other enzymes involved in purine and pyrimidine biosynthesis pathways. Due to the large size of the RR structure, we speculate that RR may be composed of other additional components. For example, in GW bodies which are known range from 0.1 to 0.3 μm in diameter, more than 10 proteins have been identified (10,121) . With rods being ~3-10 μm in length and rings ~2-5 μm in diameter, it is very reasonable to postulate that RR are composed of additional enzymes involved in nucleotide biosynthesis. There is experimental support for this consideration because RR formation was observed in cells that were treated with 10 μM pemetrexed for 24 hours. Pemetrexed is a chemotherapeutic drug that inhibits thymidine synthetase, dihydrofolate reductase, glycinamide ribonucleotide formyltransferase (GARFT), and aminoimidazole carboxamide ribonucleotide formyltransferase (AICARFT). The fact that pemetrexed induced RR formation in HeLa cells suggests that some of these enzymes are components of RR. Thymidine synthetase was an interesting candidate RR protein for obvious reason because it is the critical enzyme for the production of thymidine triphosphate (TTP). Additional thymidine synthetase inhibitors, 5-Fluorouracil and gemcitibane, were also tested but they did not induce RR formation. Also we were not

able to detect RR using a mouse antibody to thymidine synthetase (TS antibody generously provided by Dr. Maria Zajac-Kaye); however, this data cannot completely rule out TS may still be localized to RR. Similarily, rabbit anti-dihydrofolate reducatase antibody (E18220, Spring Bioscience; Pleasanton, CA, USA) was unable to detect RR formed after treatment with pemetrexed. Thus, it remains necessary to examine whether RR may be composed of GARFT or AICARFT enzymes involved in purine biosynthesis pathway (Figure 7-3). In addition, these enzymes may also be affected by glutamine deprivation, although they do not require the use of glutamine, other steps before and after in the same purine biosynthetic pathway require glutamine (Figure 5-4). Interfering with enzymes within the purine biosynthesis pathways will likely have an effect on others enzymes within the pathway; therefore, glutamine might have an indirect effect on GARFT and AICARFT.

RR that are induced by CTPS/IMPDH inhibitors are readily dissociated after cell lysis with detergents, such as 0.3% Nonidet P40 and 0.5% triton-X; therefore, attempts to purify RR for the identification of additional components using mass spectroscopy has not been feasible to date. However, crosslinking RR may help stabilize these structures and allow immunoaffinity purification and identification of additional components via mass spectroscopy. In order to isolate RR, we have used a homobifunctional cleavable crosslinker dimethyl 3,3' -dithiobispropionimidate·2HCl (Cat# 20665; Thermo Scientific; Rockford, IL, USA). The cleavable crosslinker should allow us to isolate intact RR that can then be analyzed to identify novel components by mass spectroscopy. If these components are the proposed enzymes as discussed above, they can be verified as RR components by using inhibitors to those enzymes to

detect whether RR are formed. Many antibodies of known RR components would not recognize RR, as shown in Table 7-2. This inability of certain antibodies to recognize RR structures may depend on the conformational changes of the individual component; therefore, verification with an inhibitor, if the component is an enzyme or other antibodies is required.

Cytoplasmic Versus Nuclear RR

In addition to the cytoplasmic RR structures discuss so far, recent data show RR were detected within the nucleus. Nuclear RR are observed after treatment of CTPS1 or IMPDH2 inhibitors or glutamine deprivation; although they are located within the nucleus they may be similar to cytoplasmic RR. Multiple z-stack images of a nucleus containing a short rod clearly demonstrated the structure within the nucleus (Figure 7-4); additional cells were observed with rings within the nucleus. These rod and ring structures were present within the nucleus and were co-stained by both patient autoantibodies and rabbit anti-IMPDH2 antibody (data not shown). Nuclear rods were determined to range in size from 1.6 µm to 4.5 µm, while cytoplasmic rods were from 2.5 µm to 16.8 µm when counted from the same cell preparations. The mean size of cytoplasmic rods was 8.4 µm and the mean size of nuclear rods was 3.2 µm. This was determined by quantitating nuclear and cytoplasmic RR from 66 cells. Nuclear rods were substantially shorter than cytoplasmic rods. Although nuclear rods and cytoplasmic rods are highly similar structures, it is unknown whether they have the same function due to the difference in their subcellular locations. Studies suggest that IMPDH binds single stranded RNA/DNA and modulate localization or degradation of a set of mRNAs (175,176).

Technical Difficulties in RR Detection

The study of RR formation and function has been limited by several obstacles. First, detection of RR antibodies in patient sera depends on the commercial ANA slides used. Most ANA slides do not give RR staining; for example ANA slides from INOVA diagnostics, Inc. (San Diego, CA) consistently give RR staining with our prototype anti-RR serum but ANA slides from Immuno Concepts (Sacramento, CA) are negative. After determining that RR can be induced with glutamine deprivation, we speculate that RR detected in INOVA slides may be due to techniques used to increase proliferation and therefore may cause limitations in availability of nutrients in medium. Additionally, not all antibodies can detect the apparently conformational epitope(s) expressed on the RR structures as compared to monomeric proteins in the cytoplasm. Table 7-2 includes all the available antibodies we have tested for their ability to recognize RR on INOVA or home-made slides to date. While all the antibodies can detect monomeric proteins by Western blot only one anti-IMPDH2 antibody was able to detect RR structures. Liu detected RR-like structures in Drosophila using an anti-CTPS1 antibody (77). However, the same anti-CTPS1 antibody did not detect RR when tested in our laboratory and this was apparently because of lot-to-lot variation and that not all lots were able to detect RR. Therefore, inability of RR detection with an antibody does not rule out that the protein as being part of the RR structure.

Clinical Implication of Anti-RR

Ribavirin as a Therapeutic Agent

Ribavirin is believed to be the cause for RR formation in HCV patients who have undergone months of therapeutic exposure, leading to the production of anti-RR autoantibodies. Due to ribavirin induction of RR *in vitro*, it is unknown whether ribavirin

alone or the co-exposure to interferon in HCV treatment is required for the production of anti-RR in selected patients. Ribavirin is only approved for the treatment of HCV; however it is currently in trial for the treatment of other viral infections. Although there are a few cases of patients with anti-RR antibodies that do not have HCV, anti-RR antibodies in HCV patients is highly correlated to the effects of ribavirin treatment, leading to RR formation and stimulation of the host immune system.

MPA as a Therapeutic Agent

MPA is currently used for the treatment of systemic lupus erythematosus and to prevent organ rejection. Although MPA has been shown to induce RR formation *in vitro*, lupus patients treated with MPA do not develop anti-RR antibodies, with just one exception to our knowledge. Interestingly, lupus patients are also often continuously exposed to type I interferon, the cytokine that is playing a major role in the disease pathogenesis (177,178). Thus, continuous exposure of interferon does not help induce anti-RR antibodies in lupus patients undergoing MPA treatment. This suggests that the inhibitor of IMPDH alone is not sufficient to induce autoantibody formation and additional factors are likely required.

Development of RR Antibodies and Resistance to Treatment

We have determined that a subset of patients that develop anti-RR antibodies either are non-responsive to therapy or relapse. It was previously determined that equilibrative nucleoside transporter 1 (ENT1), the known transporter for ribavirin from extracellular source into cytoplasm, becomes resistance after exposure to ribavirin and prevents further transport of ribavirin into the cell (132). Studies using other IMPDH inhibitors have determined that ENT1 becomes resistant to transport after cells are treated with IMPDH inhibitors (179). ENT1 is sensitive to inactivation via IMPDH

inhibitors. Since ribavirin induces formation *in vitro* in all cell types, we speculate that there is a linkage between RR and ENT1 that leads to patients becoming non-responders or relapsers after therapy. After a patient is infected by HCV, cells may have varying levels of HCV (Figure 7-5A). When the patient is treated with interferon-alpha and ribavirin, this leads to the formation of RR within some hepatocytes, ribavirin may be utilized by the virus and may not be present at a high enough concentration to induce RR formation in infected cells (Figure 7-5B). RR may either interact directly with ENT1 or indirectly with activation proteins, such as protein kinase C (180,181) and thus inactivate further uptake of ribavirin. Additional studies have identified that ribavirin treatment can decrease the mRNA levels of protein kinase C, this decrease due to ribavirin may cause the ENT1 resistance (182). For the cells that were infected and received ribavirin treatment, some become virus free as to be expected (Figure 7-5C). After continuous treatment, cells that have formed RR may be resistant to further uptake of ribavirin, allowing the infection to spread. The infection that has remained may then spread to all cells causing the patient to have a negative outcome to the interferon-alpha and ribavirin therapy (Figure 7-5D). In other words, patients with more RR-positive hepatocytes will likely induce autoantibodies to RR and become at a later time resistant to viral clearance. This hypothesis can be tested by pretreating cells with ribavirin to induce RR formation and cause cellular resistance in the pretreated cells and then infecting with HCV as shown in Figure 7-6. Pretreating hepatocytes with ribavirin will help simulate the *in vitro* effect that not all cells are infected in HCV infected patients at time of treatment. Untreated cells (Figure 7-6A) and ribavirin treated cells are left overnight for the induction of RR (Figure 7-6B) and both will then be infected with HCV.

Infected cells will be treated with ribavirin. If ribavirin causes ENT1 resistance due to presence of RR then viral RNA will be detected at high levels in cell with RR after ribavirin treatment. While cells that are not pretreated with ribavirin will clear the virus after ribavirin treatment.

We also speculate that anti-RR antibodies production is resulted from interactions of HCV viral proteins/RNA with ribavirin-induced RR. Ribavirin has a similar chemical structure as GTP (Figure 7-7 A vs B). Since IMPDH2 is inhibited by ribavirin and can induce RR formation, we speculate that viral proteins may bind to IMPDH2 with or without ribavirin in RR (Figure 7-7C-D). The viral proteins that may interact with RR are HCV structural and non-structural proteins such as core, E1, E2, p7, NS2, NS3, NS4A, NS4B, NS5A and NS5B. Our data has shown that approximately 20% of HCV patients develop anti-RR antibodies (139), while the other 80% do not develop these specific antibodies. This observation can be related to the genetic background of individual patients. However, development of anti-RR may be due to an intracellular level of IMPDH2. We previously determined that cells overexpressing IMPDH2 do not form RR (Figure 2-8). If overexpression of IMPDH2 prevents formation of RR, it may also prevent formation of RR within patients and lead to the prevention of development of anti-RR antibodies. Therefore, the heterogeneity of patients and levels of IMPDH2 may contribute to the variable development of anti-RR antibodies. HCV viral protein/RNA-RR complexes may be recognized by the host immune system and the productive immune response target the viral protein/RNA complex but also develop autoantibody to RR from epitope spreading or simply crossreaction.

Conclusions

Rods and rings were identified using human autoantibodies produced by HCV patients treated with interferon-alpha and ribavirin. HCV patients that do not respond to therapy or develop relapse tend to have higher anti-RR antibody titers. RR were determined to be composed of nucleotide biosynthesis enzymes: CTPS1 and IMPDH2. We speculate that RR are composed of additional nucleotide biosynthetic enzymes, such as GARFT or AICARFT. RR currently formed from the inhibition of CTPS1 or IMPDH2 or in response to depletion of glutamine, are consistently correlated to a decrease in intracellular levels of CTP/GTP. Therefore, RR may represent polymerization of nucleotide biosynthetic enzymes in response to decrease in intracellular CTP or GTP levels in order to increase CTP/GTP levels necessary for cellular function. This working hypothesis will require further experiments.

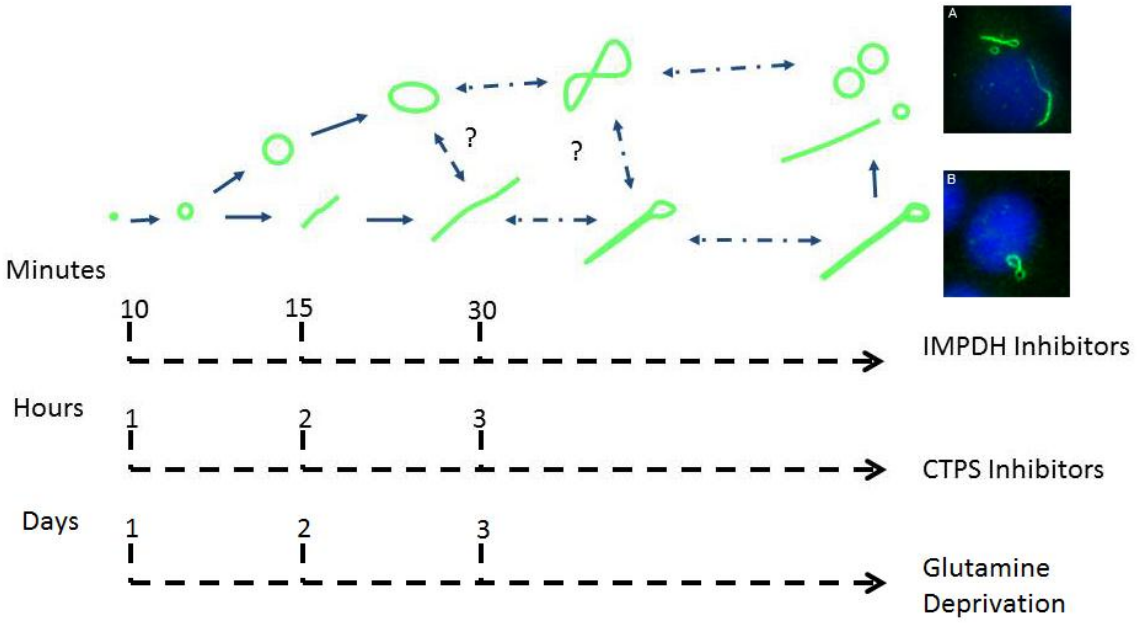

Figure 7-1. RR induction pathway showing hypothetical exchange between rods and rings. This figure summarizes the overall timeline when IMPDH and CTPS inhibitors or glutamine deprivation induce the formation of RR in different cell lines. Some RR structures maybe interchangeable as indicated by double sided arrows. The timelines indicate induction time for RR using IMPDH inhibitors, ribavirin or mycophenolic acid (MPA), CTPS inhibitors 6-diazo-5-oxo-L-norleucine (DON) or acivicin, and by glutamine deprivation. Representatives RR intermediate structures sewing pin A) and the figure "8" B) are shown respectively as described in Carcamo *et al*. (122).

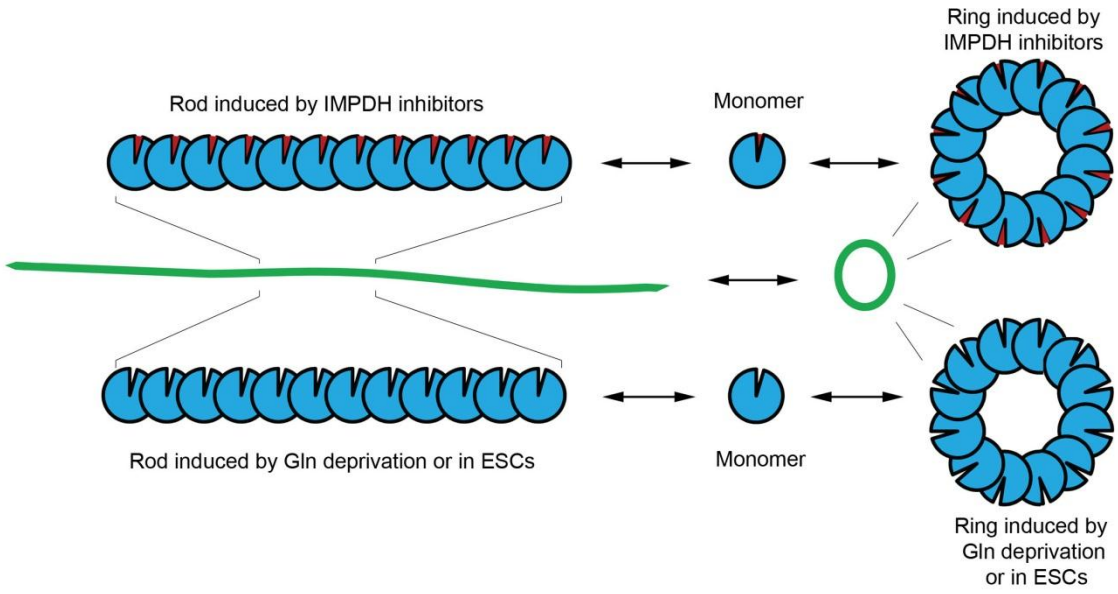

Figure 7-2. Schematic of RR assembly. Rods and rings formed from monomers after induction with CTPS/IMPDH inhibitors (red inserts). RR may also form from monomers without inhibitors as in ESCs or after glutamine deprivation. These represent a detail view of rods and rings (green).

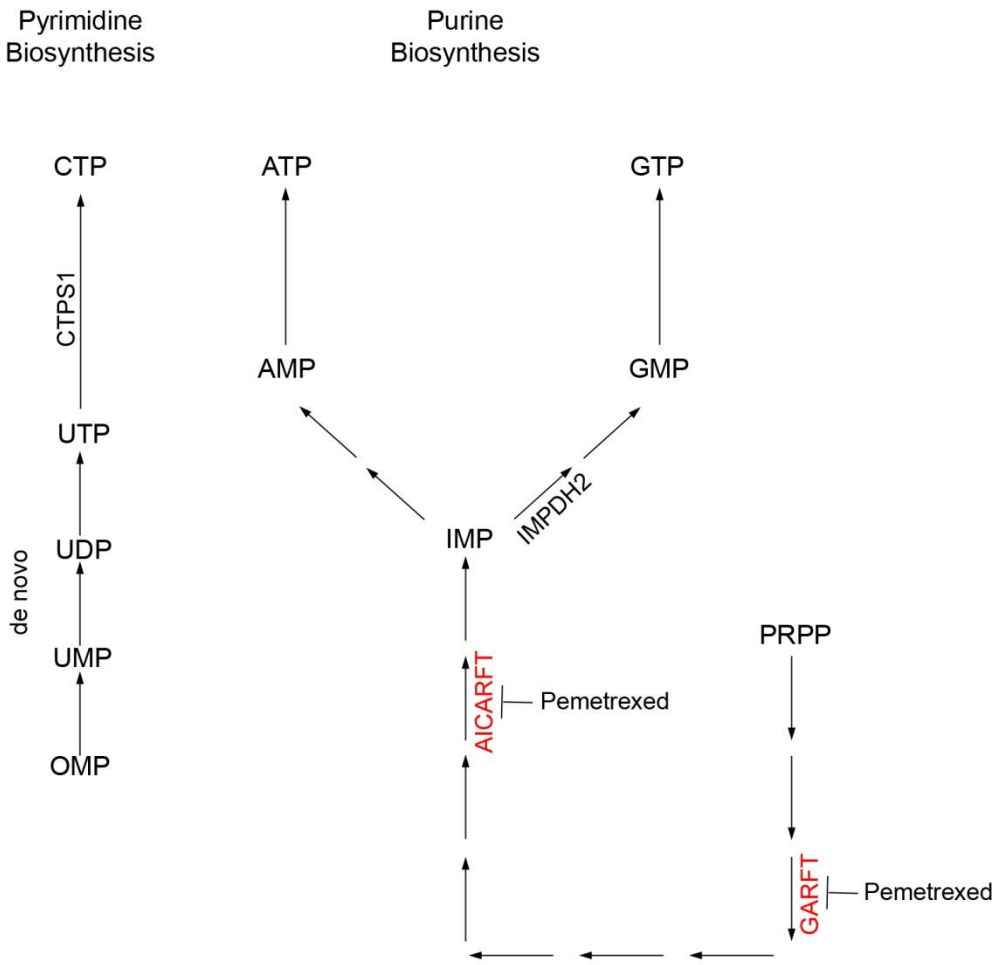

Figure 7-3. A schematic of putative RR components AICARFT and GARFT along the purine and pyrimidine biosynthesis pathways. Putative RR components are shown in red. The site of inhibition is indicated for pemetrexed. Arrows signify a step in the pathway. The pathway schematic is adapted from Hofer *et al.* (57).

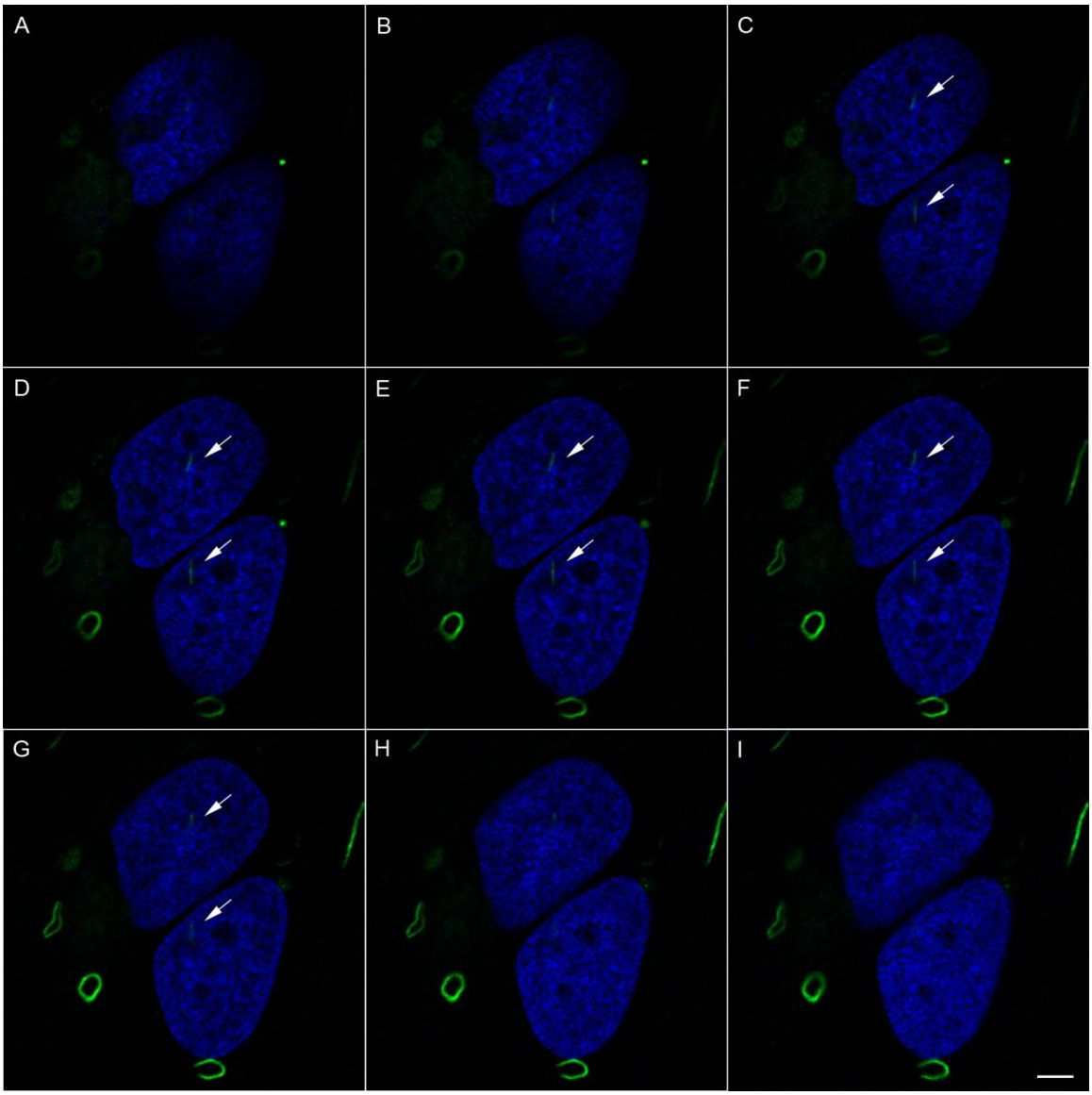

Figure 7-4. Rods and rings located within the nucleus. HeLa cells treated with DON form RR detected by human It2006 (green).A-I) A confocal z-stack cuttings of rod within nucleus. 0.39 µm thickness per section. Arrow signifies location of visible nuclear RR. Nuclei are counterstained with DAPI. Scale bar 5 µm.

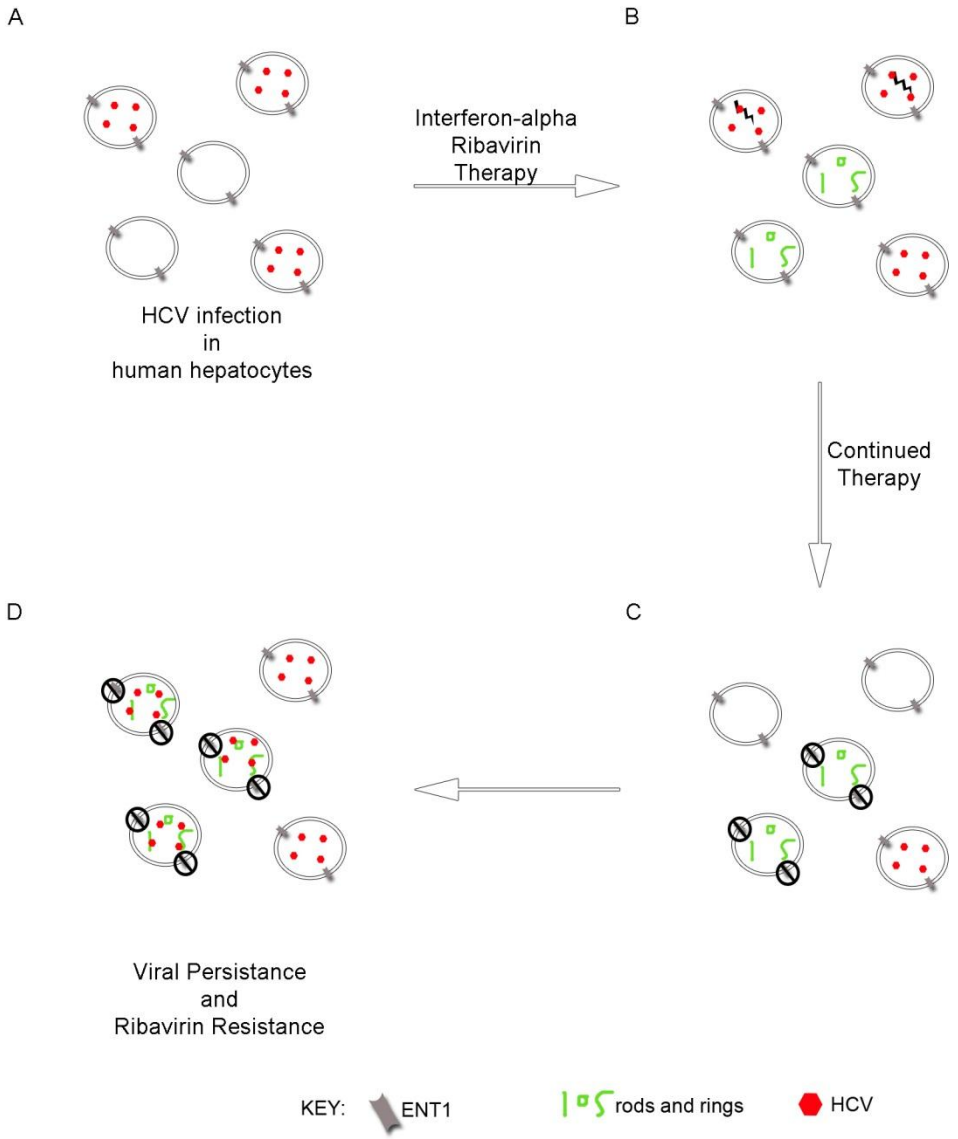

Figure 7-5. Hypothetical role of ENT1 contributing to resistance to ribavirin therapy and HCV viral persistence *in vivo*. A) After HCV infection some hepatocytes are infected with virus while others are not infected. B) Patient then receives pegylated-interferon-alpha and ribavirin therapy, causes RR formation in uninfected cells. C) Therapy is continued and clears virus from some cells and yet causes resistance to ribavirin in cells with RR. D) Virus replicated and infects cells with RR, which are resistant to ribavirin and viral persistence occurs.

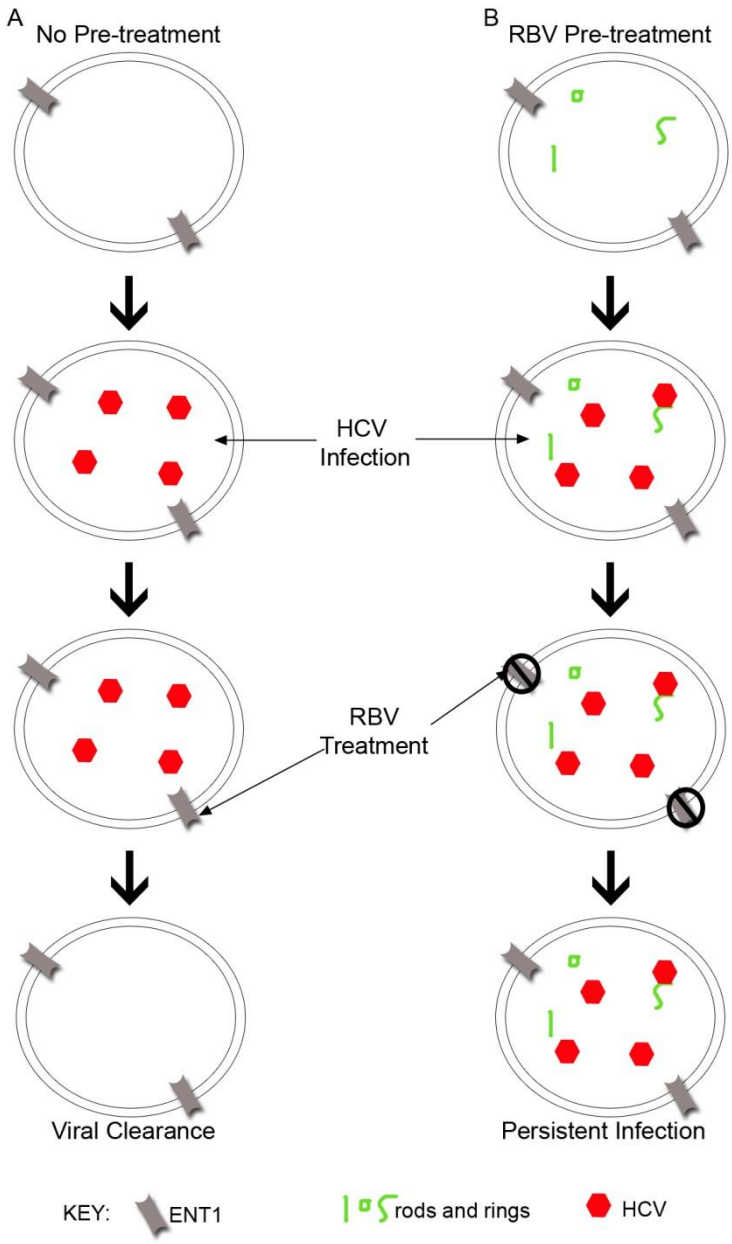

Figure 7-6. Experimental schematic to test whether ENT1 resistance is linked to viral persistence. A) The hepatocyte is not pre-treated and then gets infected with HCV. After viral infection it receives ribavirin treatment. After treatment viral infection is cleared. B) The hepatocyte is pre-treated with ribavirin to induce RR and then gets infected with HCV. After viral infection it receives ribavirin treatment. After treatment viral infection persists. Each column represents one cell, which represents multiple cells.

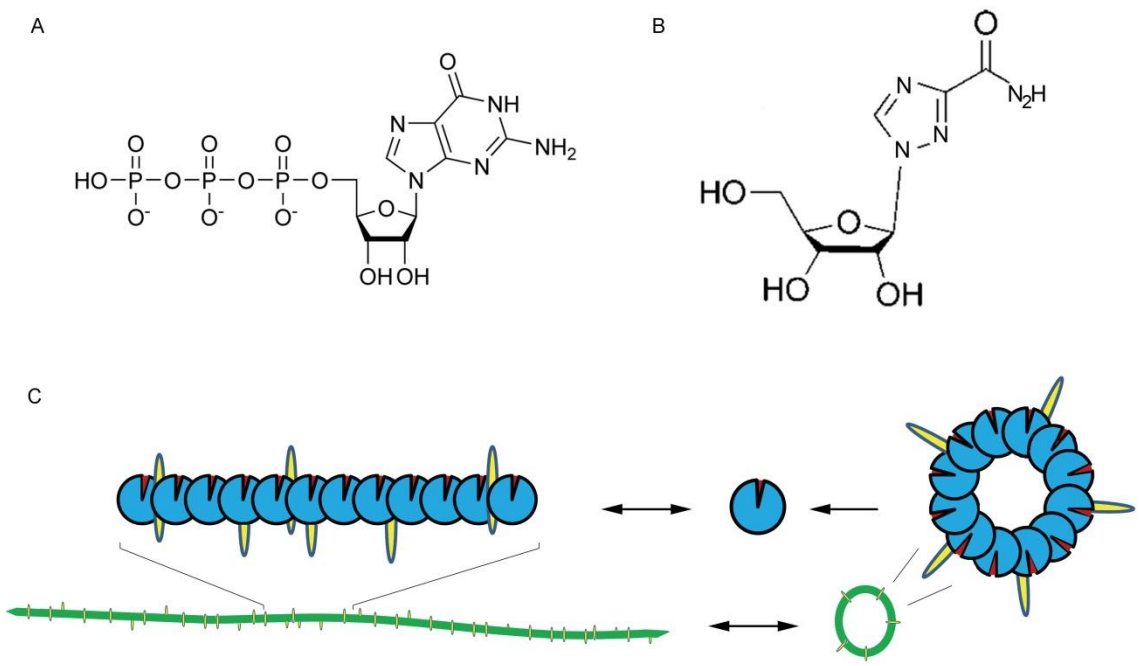

Figure 7-7. Postulation of HCV antigens associated with RR. A) Structure of GTP and B) ribavirin. C) Schematic of HCV viral protein or viral RNA (yellow spikes) interacting with rod or ring (blue) induced to form from exposure to ribavirin (red).

Table 7-1. Methods of RR induction and quantification of rods vs rings.

Induction Method	Cell Types	Rods vs rings percentage
IMPDH/CTPS inhibitors	Cancer and primary cell lines	90% rods
Glutamine Deprivation	HeLa	90% rods
Uninduced	ESCs	91% rings

Table 7-2. Antibodies tested for RR detection by direct immunofluorescence.

Investigator	Rods/rings; Components	Sizes	Induction method	Detection
IMPDH2	Rabbit	Abcam	Ab75790	NO
IMPDH2	Rabbit	Proteintech	12948-1-AP	YES-1:100
CTPS1	Rabbit	Abcam	Ab65045	NO
CTPS1	Rabbit	Proteintech	15914-1-AP	NO
CTPS1	Mouse	Sigma-Aldrich	WH0001503M1	NO
CTPS1	Rabbit	Santa Cruz	Sc-101925	NO (lot specific*)
TS-106	Mouse	Not a commercial antibody		NO
DHFR	Rabbit	Spring Bioscience	E18220	NO
UMPS	Mouse	Abgent	AT4467a	NO
PCYT1A	Mouse	Abgent	AT3244a	NO

*CTPS1 antibody from Santa Cruz was tested 3 times due to inconsistent reports; Liu reported that this antibody detected RR (77). However, we determined that detection of RR with this antibody was lot specific and only one lot was able to detect RR while another lot could only detect RR at 1:50 and were very faint required co-staining to visualize RR.

LIST OF REFERENCES

1. Tan, E.M. (1989) Antinuclear antibodies: diagnostic markers for autoimmune diseases and probes for cell biology. *Advances in immunology*, **44**, 93-151.

2. Tan, E.M. (1991) Autoantibodies in pathology and cell biology. *Cell*, **67**, 841-842.

3. Tan, E.M., Chan, E.K., Sullivan, K.F. and Rubin, R.L. (1988) Antinuclear antibodies (ANAs): diagnostically specific immune markers and clues toward the understanding of systemic autoimmunity. *Clinical immunology and immunopathology*, **47**, 121-141.

4. Fritzler, M.J. (1993) Autoantibodies in scleroderma. *The Journal of dermatology*, **20**, 257-268.

5. Chan, E.K. and Andrade, L.E. (1992) Antinuclear antibodies in Sjogren's syndrome. *Rheumatic diseases clinics of North America*, **18**, 551-570.

6. Tillman, D.M., Jou, N.T., Hill, R.J. and Marion, T.N. (1992) Both IgM and IgG anti-DNA antibodies are the products of clonally selective B cell stimulation in (NZB x NZW)F1 mice. *The Journal of experimental medicine*, **176**, 761-779.

7. Radic, M.Z. and Weigert, M. (1994) Genetic and structural evidence for antigen selection of anti-DNA antibodies. *Annual review of immunology*, **12**, 487-520.

8. Hardin, J.A. (1986) The lupus autoantigens and the pathogenesis of systemic lupus erythematosus. *Arthritis and rheumatism*, **29**, 457-460.

9. Andrade, L.E., Chan, E.K., Raska, I., Peebles, C.L., Roos, G. and Tan, E.M. (1991) Human autoantibody to a novel protein of the nuclear coiled body: immunological characterization and cDNA cloning of p80-coilin. *The Journal of experimental medicine*, **173**, 1407-1419.

10. Eystathioy, T., Chan, E.K., Tenenbaum, S.A., Keene, J.D., Griffith, K. and Fritzler, M.J. (2002) A phosphorylated cytoplasmic autoantigen, GW182, associates with a unique population of human mRNAs within novel cytoplasmic speckles. *Mol Biol Cell*, **13**, 1338-1351.

11. Alderuccio, F., Chan, E.K. and Tan, E.M. (1991) Molecular characterization of an autoantigen of PM-Scl in the polymyositis/scleroderma overlap syndrome: a unique and complete human cDNA encoding an apparent 75-kD acidic protein of the nucleolar complex. *The Journal of experimental medicine*, **173**, 941-952.

12. Chan, E.K., Imai, H., Hamel, J.C. and Tan, E.M. (1991) Human autoantibody to RNA polymerase I transcription factor hUBF. Molecular identity of nucleolus organizer region autoantigen NOR-90 and ribosomal RNA transcription upstream binding factor. *The Journal of experimental medicine*, **174**, 1239-1244.

13. Chan, E.K.L. and Fritzler, M.J. (1998) In Conrad, K., Humbel, R. L., Meurer, M., Shoenfeld, Y. and Tan, E. M. (eds.). Pabst Science Publishers, Lengerich, Germany, pp. 85-100.

14. Hoofnagle, J.H. (2002) Course and outcome of hepatitis C. *Hepatology*, **36**, S21-29.

15. (2002) National Institutes of Health Consensus Development Conference Statement: Management of hepatitis C 2002 (June 10-12, 2002). *Gastroenterology*, **123**, 2082-2099.

16. Alter, H.J. and Seeff, L.B. (2000) Recovery, persistence, and sequelae in hepatitis C virus infection: a perspective on long-term outcome. *Seminars in liver disease*, **20**, 17-35.

17. Charlton, M. (2001) Hepatitis C infection in liver transplantation. *American journal of transplantation : official journal of the American Society of Transplantation and the American Society of Transplant Surgeons*, **1**, 197-203.

18. Seeff, L.B. (1997) Natural history of hepatitis C. *Hepatology*, **26**, 21S-28S.

19. Foy, E., Li, K., Wang, C., Sumpter, R., Jr., Ikeda, M., Lemon, S.M. and Gale, M., Jr. (2003) Regulation of interferon regulatory factor-3 by the hepatitis C virus serine protease. *Science*, **300**, 1145-1148.

20. Fried, M.W., Shiffman, M.L., Reddy, K.R., Smith, C., Marinos, G., Goncales, F.L., Jr., Haussinger, D., Diago, M., Carosi, G., Dhumeaux, D. *et al.* (2002) Peginterferon alfa-2a plus ribavirin for chronic hepatitis C virus infection. *The New England journal of medicine*, **347**, 975-982.

21. Hadziyannis, S.J., Sette, H., Jr., Morgan, T.R., Balan, V., Diago, M., Marcellin, P., Ramadori, G., Bodenheimer, H., Jr., Bernstein, D., Rizzetto, M. *et al.* (2004) Peginterferon-alpha2a and ribavirin combination therapy in chronic hepatitis C: a randomized study of treatment duration and ribavirin dose. *Annals of internal medicine*, **140**, 346-355.

22. Manns, M.P., McHutchison, J.G., Gordon, S.C., Rustgi, V.K., Shiffman, M., Reindollar, R., Goodman, Z.D., Koury, K., Ling, M. and Albrecht, J.K. (2001) Peginterferon alfa-2b plus ribavirin compared with interferon alfa-2b plus ribavirin for initial treatment of chronic hepatitis C: a randomised trial. *Lancet*, **358**, 958-965.

23. Kau, A., Vermehren, J. and Sarrazin, C. (2008) Treatment predictors of a sustained virologic response in hepatitis B and C. *J Hepatol*, **49**, 634-651.

24. Smith, K.R., Suppiah, V., O'Connor, K., Berg, T., Weltman, M., Abate, M.L., Spengler, U., Bassendine, M., Matthews, G., Irving, W.L. *et al.* (2011) Identification of improved IL28B SNPs and haplotypes for prediction of drug response in treatment of hepatitis C using massively parallel sequencing in a cross-sectional European cohort. *Genome medicine*, **3**, 57.

25. Simmonds, P., Bukh, J., Combet, C., Deleage, G., Enomoto, N., Feinstone, S., Halfon, P., Inchauspe, G., Kuiken, C., Maertens, G. *et al.* (2005) Consensus proposals for a unified system of nomenclature of hepatitis C virus genotypes. *Hepatology*, **42**, 962-973.

26. Choo, Q.L., Kuo, G., Weiner, A.J., Overby, L.R., Bradley, D.W. and Houghton, M. (1989) Isolation of a cDNA clone derived from a blood-borne non-A, non-B viral hepatitis genome. *Science*, **244**, 359-362.

27. Lauer, G.M. and Walker, B.D. (2001) Hepatitis C virus infection. *The New England journal of medicine*, **345**, 41-52.

28. Dustin, L.B. and Rice, C.M. (2007) Flying under the radar: the immunobiology of hepatitis C. *Annual review of immunology*, **25**, 71-99.

29. Rosenberg, S. (2001) Recent advances in the molecular biology of hepatitis C virus. *Journal of molecular biology*, **313**, 451-464.

30. Op De Beeck, A. and Dubuisson, J. (2003) Topology of hepatitis C virus envelope glycoproteins. *Reviews in medical virology*, **13**, 233-241.

31. Kato, N. (2000) Genome of human hepatitis C virus (HCV): gene organization, sequence diversity, and variation. *Microbial & comparative genomics*, **5**, 129-151.

32. Ohba, K., Mizokami, M., Lau, J.Y., Orito, E., Ikeo, K. and Gojobori, T. (1996) Evolutionary relationship of hepatitis C, pesti-, flavi-, plantviruses, and newly discovered GB hepatitis agents. *FEBS Lett*, **378**, 232-234.

33. Penin, F., Dubuisson, J., Rey, F.A., Moradpour, D. and Pawlotsky, J.M. (2004) Structural biology of hepatitis C virus. *Hepatology*, **39**, 5-19.

34. Lohmann, V., Koch, J.O. and Bartenschlager, R. (1996) Processing pathways of the hepatitis C virus proteins. *Journal of hepatology*, **24**, 11-19.

35. Bartenschlager, R. and Lohmann, V. (2000) Replication of hepatitis C virus. *The Journal of general virology*, **81**, 1631-1648.

36. Evans, M.J., von Hahn, T., Tscherne, D.M., Syder, A.J., Panis, M., Wolk, B., Hatziioannou, T., McKeating, J.A., Bieniasz, P.D. and Rice, C.M. (2007) Claudin-1 is a hepatitis C virus co-receptor required for a late step in entry. *Nature*, **446**, 801-805.

37. Bartosch, B. and Cosset, F.L. (2006) Cell entry of hepatitis C virus. *Virology*, **348**, 1-12.

38. Cocquerel, L., Voisset, C. and Dubuisson, J. (2006) Hepatitis C virus entry: potential receptors and their biological functions. *The Journal of general virology*, **87**, 1075-1084.

39. Kohaar, I., Ploss, A., Korol, E., Mu, K., Schoggins, J.W., O'Brien, T.R., Rice, C.M. and Prokunina-Olsson, L. (2010) Splicing diversity of the human OCLN gene and its biological significance for hepatitis C virus entry. *Journal of virology*, **84**, 6987-6994.

40. Ray, K. (2012) Hepatitis: NPC1L1 identified as a novel HCV entry factor. *Nature reviews. Gastroenterology & hepatology*, **9**, 124.

41. Sainz, B., Jr., Barretto, N., Martin, D.N., Hiraga, N., Imamura, M., Hussain, S., Marsh, K.A., Yu, X., Chayama, K., Alrefai, W.A. *et al.* (2012) Identification of the Niemann-Pick C1-like 1 cholesterol absorption receptor as a new hepatitis C virus entry factor. *Nature medicine*, **18**, 281-285.

42. Lindenbach, B.D. and Rice, C.M. (2005) Unravelling hepatitis C virus replication from genome to function. *Nature*, **436**, 933-938.

43. Pavio, N. and Lai, M.M. (2003) The hepatitis C virus persistence: how to evade the immune system? *Journal of biosciences*, **28**, 287-304.

44. Hadziyannis, S.J. (1997) The spectrum of extrahepatic manifestations in hepatitis C virus infection. *J Viral Hepat*, **4**, 9-28.

45. Cresta, P., Musset, L., Cacoub, P., Frangeul, L., Vitour, D., Poynard, T., Opolon, P., Nguyen, D.T., Golliot, F., Piette, J.C. *et al.* (1999) Response to interferon alpha treatment and disappearance of cryoglobulinaemia in patients infected by hepatitis C virus. *Gut*, **45**, 122-128.

46. Ferri, C. and Zignego, A.L. (2000) Relation between infection and autoimmunity in mixed cryoglobulinemia. *Current opinion in rheumatology*, **12**, 53-60.

47. Bortolotti, F., Vajro, P., Balli, F., Giacchino, R., Crivellaro, C., Barbera, C., Cataleta, M., Muratori, L., Pontisso, P., Nebbia, G. *et al.* (1996) Non-organ specific autoantibodies in children with chronic hepatitis C. *Journal of hepatology*, **25**, 614-620.

48. Lenzi, M., Bellentani, S., Saccoccio, G., Muratori, P., Masutti, F., Muratori, L., Cassani, F., Bianchi, F.B. and Tiribelli, C. (1999) Prevalence of non-organ-specific autoantibodies and chronic liver disease in the general population: a nested case-control study of the Dionysos cohort. *Gut*, **45**, 435-441.

49. Luo, J.C., Hwang, S.J., Li, C.P., Lu, R.H., Chan, C.Y., Wu, J.C., Chang, F.Y. and Lee, S.D. (1998) Clinical significance of serum auto-antibodies in Chinese patients with chronic hepatitis C: negative role of serum viral titre and genotype. *Journal of gastroenterology and hepatology*, **13**, 475-479.

50. Kammer, A.R., van der Burg, S.H., Grabscheid, B., Hunziker, I.P., Kwappenberg, K.M., Reichen, J., Melief, C.J. and Cerny, A. (1999) Molecular mimicry of human cytochrome P450 by hepatitis C virus at the level of cytotoxic T cell recognition. *The Journal of experimental medicine*, **190**, 169-176.

51. Drygiannakis, D., Lionis, C., Drygiannakis, I., Pappas, G. and Kouroumalis, E. (2001) Low prevalence of liver-kidney microsomal autoantibodies of type 1 (LKM1) in hepatitis C seropositive subjects on Crete, Greece. *BMC gastroenterology*, **1**, 4.

52. Dammacco, F., Sansonno, D., Piccoli, C., Racanelli, V., D'Amore, F.P. and Lauletta, G. (2000) The lymphoid system in hepatitis C virus infection: autoimmunity, mixed cryoglobulinemia, and Overt B-cell malignancy. *Seminars in liver disease*, **20**, 143-157.

53. Obermayer-Straub, P. and Manns, M.P. (2001) Hepatitis C and D, retroviruses and autoimmune manifestations. *Journal of autoimmunity*, **16**, 275-285.

54. McMurray, R.W. and Elbourne, K. (1997) Hepatitis C virus infection and autoimmunity. *Seminars in arthritis and rheumatism*, **26**, 689-701.

55. Valentini, G., Mantelli, A., Persico, M., Tuccillo, C., Del Vecchio Blanco, G., Morisco, F., Improta, R.D., Migliaresi, S., Gualdieri, L. and Caporaso, N. (1999) Serological and clinical markers of autoimmune disease in HCV-infected subjects with different disease conditions. *Clinical and experimental rheumatology*, **17**, 75-79.

56. Kursula, P., Flodin, S., Ehn, M., Hammarstrom, M., Schuler, H., Nordlund, P. and Stenmark, P. (2006) Structure of the synthetase domain of human CTP synthetase, a target for anticancer therapy. *Acta Crystallogr Sect F Struct Biol Cryst Commun*, **62**, 613-617.

57. Hofer, A., Steverding, D., Chabes, A., Brun, R. and Thelander, L. (2001) Trypanosoma brucei CTP synthetase: a target for the treatment of African sleeping sickness. *Proc Natl Acad Sci U S A*, **98**, 6412-6416.

58. Carr, S.F., Papp, E., Wu, J.C. and Natsumeda, Y. (1993) Characterization of human type I and type II IMP dehydrogenases. *J Biol Chem*, **268**, 27286-27290.

59. Ji, Y., Gu, J., Makhov, A.M., Griffith, J.D. and Mitchell, B.S. (2006) Regulation of the interaction of inosine monophosphate dehydrogenase with mycophenolic Acid by GTP. *The Journal of biological chemistry*, **281**, 206-212.

60. Franchetti, P. and Grifantini, M. (1999) Nucleoside and non-nucleoside IMP dehydrogenase inhibitors as antitumor and antiviral agents. *Curr Med Chem*, **6**, 599-614.

61. Kaur, R., Klichko, V. and Margolis, D. (2005) Ex vivo modeling of the effects of mycophenolic acid on HIV infection: considerations for antiviral therapy. *AIDS Res Hum Retroviruses*, **21**, 116-124.

62. Robertson, C.M., Hermann, L.L. and Coombs, K.M. (2004) Mycophenolic acid inhibits avian reovirus replication. *Antiviral Res*, **64**, 55-61.

63. Zhou, S., Liu, R., Baroudy, B.M., Malcolm, B.A. and Reyes, G.R. (2003) The effect of ribavirin and IMPDH inhibitors on hepatitis C virus subgenomic replicon RNA. *Virology*, **310**, 333-342.

64. Hamazaki, T., Oka, M., Yamanaka, S. and Terada, N. (2004) Aggregation of embryonic stem cells induces Nanog repression and primitive endoderm differentiation. *J. Cell Sci.*, **117**, 5681-5686.

65. Gu, P., LeMenuet, D., Chung, A.C., Mancini, M., Wheeler, D.A. and Cooney, A.J. (2005) Orphan nuclear receptor GCNF is required for the repression of pluripotency genes during retinoic acid-induced embryonic stem cell differentiation. *Mol. Cell. Biol.*, **25**, 8507-8519.

66. Chan, J.Y., Takeda, M., Briggs, L.E., Graham, M.L., Lu, J.T., Horikoshi, N., Weinberg, E.O., Aoki, H., Sato, N., Chien, K.R. *et al.* (2008) Identification of cardiac-specific myosin light chain kinase. *Circ Res*, **102**, 571-580.

67. Satoh, M., Langdon, J.J., Hamilton, K.J., Richards, H.B., Panka, D., Eisenberg, R.A. and Reeves, W.H. (1996) Distinctive immune response patterns of human and murine autoimmune sera to U1 small nuclear ribonucleoprotein C protein. *The Journal of clinical investigation*, **97**, 2619-2626.

68. Fritzler, M.J., Hamel, J.C., Ochs, R.L. and Chan, E.K.L. (1993) Molecular characterization of two human autoantigens: unique cDNAs encoding 95- and 160-kD proteins of a putative family in the Golgi complex. *J. Exp. Med.*, **178**, 49-62.

69. Jakymiw, A., Ikeda, K., Fritzler, M.J., Reeves, W.H., Satoh, M. and Chan, E.K.L. (2006) Autoimmune targeting of key components of RNA interference. *Arthritis Res.Ther.*, **8**, R87.

70. Pauley, K.M., Satoh, M., Pauley, B.A., Dominguez-Gutierrez, P.R., Wallet, S.M., Holliday, L.S., Cha, S., Reeves, W.H. and Chan, E.K.L. (2010) Formation of GW/P bodies as marker for microRNA-mediated regulation of innate immune signaling in THP-1 cells. *Immunol. Cell Biol.*, **88**, 205-212.

71. Nozawa, K., Casiano, C.A., Hamel, J.C., Molinaro, C., Fritzler, M.J. and Chan, E.K.L. (2002) Fragmentation of Golgi complex and Golgi autoantigens during apoptosis and necrosis. *Arthritis Res.*, **4**, R3.

72. Lian, S., Fritzler, M.J., Katz, J., Hamazaki, T., Terada, N., Satoh, M. and Chan, E.K.L. (2007) Small interfering RNA-mediated silencing induces target-dependent assembly of GW/P bodies. *Mol Biol Cell*, **18**, 3375-3387.

73. Moser, J.J., Chan, E.K.L. and Fritzler, M.J. (2009) Optimization of immunoprecipitation-western blot analysis in detecting GW182-associated components of GW/P bodies. *Nat Protoc*, **4**, 674-685.

74. Southwick, F.S., Li, W., Zhang, F., Zeile, W.L. and Purich, D.L. (2003) Actin-based endosome and phagosome rocketing in macrophages: activation by the secretagogue antagonists lanthanum and zinc. *Cell Motil. Cytoskeleton*, **54**, 41-55.

75. Christensen, S.T., Pedersen, S.F., Satir, P., Veland, I.R. and Schneider, L. (2008) The primary cilium coordinates signaling pathways in cell cycle control and migration during development and tissue repair. *Curr. Top. Dev. Biol.*, **85**, 261-301.

76. Buszczak, M., Paterno, S., Lighthouse, D., Bachman, J., Planck, J., Owen, S., Skora, A.D., Nystul, T.G., Ohlstein, B., Allen, A. *et al.* (2007) The carnegie protein trap library: a versatile tool for Drosophila developmental studies. *Genetics*, **175**, 1505-1531.

77. Liu, J.L. (2010) Intracellular compartmentation of CTP synthase in Drosophila. *J Genet Genomics*, **37**, 281-296.

78. Blüthner, M., Appelhans, H., Moosbrugger, I., Wiemann, C., Lenz, D. and Seeling, H.P. (2009) In Conrad, K., Chan, E. K. L., Fritzler, M. J., Humbel, R. L., von Landenberg, P. and Shoenfeld, Y. (eds.), *Proceedings 9th Dresden Symposium on Autoantibodies.* Pabst Science Publishers, Lengerich, Germany, Vol. 6, pp. 125-126.

79. Wu, F., Lukinius, A., Bergstrom, M., Eriksson, B., Watanabe, Y. and Langstrom, B. (1999) A mechanism behind the antitumour effect of 6-diazo-5-oxo-L-norleucine (DON): disruption of mitochondria. *Eur J Cancer*, **35**, 1155-1161.

80. Shan, G., Li, Y., Zhang, J., Li, W., Szulwach, K.E., Duan, R., Faghihi, M.A., Khalil, A.M., Lu, L., Paroo, Z. *et al.* (2008) A small molecule enhances RNA interference and promotes microRNA processing. *Nat.Biotechnol.*, **26**, 933-940.

81. Willingham, M.C., Richert, N.D. and Rutherford, A.V. (1987) A novel fibrillar structure in cultured cells detected by a monoclonal antibody. *Exp Cell Res*, **171**, 284-295.

82. Ingerson-Mahar, M., Briegel, A., Werner, J.N., Jensen, G.J. and Gitai, Z. (2010) The metabolic enzyme CTP synthase forms cytoskeletal filaments. *Nature cell biology*, **12**, 739-746.

83. Noree, C., Sato, B.K., Broyer, R.M. and Wilhelm, J.E. (2010) Identification of novel filament-forming proteins in Saccharomyces cerevisiae and Drosophila melanogaster. *J Cell Biol*, **190**, 541-551.

84. Ramer, M.S., Cruz Cabrera, M.A., Alan, N., Scott, A.L. and Inskip, J.A. (2010) A new organellar complex in rat sympathetic neurons. *PLoS One*, **5**, e10872.

85. Allison, A.C., Kowalski, W.J., Muller, C.D. and Eugui, E.M. (1993) Mechanisms of action of mycophenolic acid. *Ann N Y Acad Sci*, **696**, 63-87.

86. Liu, J.L. (2011) The enigmatic cytoophidium: compartmentation of CTP synthase via filament formation. *Bioessays*, **33**, 159-164.

87. He, Y., Mou, Z., Li, W., Liu, B., Fu, T., Zhao, S., Xiang, D. and Wu, Y. (2009) Identification of IMPDH2 as a tumor-associated antigen in colorectal cancer using immunoproteomics analysis. *Int J Colorectal Dis*, **24**, 1271-1279.

88. Cassani, F., Cataleta, M., Valentini, P., Muratori, P., Giostra, F., Francesconi, R., Muratori, L., Lenzi, M., Bianchi, G., Zauli, D. *et al.* (1997) Serum autoantibodies in chronic hepatitis C: comparison with autoimmune hepatitis and impact on the disease profile. *Hepatology*, **26**, 561-566.

89. Clifford, B.D., Donahue, D., Smith, L., Cable, E., Luttig, B., Manns, M. and Bonkovsky, H.L. (1995) High prevalence of serological markers of autoimmunity in patients with chronic hepatitis C. *Hepatology*, **21**, 613-619.

90. Fried, M.W., Draguesku, J.O., Shindo, M., Simpson, L.H., Banks, S.M., Hoofnagle, J.H. and Di Bisceglie, A.M. (1993) Clinical and serological differentiation of autoimmune and hepatitis C virus-related chronic hepatitis. *Digestive diseases and sciences*, **38**, 631-636.

91. Preziati, D., La Rosa, L., Covini, G., Marcelli, R., Rescalli, S., Persani, L., Del Ninno, E., Meroni, P.L., Colombo, M. and Beck-Peccoz, P. (1995) Autoimmunity and thyroid function in patients with chronic active hepatitis treated with recombinant interferon alpha-2a. *European journal of endocrinology / European Federation of Endocrine Societies*, **132**, 587-593.

92. Abuaf, N., Lunel, F., Giral, P., Borotto, E., Laperche, S., Poupon, R., Opolon, P., Huraux, J.M. and Homberg, J.C. (1993) Non-organ specific autoantibodies associated with chronic C virus hepatitis. *Journal of hepatology*, **18**, 359-364.

93. Tran, A., Quaranta, J.F., Benzaken, S., Thiers, V., Chau, H.T., Hastier, P., Regnier, D., Dreyfus, G., Pradier, C., Sadoul, J.L. *et al.* (1993) High prevalence of thyroid autoantibodies in a prospective series of patients with chronic hepatitis C before interferon therapy. *Hepatology*, **18**, 253-257.

94. Lenzi, M., Johnson, P.J., McFarlane, I.G., Ballardini, G., Smith, H.M., McFarlane, B.M., Bridger, C., Vergani, D., Bianchi, F.B. and Williams, R. (1991) Antibodies to hepatitis C virus in autoimmune liver disease: evidence for geographical heterogeneity. *Lancet*, **338**, 277-280.

95. Williams, M.J., Lawson, A., Neal, K.R., Ryder, S.D. and Irving, W.L. (2009) Autoantibodies in chronic hepatitis C virus infection and their association with disease profile. *J Viral Hepat*, **16**, 325-331.

96. Covini, G., von Muhlen, C.A., Pacchetti, S., Colombo, M., Chan, E.K. and Tan, E.M. (1997) Diversity of antinuclear antibody responses in hepatocellular carcinoma. *Journal of hepatology*, **26**, 1255-1265.

97. Pileri, P., Uematsu, Y., Campagnoli, S., Galli, G., Falugi, F., Petracca, R., Weiner, A.J., Houghton, M., Rosa, D., Grandi, G. *et al.* (1998) Binding of hepatitis C virus to CD81. *Science*, **282**, 938-941.

98. Maecker, H.T., Do, M.S. and Levy, S. (1998) CD81 on B cells promotes interleukin 4 secretion and antibody production during T helper type 2 immune responses. *Proc Natl Acad Sci U S A*, **95**, 2458-2462.

99. Gregorio, G.V., Choudhuri, K., Ma, Y., Pensati, P., Iorio, R., Grant, P., Garson, J., Bogdanos, D.P., Vegnente, A., Mieli-Vergani, G. *et al.* (2003) Mimicry between the hepatitis C virus polyprotein and antigenic targets of nuclear and smooth muscle antibodies in chronic hepatitis C virus infection. *Clinical and experimental immunology*, **133**, 404-413.

100. Sutti, S., Vidali, M., Mombello, C., Sartori, M., Ingelman-Sundberg, M. and Albano, E. (2010) Breaking self-tolerance toward cytochrome P4502E1 (CYP2E1) in chronic hepatitis C: possible role for molecular mimicry. *Journal of hepatology*, **53**, 431-438.

101. Yamamoto, A.M., Cresteil, D., Boniface, O., Clerc, F.F. and Alvarez, F. (1993) Identification and analysis of cytochrome P450IID6 antigenic sites recognized by anti-liver-kidney microsome type-1 antibodies (LKM1). *European journal of immunology*, **23**, 1105-1111.

102. Shindo, M., Di Bisceglie, A.M. and Hoofnagle, J.H. (1992) Acute exacerbation of liver disease during interferon alfa therapy for chronic hepatitis C. *Gastroenterology*, **102**, 1406-1408.

103. Papo, T., Marcellin, P., Bernuau, J., Durand, F., Poynard, T. and Benhamou, J.P. (1992) Autoimmune chronic hepatitis exacerbated by alpha-interferon. *Annals of internal medicine*, **116**, 51-53.

104. Todros, L., Saracco, G., Durazzo, M., Abate, M.L., Touscoz, G., Scaglione, L., Verme, G. and Rizzetto, M. (1995) Efficacy and safety of interferon alfa therapy in chronic hepatitis C with autoantibodies to liver-kidney microsomes. *Hepatology*, **22**, 1374-1378.

105. Garcia-Buey, L., Garcia-Monzon, C., Rodriguez, S., Borque, M.J., Garcia-Sanchez, A., Iglesias, R., DeCastro, M., Mateos, F.G., Vicario, J.L., Balas, A. *et al.* (1995) Latent autoimmune hepatitis triggered during interferon therapy in patients with chronic hepatitis C. *Gastroenterology*, **108**, 1770-1777.

106. Fabbri, C., Jaboli, M.F., Giovanelli, S., Azzaroli, F., Pezzoli, A., Accogli, E., Liva, S., Nigro, G., Miracolo, A., Festi, D. *et al.* (2003) Gastric autoimmune disorders in patients with chronic hepatitis C before, during and after interferon-alpha therapy. *World J Gastroenterol*, **9**, 1487-1490.

107. Wesche, B., Jaeckel, E., Trautwein, C., Wedemeyer, H., Falorni, A., Frank, H., von zur Muhlen, A., Manns, M.P. and Brabant, G. (2001) Induction of autoantibodies to the adrenal cortex and pancreatic islet cells by interferon alpha therapy for chronic hepatitis C. *Gut*, **48**, 378-383.

108. Fabris, P., Betterle, C., Greggio, N.A., Zanchetta, R., Bosi, E., Biasin, M.R. and de Lalla, F. (1998) Insulin-dependent diabetes mellitus during alpha-interferon therapy for chronic viral hepatitis. *Journal of hepatology*, **28**, 514-517.

109. Dalekos, G.N., Wedemeyer, H., Obermayer-Straub, P., Kayser, A., Barut, A., Frank, H. and Manns, M.P. (1999) Epitope mapping of cytochrome P4502D6 autoantigen in patients with chronic hepatitis C during alpha-interferon treatment. *Journal of hepatology*, **30**, 366-375.

110. Fabris, P., Betterle, C., Floreani, A., Greggio, N.A., de Lazzari, F., Naccarato, R. and Chiaramonte, M. (1992) Development of type 1 diabetes mellitus during interferon alfa therapy for chronic HCV hepatitis. *Lancet*, **340**, 548.

111. Imagawa, A., Itoh, N., Hanafusa, T., Waguri, M., Kuwajima, M. and Matsuzawa, Y. (1996) Antibodies to glutamic acid decarboxylase induced by interferon-alpha therapy for chronic viral hepatitis. *Diabetologia*, **39**, 126.

112. Baron, S., Tyring, S.K., Fleischmann, W.R., Jr., Coppenhaver, D.H., Niesel, D.W., Klimpel, G.R., Stanton, G.J. and Hughes, T.K. (1991) The interferons. Mechanisms of action and clinical applications. *JAMA : the journal of the American Medical Association*, **266**, 1375-1383.

113. Kogure, T., Ueno, Y., Fukushima, K., Nagasaki, F., Inoue, J., Kakazu, E., Matsuda, Y., Kido, O., Nakagome, Y., Kimura, O. *et al.* (2007) Fulminant hepatic failure in a case of autoimmune hepatitis in hepatitis C during peg-interferon-alpha 2b plus ribavirin treatment. *World J Gastroenterol*, **13**, 4394-4397.

114. Narciso-Schiavon, J.L., Freire, F.C., Suarez, M.M., Ferrari, M.V., Scanhola, G.Q., Schiavon Lde, L., de Carvalho Filho, R.J., Ferraz, M.L. and Silva, A.E. (2009) Antinuclear antibody positivity in patients with chronic hepatitis C: clinically relevant or an epiphenomenon? *European journal of gastroenterology & hepatology*, **21**, 440-446.

115. Wasmuth, H.E., Stolte, C., Geier, A., Dietrich, C.G., Gartung, C., Lorenzen, J., Matern, S. and Lammert, F. (2004) The presence of non-organ-specific autoantibodies is associated with a negative response to combination therapy with interferon and ribavirin for chronic hepatitis C. *BMC infectious diseases*, **4**, 4.

116. Gatselis, N.K., Georgiadou, S.P., Koukoulis, G.K., Tassopoulos, N., Zachou, K., Liaskos, C., Hatzakis, A. and Dalekos, G.N. (2006) Clinical significance of organ- and non-organ-specific autoantibodies on the response to anti-viral treatment of patients with chronic hepatitis C. *Alimentary pharmacology & therapeutics*, **24**, 1563-1573.

117. Ferri, S., Muratori, L., Quarneti, C., Muratori, P., Menichella, R., Pappas, G., Granito, A., Ballardini, G., Bianchi, F.B. and Lenzi, M. (2009) Clinical features and effect of antiviral therapy on anti-liver/kidney microsomal antibody type 1 positive chronic hepatitis C. *Journal of hepatology*, **50**, 1093-1101.

118. Yee, L.J., Kelleher, P., Goldin, R.D., Marshall, S., Thomas, H.C., Alberti, A., Chiaramonte, M., Braconier, J.H., Hall, A.J. and Thursz, M.R. (2004) Antinuclear antibodies (ANA) in chronic hepatitis C virus infection: correlates of positivity and clinical relevance. *J Viral Hepat*, **11**, 459-464.

119. Dienstag, J.L. and McHutchison, J.G. (2006) American Gastroenterological Association technical review on the management of hepatitis C. *Gastroenterology*, **130**, 231-264; quiz 214-237.

120. Alvarez, F., Berg, P.A., Bianchi, F.B., Bianchi, L., Burroughs, A.K., Cancado, E.L., Chapman, R.W., Cooksley, W.G., Czaja, A.J., Desmet, V.J. *et al.* (1999) International Autoimmune Hepatitis Group Report: review of criteria for diagnosis of autoimmune hepatitis. *Journal of hepatology*, **31**, 929-938.

121. Jakymiw, A., Pauley, K.M., Li, S., Ikeda, K., Lian, S., Eystathioy, T., Satoh, M., Fritzler, M.J. and Chan, E.K. (2007) The role of GW/P-bodies in RNA processing and silencing. *J Cell Sci*, **120**, 1317-1323.

122. Carcamo, W.C., Satoh, M., Kasahara, H., Terada, N., Hamazaki, T., Chan, J.Y., Yao, B., Tamayo, S., Covini, G., von Muhlen, C.A. *et al.* (2011) Induction of cytoplasmic rods and rings structures by inhibition of the CTP and GTP synthetic pathway in mammalian cells. *PLoS One*, **6**, e29690.

123. Homberg, J.C., Andre, C. and Abuaf, N. (1984) A new anti-liver-kidney microsome antibody (anti-LKM2) in tienilic acid-induced hepatitis. *Clinical and experimental immunology*, **55**, 561-570.

124. Matsuda, J., Saitoh, N., Gotoh, M., Gohchi, K., Tsukamoto, M., Syoji, S., Miyake, K. and Yamanaka, M. (1995) High prevalence of anti-phospholipid antibodies and anti-thyroglobulin antibody in patients with hepatitis C virus infection treated with interferon-alpha. *The American journal of gastroenterology*, **90**, 1138-1141.

125. Stroffolini, T., Colloredo, G., Gaeta, G.B., Sonzogni, A., Angeletti, S., Marignani, M., Pasquale, G., Venezia, G., Craxi, A. and Almasio, P. (2004) Does an 'autoimmune' profile affect the clinical profile of chronic hepatitis C? An Italian multicentre survey. *J Viral Hepat*, **11**, 257-262.

126. van Regenmortel, M.H., Mayo, M.A., Fauquet, C.M. and Maniloff, J. (2000) Virus nomenclature: consensus versus chaos. *Archives of virology*, **145**, 2227-2232.

127. Ikeda, K., Saitoh, S., Koida, I., Arase, Y., Tsubota, A., Chayama, K., Kumada, H. and Kawanishi, M. (1993) A multivariate analysis of risk factors for hepatocellular carcinogenesis: a prospective observation of 795 patients with viral and alcoholic cirrhosis. *Hepatology*, **18**, 47-53.

128. Houghton, M. and Abrignani, S. (2005) Prospects for a vaccine against the hepatitis C virus. *Nature*, **436**, 961-966.

129. Bartenschlager, R., Frese, M. and Pietschmann, T. (2004) Novel insights into hepatitis C virus replication and persistence. *Advances in virus research*, **63**, 71-180.

130. Moradpour, D., Penin, F. and Rice, C.M. (2007) Replication of hepatitis C virus. *Nature reviews. Microbiology*, **5**, 453-463.

131. Simmonds, P. (1995) Variability of hepatitis C virus. *Hepatology*, **21**, 570-583.

132. Ibarra, K.D., Jain, M.K. and Pfeiffer, J.K. (2011) Host-based ribavirin resistance influences hepatitis C virus replication and treatment response. *Journal of virology*, **85**, 7273-7283.

133. Ghany, M.G., Strader, D.B., Thomas, D.L. and Seeff, L.B. (2009) Diagnosis, management, and treatment of hepatitis C: an update. *Hepatology*, **49**, 1335-1374.

134. Ferri, S., Muratori, L., Lenzi, M., Granito, A., Bianchi, F.B. and Vergani, D. (2008) HCV and autoimmunity. *Current pharmaceutical design*, **14**, 1678-1685.

135. Manns, M.P. and Rambusch, E.G. (1999) Autoimmunity and extrahepatic manifestations in hepatitis C virus infection. *Journal of hepatology*, **31 Suppl 1**, 39-42.

136. Zignego, A.L. and Brechot, C. (1999) Extrahepatic manifestations of HCV infection: facts and controversies. *Journal of hepatology*, **31**, 369-376.

137. Satoh, M., Vazquez-Del Mercado, M. and Chan, E.K.L. (2009) Clinical interpretation of antinuclear antibody tests in systemic rheumatic diseases. *Mod Rheumatol*, **19**, 219-228.

138. Muratori, P., Muratori, L., Guidi, M., Granito, A., Susca, M., Lenzi, M. and Bianchi, F.B. (2005) Clinical impact of non-organ-specific autoantibodies on the response to combined antiviral treatment in patients with hepatitis C. *Clinical infectious diseases : an official publication of the Infectious Diseases Society of America*, **40**, 501-507.

139. Covini, G., Carcamo, W.C., Bredi, E., von Muhlen, C.A., Colombo, M. and Chan, E.K. (2011) Cytoplasmic rods and rings autoantibodies developed during pegylated interferon and ribavirin therapy in patients with chronic hepatitis C. *Antivir Ther*.

140. Seelig, H.P., Appelhans, H., Bauer, O., Bluthner, M., Hartung, K., Schranz, P., Schultze, D., Seelig, C.A. and Volkmann, M. (2011) Autoantibodies against inosine-5'-monophosphate dehydrogenase 2--characteristics and prevalence in patients with HCV-infection. *Clin Lab*, **57**, 753-765.

141. Goto, M., Omi, R., Nakagawa, N., Miyahara, I. and Hirotsu, K. (2004) Crystal structures of CTP synthetase reveal ATP, UTP, and glutamine binding sites. *Structure*, **12**, 1413-1423.

142. Long, C.W. and Pardee, A.B. (1967) Cytidine triphosphate synthetase of Escherichia coli B. I. Purification and kinetics. *The Journal of biological chemistry*, **242**, 4715-4721.

143. Endrizzi, J.A., Kim, H., Anderson, P.M. and Baldwin, E.P. (2005) Mechanisms of product feedback regulation and drug resistance in cytidine triphosphate synthetases from the structure of a CTP-inhibited complex. *Biochemistry*, **44**, 13491-13499.

144. Willemoes, M. and Sigurskjold, B.W. (2002) Steady-state kinetics of the glutaminase reaction of CTP synthase from Lactococcus lactis. The role of the allosteric activator GTP incoupling between glutamine hydrolysis and CTP synthesis. *European journal of biochemistry / FEBS*, **269**, 4772-4779.

145. Weber, G. (1983) Enzymes of purine metabolism in cancer. *Clinical biochemistry*, **16**, 57-63.

146. Weber, G., Prajda, N., Abonyi, M., Look, K.Y. and Tricot, G. (1996) Tiazofurin: molecular and clinical action. *Anticancer Res*, **16**, 3313-3322.

147. Franklin, T.J., Edwards, G. and Hedge, P. (1994) Inosine 5'-monophosphate dehydrogenase as a chemotherapeutic target. *Adv Exp Med Biol*, **370**, 155-160.

148. Nair, V. and Shu, Q. (2007) Inosine monophosphate dehydrogenase as a probe in antiviral drug discovery. *Antivir Chem Chemother*, **18**, 245-258.

149. Curi, R., Lagranha, C.J., Doi, S.Q., Sellitti, D.F., Procopio, J., Pithon-Curi, T.C., Corless, M. and Newsholme, P. (2005) Molecular mechanisms of glutamine action. *Journal of cellular physiology*, **204**, 392-401.

150. Engstrom, W. and Zetterberg, A. (1984) The relationship between purines, pyrimidines, nucleosides, and glutamine for fibroblast cell proliferation. *Journal of cellular physiology*, **120**, 233-241.

151. Newsholme, P., Procopio, J., Lima, M.M., Pithon-Curi, T.C. and Curi, R. (2003) Glutamine and glutamate--their central role in cell metabolism and function. *Cell biochemistry and function*, **21**, 1-9.

152. Curi, R., Lagranha, C.J., Doi, S.Q., Sellitti, D.F., Procopio, J. and Pithon-Curi, T.C. (2005) Glutamine-dependent changes in gene expression and protein activity. *Cell biochemistry and function*, **23**, 77-84.

153. Geisbuhler, T.P. and Rovetto, M.J. (1991) Guanosine metabolism in adult rat cardiac myocytes: ribose-enhanced GTP synthesis from extracellular guanosine. *Pflugers Archiv : European journal of physiology*, **419**, 160-165.

154. Jones, M.E. (1980) Pyrimidine nucleotide biosynthesis in animals: genes, enzymes, and regulation of UMP biosynthesis. *Annual review of biochemistry*, **49**, 253-279.

155. Chen, K., Zhang, J., Tastan, O.Y., Deussen, Z.A., Siswick, M.Y. and Liu, J.L. (2011) Glutamine analogs promote cytoophidium assembly in human and Drosophila cells. *J Genet Genomics*, **38**, 391-402.

156. Rapaport, E., Christopher, C.W., Svihovec, S.K., Ullrey, D. and Kalckar, H.M. (1979) Selective high metabolic lability of uridine, guanosine and cytosine triphosphates in response to glucose deprivation and refeeding of untransformed and polyoma virus-transformed hamster fibroblasts. *Journal of cellular physiology*, **101**, 229-235.

157. Bode, B.P. (2001) Recent molecular advances in mammalian glutamine transport. *The Journal of nutrition*, **131**, 2475S-2485S; discussion 2486S-2477S.

158. Boza, J.J., Moennoz, D., Bournot, C.E., Blum, S., Zbinden, I., Finot, P.A. and Ballevre, O. (2000) Role of glutamine on the de novo purine nucleotide synthesis in Caco-2 cells. *European journal of nutrition*, **39**, 38-46.

159. Dereuddre-Bosquet, N., Roy, B., Routledge, K., Clayette, P., Foucault, G. and Lepoivre, M. (2004) Inhibitors of CTP biosynthesis potentiate the anti-human immunodeficiency virus type 1 activity of 3TC in activated peripheral blood mononuclear cells. *Antiviral Res*, **61**, 67-70.

160. Verschuur, A.C., Van Gennip, A.H., Leen, R., Meinsma, R., Voute, P.A. and van Kuilenburg, A.B. (2000) In vitro inhibition of cytidine triphosphate synthetase activity by cyclopentenyl cytosine in paediatric acute lymphocytic leukaemia. *Br J Haematol*, **110**, 161-169.

161. Jackson, R.C., Weber, G. and Morris, H.P. (1975) IMP dehydrogenase, an enzyme linked with proliferation and malignancy. *Nature*, **256**, 331-333.

162. Colby, T.D., Vanderveen, K., Strickler, M.D., Markham, G.D. and Goldstein, B.M. (1999) Crystal structure of human type II inosine monophosphate dehydrogenase: implications for ligand binding and drug design. *Proceedings of the National Academy of Sciences of the United States of America*, **96**, 3531-3536.

163. Sintchak, M.D., Fleming, M.A., Futer, O., Raybuck, S.A., Chambers, S.P., Caron, P.R., Murcko, M.A. and Wilson, K.P. (1996) Structure and mechanism of inosine monophosphate dehydrogenase in complex with the immunosuppressant mycophenolic acid. *Cell*, **85**, 921-930.

164. Franklin, T.J. and Cook, J.M. (1969) The inhibition of nucleic acid synthesis by mycophenolic acid. *Biochem J*, **113**, 515-524.

165. Allison, A.C. and Eugui, E.M. (1993) Immunosuppressive and other effects of mycophenolic acid and an ester prodrug, mycophenolate mofetil. *Immunol Rev*, **136**, 5-28.

166. Hong, Z. and Cameron, C.E. (2002) Pleiotropic mechanisms of ribavirin antiviral activities. *Prog Drug Res*, **59**, 41-69.

167. Yang, Z., Jakymiw, A., Wood, M.R., Eystathioy, T., Rubin, R.L., Fritzler, M.J. and Chan, E.K. (2004) GW182 is critical for the stability of GW bodies expressed during the cell cycle and cell proliferation. *J Cell Sci*, **117**, 5567-5578.

168. An, S., Kumar, R., Sheets, E.D. and Benkovic, S.J. (2008) Reversible compartmentalization of de novo purine biosynthetic complexes in living cells. *Science*, **320**, 103-106.

169. Liu, J.L. and Gall, J.G. (2007) U bodies are cytoplasmic structures that contain uridine-rich small nuclear ribonucleoproteins and associate with P bodies. *Proceedings of the National Academy of Sciences of the United States of America*, **104**, 11655-11659.

170. Kleinschmidt, A.K., Moss, J. and Lane, D.M. (1969) Acetyl coenzyme A carboxylase: filamentous nature of the animal enzymes. *Science*, **166**, 1276-1278.

171. Schneiter, R., Hitomi, M., Ivessa, A.S., Fasch, E.V., Kohlwein, S.D. and Tartakoff, A.M. (1996) A yeast acetyl coenzyme A carboxylase mutant links very-long-chain fatty acid synthesis to the structure and function of the nuclear membrane-pore complex. *Mol Cell Biol*, **16**, 7161-7172.

172. Narayanaswamy, R., Levy, M., Tsechansky, M., Stovall, G.M., O'Connell, J.D., Mirrielees, J., Ellington, A.D. and Marcotte, E.M. (2009) Widespread reorganization of metabolic enzymes into reversible assemblies upon nutrient starvation. *Proceedings of the National Academy of Sciences of the United States of America*, **106**, 10147-10152.

173. Beaty, N.B. and Lane, M.D. (1983) Kinetics of activation of acetyl-CoA carboxylase by citrate. Relationship to the rate of polymerization of the enzyme. *The Journal of biological chemistry*, **258**, 13043-13050.

174. Vagelos, P.R., Alberts, A.W. and Martin, D.B. (1962) Activation of acetyl-CoA carboxylase and associated alteration of sedimentation characteristics of the enzyme. *Biochem Biophys Res Commun*, **8**, 4-8.

175. Hedstrom, L. (2009) IMP dehydrogenase: structure, mechanism, and inhibition. *Chem Rev*, **109**, 2903-2928.

176. McLean, J.E., Hamaguchi, N., Belenky, P., Mortimer, S.E., Stanton, M. and Hedstrom, L. (2004) Inosine 5'-monophosphate dehydrogenase binds nucleic acids in vitro and in vivo. *Biochem J*, **379**, 243-251.

177. Baechler, E.C., Batliwalla, F.M., Karypis, G., Gaffney, P.M., Ortmann, W.A., Espe, K.J., Shark, K.B., Grande, W.J., Hughes, K.M., Kapur, V. *et al.* (2003) Interferon-inducible gene expression signature in peripheral blood cells of patients with severe lupus. *Proc Natl Acad Sci U S A*, **100**, 2610-2615.

178. Bennett, L., Palucka, A.K., Arce, E., Cantrell, V., Borvak, J., Banchereau, J. and Pascual, V. (2003) Interferon and granulopoiesis signatures in systemic lupus erythematosus blood. *The Journal of experimental medicine*, **197**, 711-723.

179. Damaraju, V.L., Visser, F., Zhang, J., Mowles, D., Ng, A.M., Young, J.D., Jayaram, H.N. and Cass, C.E. (2005) Role of human nucleoside transporters in the cellular uptake of two inhibitors of IMP dehydrogenase, tiazofurin and benzamide riboside. *Mol Pharmacol*, **67**, 273-279.

180. Huang, M., Wang, Y., Cogut, S.B., Mitchell, B.S. and Graves, L.M. (2003) Inhibition of nucleoside transport by protein kinase inhibitors. *The Journal of pharmacology and experimental therapeutics*, **304**, 753-760.

181. Huang, M., Wang, Y., Mitchell, B.S. and Graves, L.M. (2004) Regulation of equilibrative nucleoside uptake by protein kinase inhibitors. *Nucleosides, nucleotides & nucleic acids*, **23**, 1445-1450.

182. Kokeny, S., Papp, J., Weber, G., Vaszko, T., Carmona-Saez, P. and Olah, E. (2009) Ribavirin acts via multiple pathways in inhibition of leukemic cell proliferation. *Anticancer Res*, **29**, 1971-1980.

BIOGRAPHICAL SKETCH

Wendy Cristina Carcamo was born in Los Angeles, California. She graduated from Piper High School in 2004 and then attended the University of Florida. During the four years she studied microbiology and volunteered in Dr. Edward Chan's laboratory. In 2008, she graduated with a Bachelor in Science in microbiology with a minor in chemistry and plant molecular and cellular biology. With the support of Dr. Chan and his graduate students she applied to the Interdisciplinary Program in Biomedical Sciences (IDP) at the University of Florida. In 2008, she joined the molecular cell biology concentration, and decided to continue in the laboratory of Dr. Edward Chan. Here, her research focused on a novel cytoplasmic structure that were detected with human autoantibodies. Her research focused on identifying the components, the function of the structure, and the correlation to the disease. After her doctorate work, Wendy plans on entering medical school where she hopes to specialize as an obstetrician/ gynecologist.